



**Calhoun: The NPS Institutional Archive**  
**DSpace Repository**

---

Theses and Dissertations

1. Thesis and Dissertation Collection, all items

---

1983

# An analysis of a PC-3 micropulsation in the geomagnetic field.

Stevens, Kurt B.

Monterey, California. Naval Postgraduate School

---

<http://hdl.handle.net/10945/19631>

---

*Downloaded from NPS Archive: Calhoun*



<http://www.nps.edu/library>

Calhoun is the Naval Postgraduate School's public access digital repository for research materials and institutional publications created by the NPS community. Calhoun is named for Professor of Mathematics Guy K. Calhoun, NPS's first appointed -- and published -- scholarly author.

**Dudley Knox Library / Naval Postgraduate School**  
**411 Dyer Road / 1 University Circle**  
**Monterey, California USA 93943**



Dudley Knox Library, NPS  
Monterey, CA 93943











# NAVAL POSTGRADUATE SCHOOL

## Monterey, California



# THESIS

AN ANALYSIS OF A PC-3 MICROPULSATION IN  
THE GEOMAGNETIC FIELD

by

Kurt B. Stevens

June 1983

Thesis Advisor:

A. Ochadlick

Approved for public release; distribution unlimited

J210157



## REPORT DOCUMENTATION PAGE

READ INSTRUCTIONS  
BEFORE COMPLETING FORM

1. REPORT NUMBER		2. GOVT ACCESSION NO.	3. RECIPIENT'S CATALOG NUMBER
4. TITLE (and Subtitle)  An Analysis of a PC-3 Micropulsation in the Geomagnetic Field		5. TYPE OF REPORT & PERIOD COVERED Master's Thesis June 1983	
7. AUTHOR(s)  Kurt B. Stevens		6. PERFORMING ORG. REPORT NUMBER	
9. PERFORMING ORGANIZATION NAME AND ADDRESS  Naval Postgraduate School Monterey, California 93940		8. CONTRACT OR GRANT NUMBER(s)	
11. CONTROLLING OFFICE NAME AND ADDRESS  Naval Postgraduate School Monterey, California 93940		10. PROGRAM ELEMENT, PROJECT, TASK AREA & WORK UNIT NUMBERS	
14. MONITORING AGENCY NAME & ADDRESS (if different from Controlling Office)		12. REPORT DATE June 1983	
		13. NUMBER OF PAGES 141	
		15. SECURITY CLASS. (of this report) Unclassified	
		15a. DECLASSIFICATION/DOWNGRADING SCHEDULE	
16. DISTRIBUTION STATEMENT (of this Report)  Approved for public release; distribution unlimited			
17. DISTRIBUTION STATEMENT (of the abstract entered in Block 20, if different from Report)			
18. SUPPLEMENTARY NOTES			
19. KEY WORDS (Continue on reverse side if necessary and identify by block number)  Micropulsation Coherence Degree of Polarization Ellipticity			
20. ABSTRACT (Continue on reverse side if necessary and identify by block number)  The Naval Postgraduate School has an ongoing effort to study geomagnetic noise and micropulsations in the ULF frequency range ( $.05 < f < 10$ Hz). Data is collected by three orthogonally mounted coils at a remote land site and telemetered to the laboratory for computer analysis. To isolate data containing a micropulsation event, time series plots of the magnetic field were generated. The (continued)			

1970-1971

## Item 20. (continued)

development of a double running average routine made possible the isolation of micropulsations in large data sets. A type PC-3 micropulsation was found and the coherence, ellipticity and polarization properties were determined as follows: Coherence = 0.99, Degree of Polarization = 0.99 and the micropulsation was elliptically polarized.

Power spectral density (PSD) plots summarizing data segments about two hours long occasionally contained structures found to be artificial and not representative of natural phenomena in the geomagnetic field. Methods to avoid this anomalous behavior in PSD plots are suggested.





Approved for public release; distribution unlimited

An Analysis of a PC-3 Micropulsation in the Geomagnetic Field

by

Kurt B. Stevens  
Captain, United States Air Force  
B.S., United States Air Force Academy, 1979

Submitted in partial fulfillment of the  
requirements for the degree of

MASTER OF SCIENCE IN PHYSICS

from the

NAVAL POSTGRADUATE SCHOOL  
June 1983

---

Thesis  
57127  
C.1

## ABSTRACT

The Naval Postgraduate School has an ongoing effort to study geomagnetic noise and micropulsations in the ULF frequency range ( $.05 < f < 10$  Hz). Data is collected by three orthogonally mounted coils at a remote land site and telemetered to the laboratory for computer analysis.

To isolate data containing a micropulsation event, time series plots of the magnetic field were generated. The development of a double running average routine made possible the isolation of micropulsations in large data sets. A type PC-3 micropulsation was found and the coherence, ellipticity and polarization properties were determined as follows: Coherence = 0.99, Degree of Polarization = 0.99 and the micropulsation was elliptically polarized.

Power spectral density (PSD) plots summarizing data segments about two hours long occasionally contained structures found to be artificial and not representative of natural phenomena in the geomagnetic field. Methods to avoid this anomalous behavior in PSD plots are suggested.



# TABLE OF CONTENTS

I.	INTRODUCTION -----	8
II.	BACKGROUND -----	10
	A. COLLECTION SYSTEM -----	10
	1. System Calibration -----	11
	B. PREVIOUS SOFTWARE -----	13
	C. ANALYSIS OF INITIAL DATA PLOTS -----	17
III.	TIME SERIES DATA -----	59
	A. TIME SERIES VOLTAGE DATA -----	59
	1. Voltage Software -----	59
	2. Time Series Voltage Data Analysis -----	61
	B. TIME SERIES MAGNETIC FIELD DATA -----	69
	1. Magnetic Field Software -----	69
	2. Smoothed Magnetic Field Data Analysis -----	79
IV.	SYSTEM AND SOFTWARE VALIDATION -----	88
	A. EXPERIMENTAL APPARATUS -----	88
	B. EXPERIMENT RESULTS -----	90
	1. Voltage -----	90
	2. Magnetic Field -----	97
V.	MICROPULSATIONS -----	110
	A. THEORY -----	110
	B. MICROPULSATION DATA ANALYSIS -----	112
VI.	CONCLUSIONS -----	118
	APPENDIX A: VOLTR COMPUTER PROGRAM -----	120
	APPENDIX B: VOLTS COMPUTER PROGRAM -----	126



APPENDIX C: LFVTC1 COMPUTER PROGRAM -----	131
LIST OF REFERENCES -----	139
INITIAL DISTRIBUTION LIST -----	140





## ACKNOWLEDGEMENTS

Special thanks to my wife Kathy, without whom I might still be doing figures. Also, thanks to my advisor, Professor Andrew Ochadlick for his patience and advice. And thanks to the Naval Air Development Center for the loan of a fluxgate magnetometer.



## I. INTRODUCTION

This thesis is part of an ongoing effort at the Naval Postgraduate School to analyze ULF geomagnetic noise and micropulsations. The results of the Naval Postgraduate School studies could impact communications systems or systems in which geomagnetic noise and/or micropulsations introduce operational difficulties.

An objective of this thesis was to develop the software necessary for obtaining computer generated plots of geomagnetic field versus time. Then, with the plots, sections of data containing obvious geomagnetic micropulsations were located. Those sections were analyzed to determine the power spectral density (PSD), coherence, degree of polarization and ellipticity of the micropulsation using already developed software [Ref. 1].

After analyzing some of the plots (PSD, coherence, etc.) produced by the software documented in [Ref. 1], it was demonstrated that problems existed in the software. New software was developed to obtain times series raw voltage and geomagnetic field plots. Validation of the software required an on-site experiment. Documented within this thesis is the software to produce time series voltage and geomagnetic field plots and the questions the validation experiment raised concerning the sensing system and software.



Using the newly developed software, a micropulsation event was located. A double running average software routine accentuated the micropulsation to permit the determination of its frequency and amplitude. The micropulsation event was further analyzed to obtain information on coherence, degree of polarization and ellipticity.



## II. BACKGROUND

### A. COLLECTION SYSTEM

The Naval Postgraduate School has two operating geomagnetic sensing systems. The land site is located at the La Mesa Village Housing Area and has three orthogonally mounted induction coils. The second operating system contains two orthogonally mounted induction coils that can be placed on the bottom of Monterey Bay. When both systems are operating, the data is collected simultaneously. The ground work has been laid for a third system located at Chew's Ridge. Three orthogonal and simultaneous measurements can be taken only between two sites since the School has only five induction coils and a sixth just calibrated. This thesis used data from the La Mesa Village site and the software associated with it.

An induction coil senses the geomagnetic field fluctuations based on Faraday's Law of induction, induced emf  $= -N \frac{d\Phi}{dt}$ , which describes the relation between the induced emf and the time rate of change of magnetic flux through the coil.  $N$  is the number of turns in the coil.

The voltage induced in the coils is sampled 32 or 64 times/second and is amplified approximately one million times. The voltage data undergoes pulse-code-modulation (PCM) for noiseless VHF radio link transmission from the La Mesa Village site, to the recording system in the Geophysics Signal





Processing Laboratory located in Spanagel 531. Data reduction on the Naval Postgraduate School's IBM 3033 computer follows digitization of the PCM data. A block diagram of the system is provided in Figure 2.1. A more detailed description of the system is given in Reference 2.

### 1. System Calibration

For purposes of documentation, the calibration of the third coil for either the Chew's Ridge or Monterey Bay system is being included in this thesis. The general method of induction coil calibration will be covered here. For a more indepth explanation, see Reference 1.

The sensing coil and its associated electronics are calibrated using a Helmholtz coil apparatus to establish a uniform magnetic field. By placing the sensing coil into the field produced by the Helmholtz coil, one can establish a relationship between the Helmholtz coil magnetic field magnitude and frequency and the coil system voltage. Once the response of the coil system is known for the frequency band of interest, it can be included in the system transfer function used in data reduction.

The experiment to determine the sixth coil system transfer function was done at the La Mesa Village site. A Wavetek Model 142 signal generator supplied a sinusoidal current to a 1.22 meter diameter, 0.61 meter high Helmholtz coil. The current was measured across a 996 ohm resistor in series with the Helmholtz coil. A Hewlett Packard HP-3582A spectrum



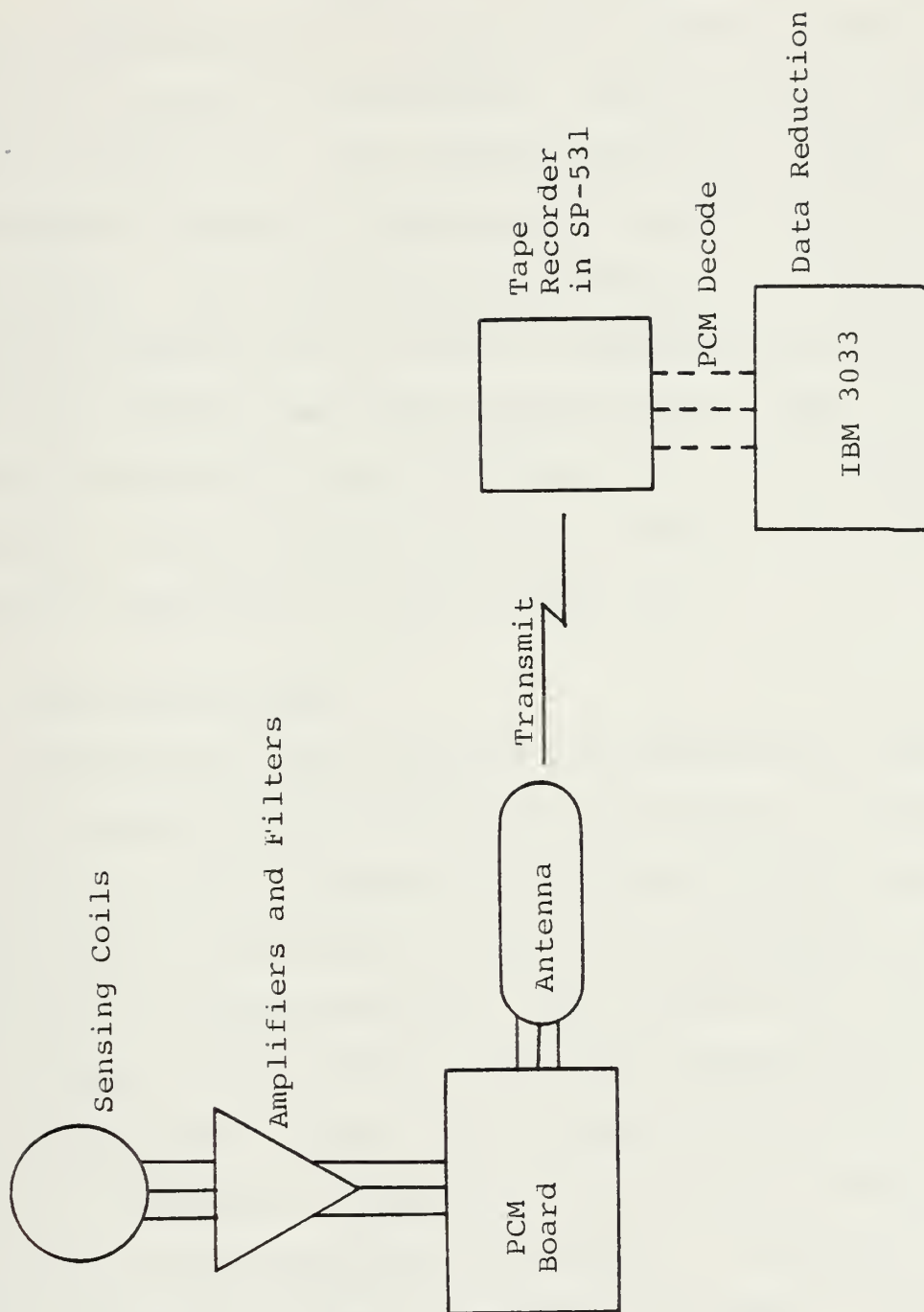


Figure 2.1. System Data Flow



analyzer measured the output voltage of the coil system as a function of frequency.

The experiment measured the response of the coil system in the frequency band .05 hertz to 20 hertz for applied fields of 0.02, 0.2 and 1.0 nanoteslas. The coil system response is shown in Figure 2.2. The transfer function of this coil system corresponds closely to those of coil systems previously calibrated. The only noticable difference is that the 0.02 nanotesla response at 15 hertz is approximately 15 volts/nanotesla higher than those measured before [Ref. 1]. It should be noted that this difference will not influence data analysis in the frequency range of interest. The transfer function algorithm is listed in Table 2.1.

#### B. PREVIOUS SOFTWARE

Software has been developed (see References 1 and 3), to extract power spectral densities for each coil, coherence between the coils, degree of polarization in the three measurement planes, ellipticity in the three measurement planes and a variety of Stokes parameters. The following is a basic description of the computer code that produces the above mentioned plots. First, the voltage data is read off the digital tape using a subroutine called RD provided by Dr. Tim Stanton of the Oceanography Department. A parameter ISEC, representing the number of seconds one wishes to advance the tape, is frequently used. ISEC establishes the number of



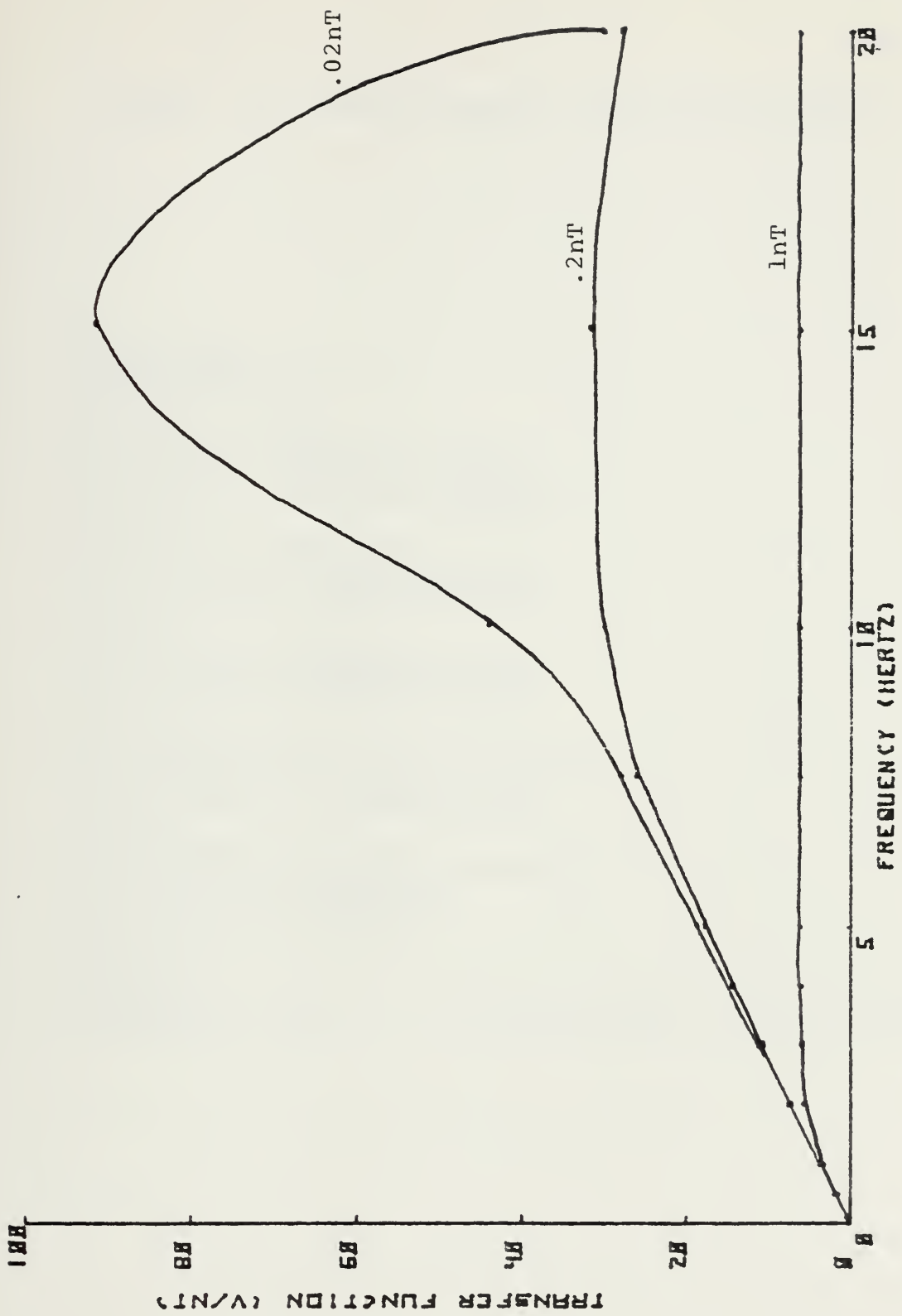


Figure 2.2. Coil Transfer Function





Table 2.1. System Transfer Function Algorithm

```

DC 9 L=1,N
FRQ=FREQ(L)
IF(FRQ.LE.25.)GO TO 1
XX(L)=XX(L)/28.
GC TO 8
1 IF(FRQ.LE.15.)GO TO 2
XX(L)=XX(L)/(105.5-3.14*FRQ)
YY(L)=YY(L)/(181.32-7.588*FRQ)
ZZ(L)=ZZ(L)/(177.26-7.484*FRQ)
GC TO 8
2 IF(FRQ.LE.10.)GO TO 3
XX(L)=XX(L)/(5.958*FRQ-30.97)
YY(L)=YY(L)/(7.166*FRQ-39.99)
ZZ(L)=ZZ(L)/(6.49*FRQ-32.35)
GC TO 8
3 IF(FRQ.LE.7.5)GO TO 4
XX(L)=XX(L)/(3.492*FRQ-6.31)
YY(L)=YY(L)/(4.252*FRQ-10.85)
ZZ(L)=ZZ(L)/(4.044*FRQ-7.69)
GC TO 3
4 IF(FRQ.LE.5.)GO TO 5
XX(L)=XX(L)/(2.6311*FRQ+0.14667)
YY(L)=YY(L)/(3.012*FRQ-1.55)
ZZ(L)=ZZ(L)/(3.184*FRQ-1.44)
GC TO 8
5 IF(FRQ.LE.3.)GO TO 6
XX(L)=XX(L)/(2.6311*FRQ+0.14667)
7 YY(L)=YY(L)/(2.702*FRQ)
ZZ(L)=ZZ(L)/(2.92*FRQ)
GC TO 8
6 XX(L)=XX(L)/(2.72*FRQ)
GC TO 7
8 CONTINUE
TF(L)=(XX(L)*COSD + YY(L)*CUSD1)*COS00 + ZZ(L)*COS30
9 CONTINUE

```



times RD is called and the data not stored. Previously, tape advances of approximately 30 seconds or ISEC = 30 were used. Once the tape is advanced the desired amount, data analysis can begin. Each digital tape contains about 90 minutes or  $1.728 \times 10^5$  pieces of data per axis resulting from the sampling rate of 32 samples/second. Because of the large amount of data, the analysis has to be accomplished in blocks. Data analysis takes place on 256 seconds or 8192 frames of data at a time. RD is called 8192 times and places the voltages for each coil in an array. The voltages are integer values from 0 to 4096 representing -5 volts to +5 volts. Ideally the value 2048 represents 0 volts. The integers between 0-4096 are normalized to  $\pm 5$  volts and placed in new complex arrays. These arrays containing 8192 pieces of data are Fourier transformed to the frequency domain where the system transfer function is applied. After applying the transfer function, the calculations begin for a determination of PSD's, coherence, ellipticity, etc. for the first block. After they are complete, the next block of 8192 pieces of data starts through the program. Once the desired amount of data has been processed, a NONIMSL subroutine called DRAWP plots the data. For a more complete description of this software, see Reference 1, Reference 3 and Reference 4.



### C. ANALYSIS OF INITIAL DATA PLOTS

Many of the PSD's, coherences, ellipticities and degree of polarization plots produced by the software of Reference 1 and Reference 3 have unexpected characteristics. The PSD's show "humps" that are shown in Figures 2.3-2.5. These "humps" are not characteristic in "normal" PSD's. The coherence plots show a coherence of essentially one degrading to hash in the frequencies greater than 2 hertz, Figures 2.6-2.8. We see a similar behavior in the plots of degree of polarization. These plots indicate a very highly polarized field from 0.02 hertz to 1.0 hertz. Figures 2.9-2.11. The ellipticity plots show a very linearly polarized field for these frequencies in Figures 2.12-2.14.

After examining the time series magnetic field plots, we noted a section of very large magnitude fluctuations (about one to three orders of magnitude greater than the general background) at the beginning of the digital tapes Figures 2.15-2.17. We found that if the digital tape was advanced past these large fluctuations the output (PSD, coherence, etc.) appeared "normal", Figures 2.18-2.29. If the program was executed on just the section containing the large fluctuations, the PSD's had the "humped" characteristic, the coherences were one, the degree of polarization was very high and the ellipticity was linear, Figures 2.30-2.41. This demonstrates that these large fluctuations dominate the output of an analysis in the frequency domain. A tape advance of 300 seconds or ISEC = 300 is



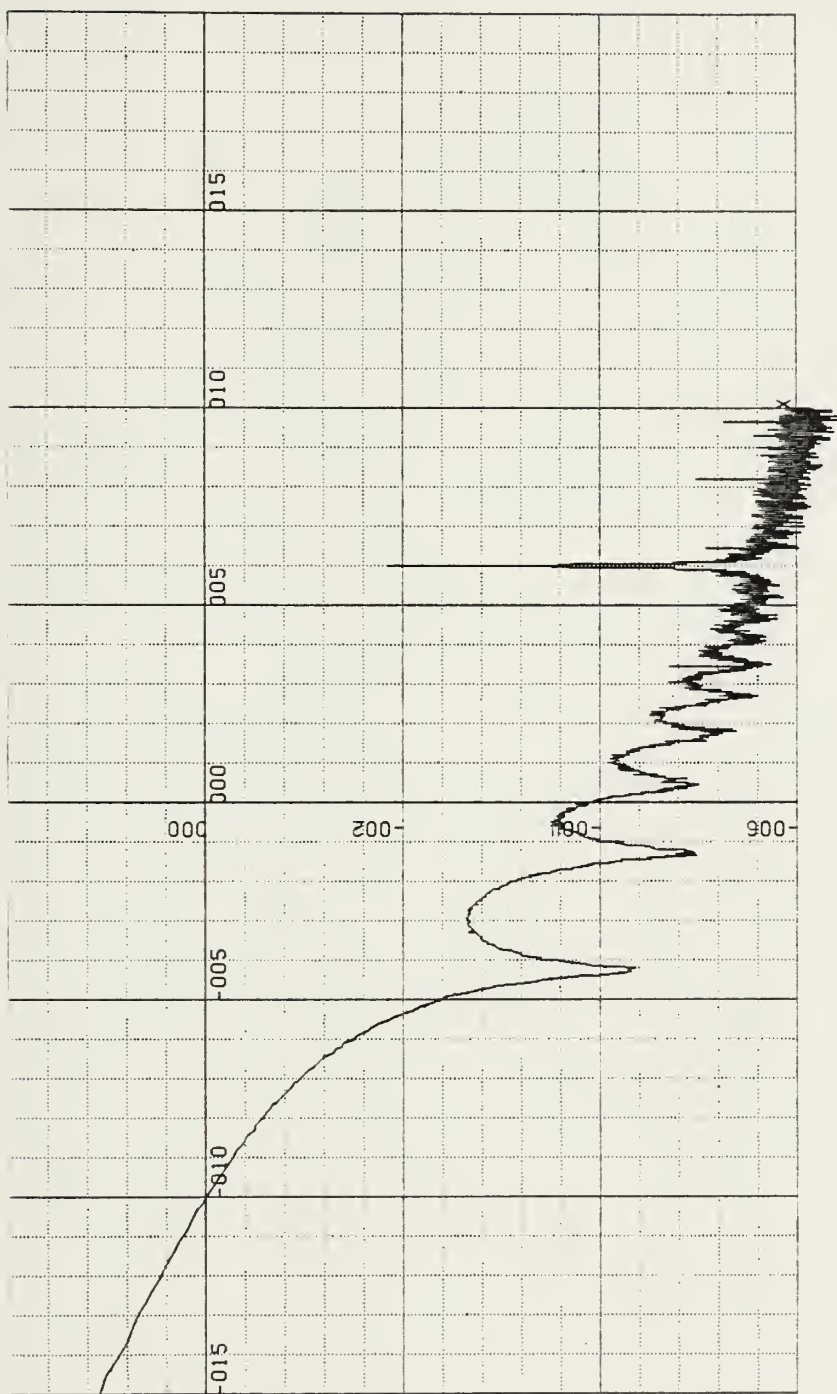


Figure 2.3. PSD X-Coil, 17 August 82, 2240-2348 Local.  
 Amplitude in dB (REF  $nT^{**2}/Hz$ ) (20 units/in) vs. Log  
 Frequency (Hz) (0.5 units/in), 16 Averages





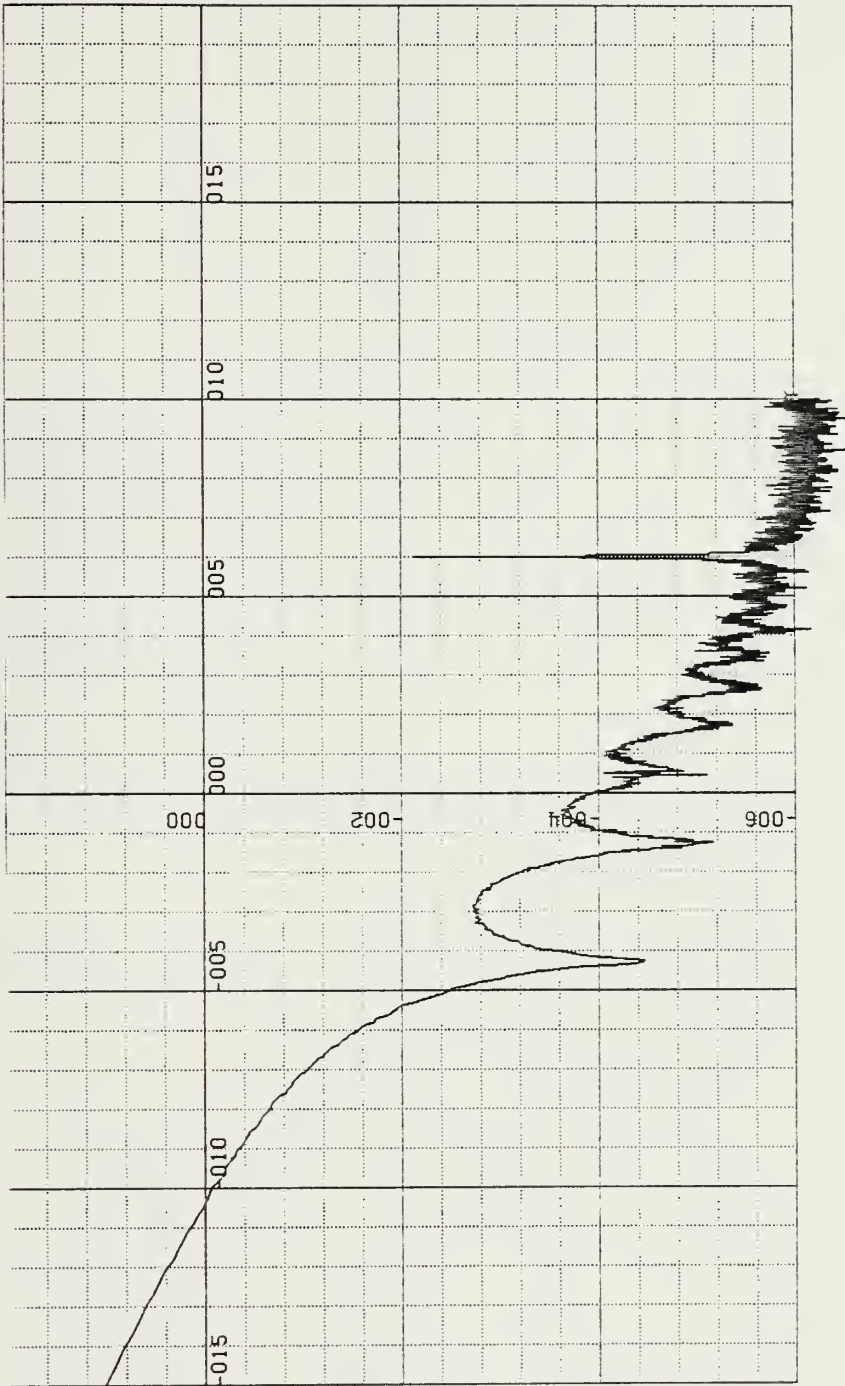


Figure 2.4. PSD Y-Coil, 17 August 82, 2240-2348 Local.  
 Amplitude in dB (REF nT\*\*2/Hz) (20 units/in)  
 vs. Log Frequency (Hz) (0.5 units/in), 16 Averages



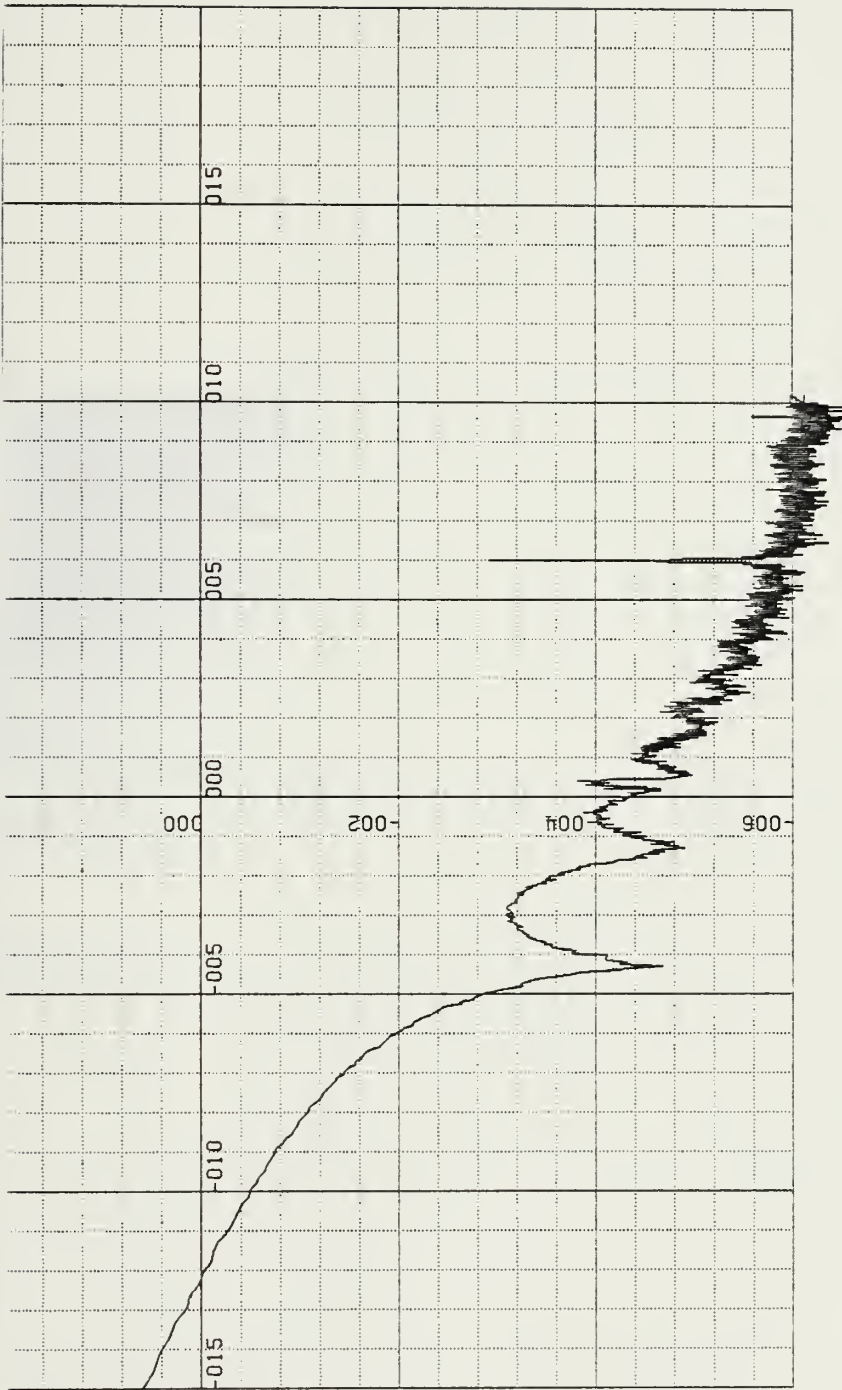


Figure 2.5. PSD Z-Coil, 17 August 82, 2240-2348 Local.  
Amplitude in dB (REF nT\*\*2/Hz) (20 units/in) vs.  
Log Frequency (Hz) (0.5 units/in), 16 Averages



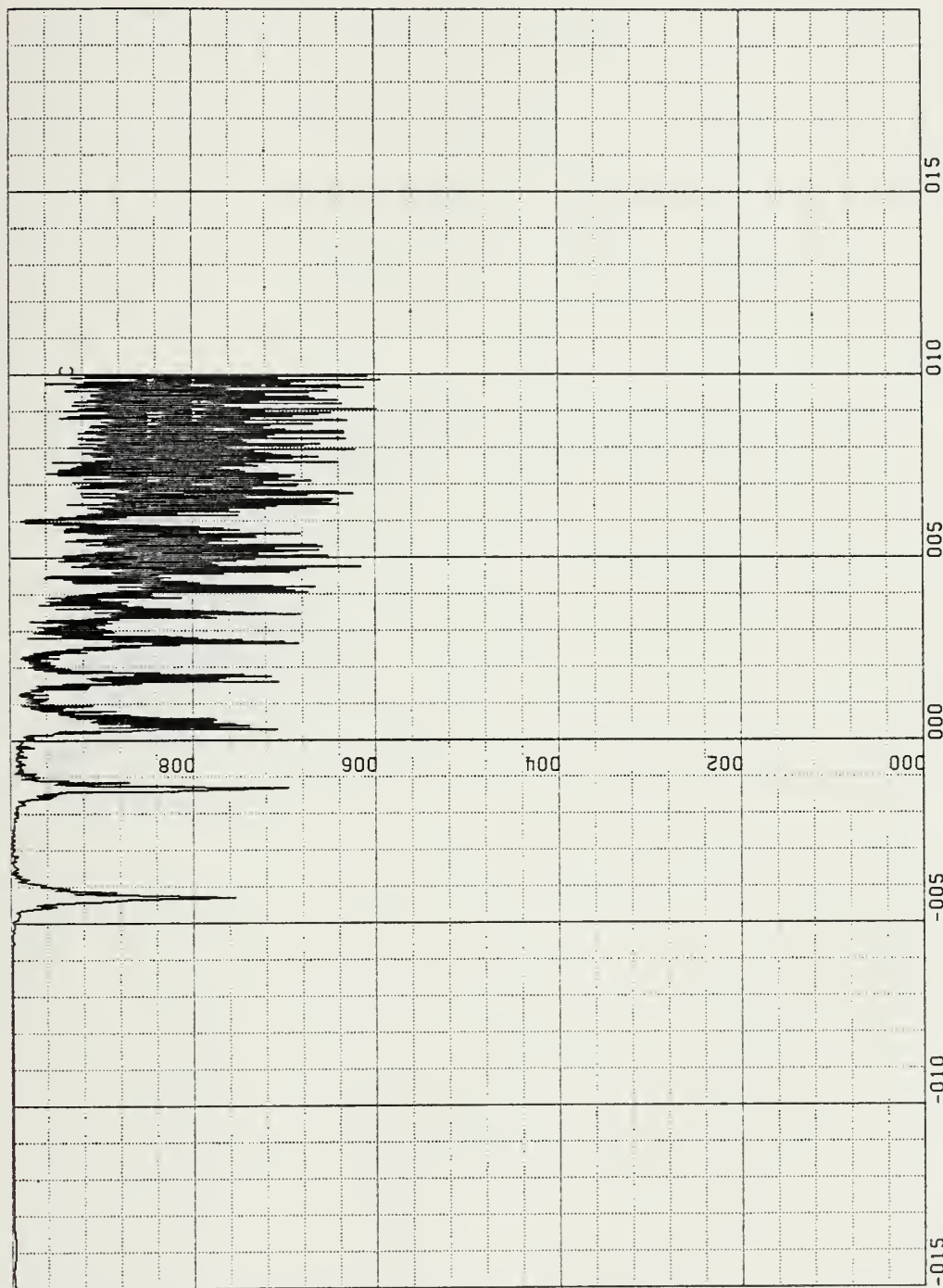


Figure 2.6. Coherence X and Y coils, 17 August 82, 2240-2348 Local.  
Coherence X and Y Coil (0.2 units/in) vs. Log Frequency  
(Hz) (0.5 units/in), 16 Averages



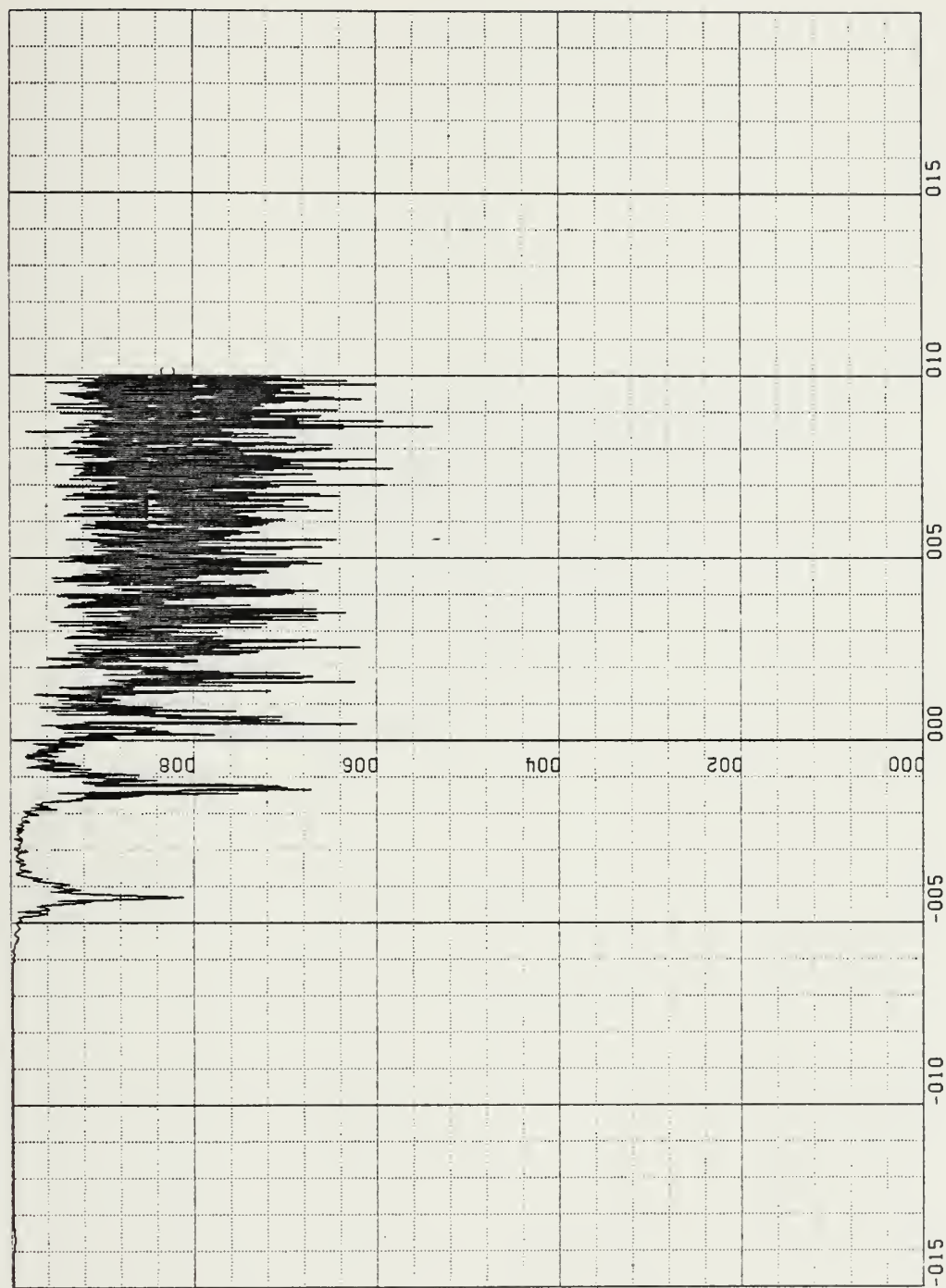


Figure 2.7. Coherence Y and Z Coils, 17 August 82, 2240-2348 Local.  
 Coherence Y and Z Coils (0.2 units/in) vs. Log Frequency  
 (Hz) (0.5 units/in), 16 Averages





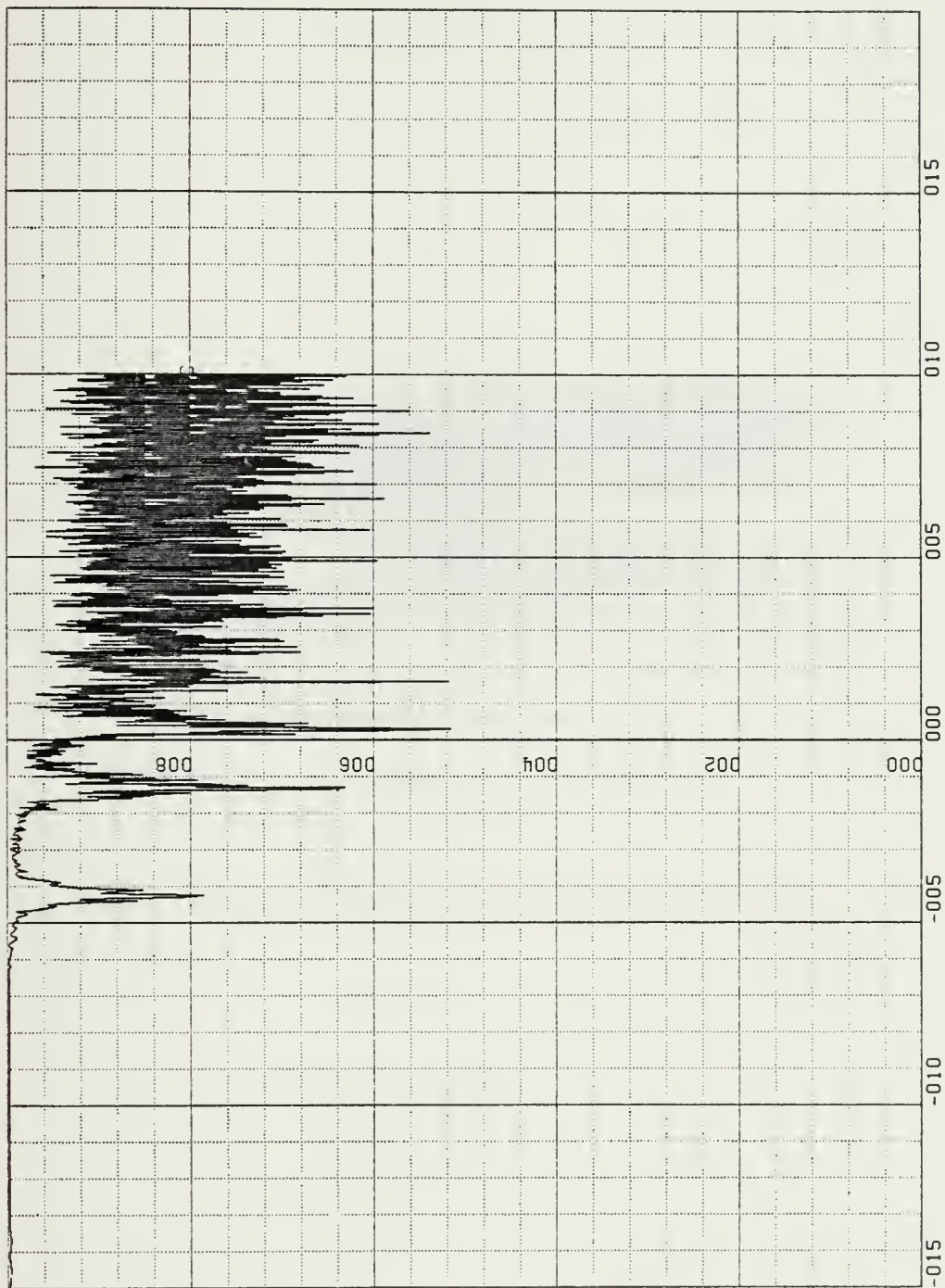


Figure 2.8. Coherence Z and Z Coils, 17 August 82, 2240-2348 Local.  
 Coherence Z and X Coils (0.2 units/in) vs. Log Frequency  
 (Hz) (0.5 units/in), 16 Averages



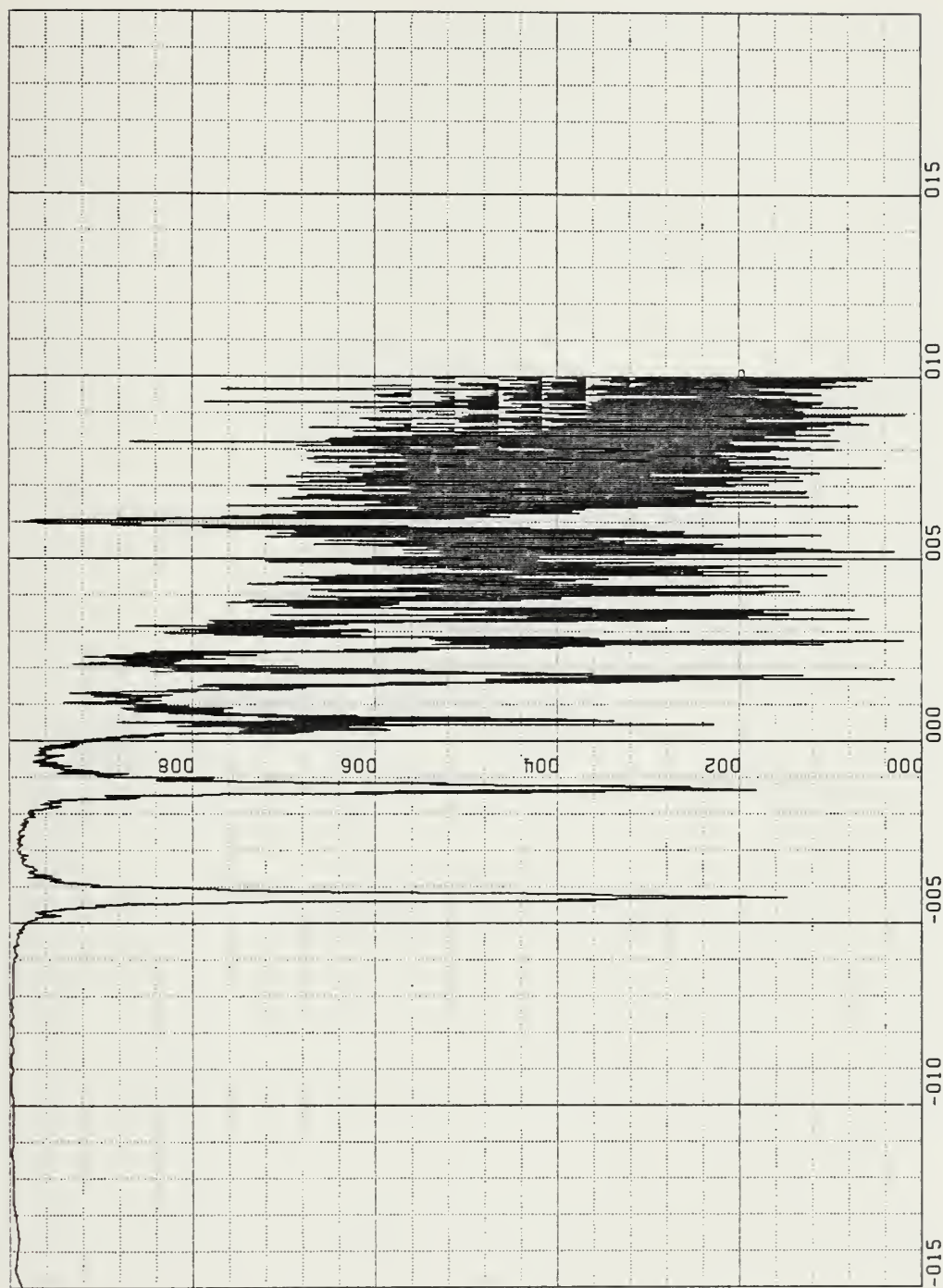


Figure 2.9. Degree of Polarization X-Y Plane, 17 August 82, 2240-2348 Local.  
 Degree of Polarization (0.2 units/in) vs. Log Frequency (Hz)  
 (0.5 units/in), 16 Averages



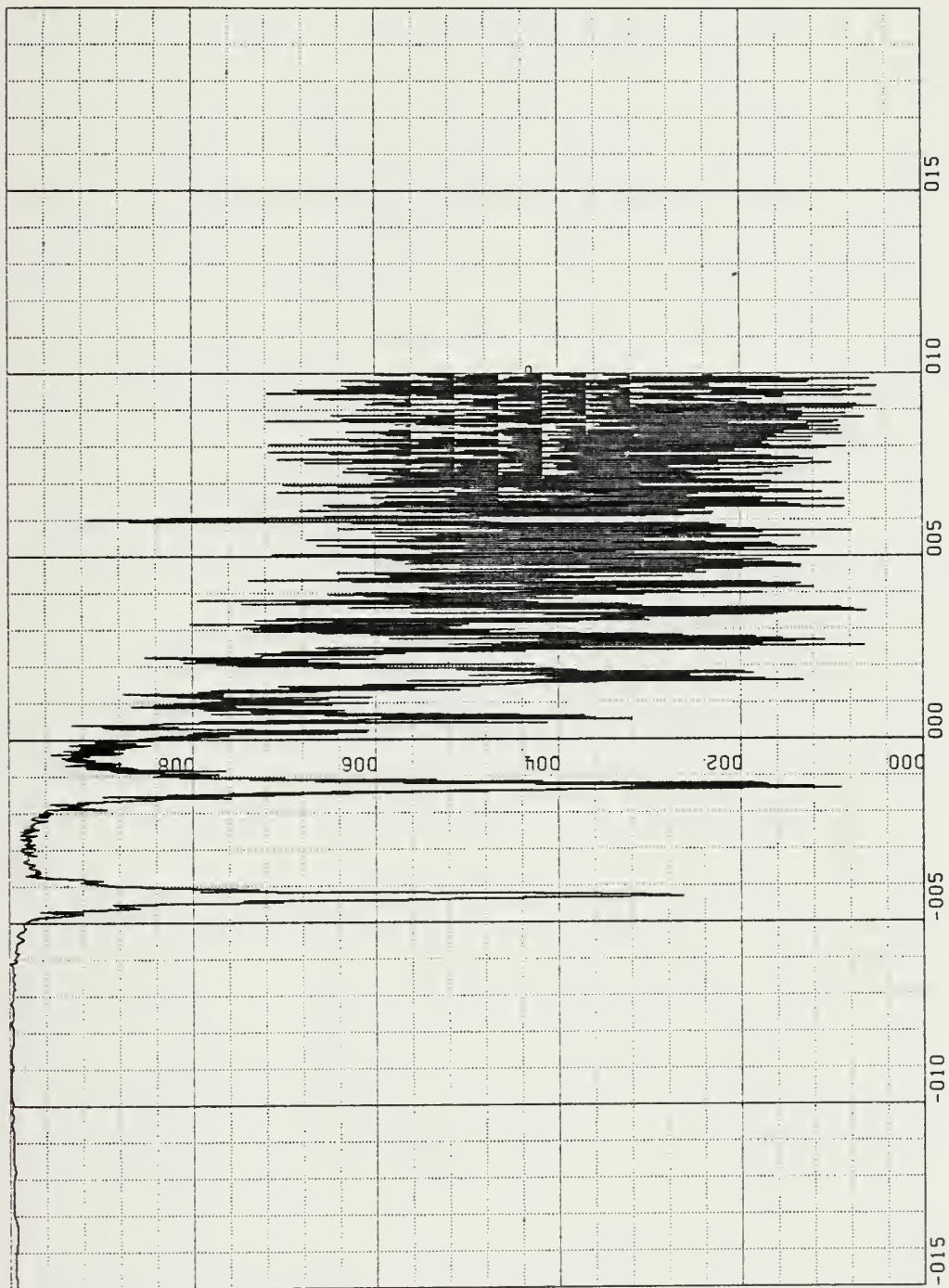


Figure 2.10. Degree of Polarization Y-Z Plane, 17 August 82, 2240-2348 Local.  
Degree of Polarization (0.2 units/in) vs. Log  
Frequency (Hz) (0.5 units/in), 16 Averages





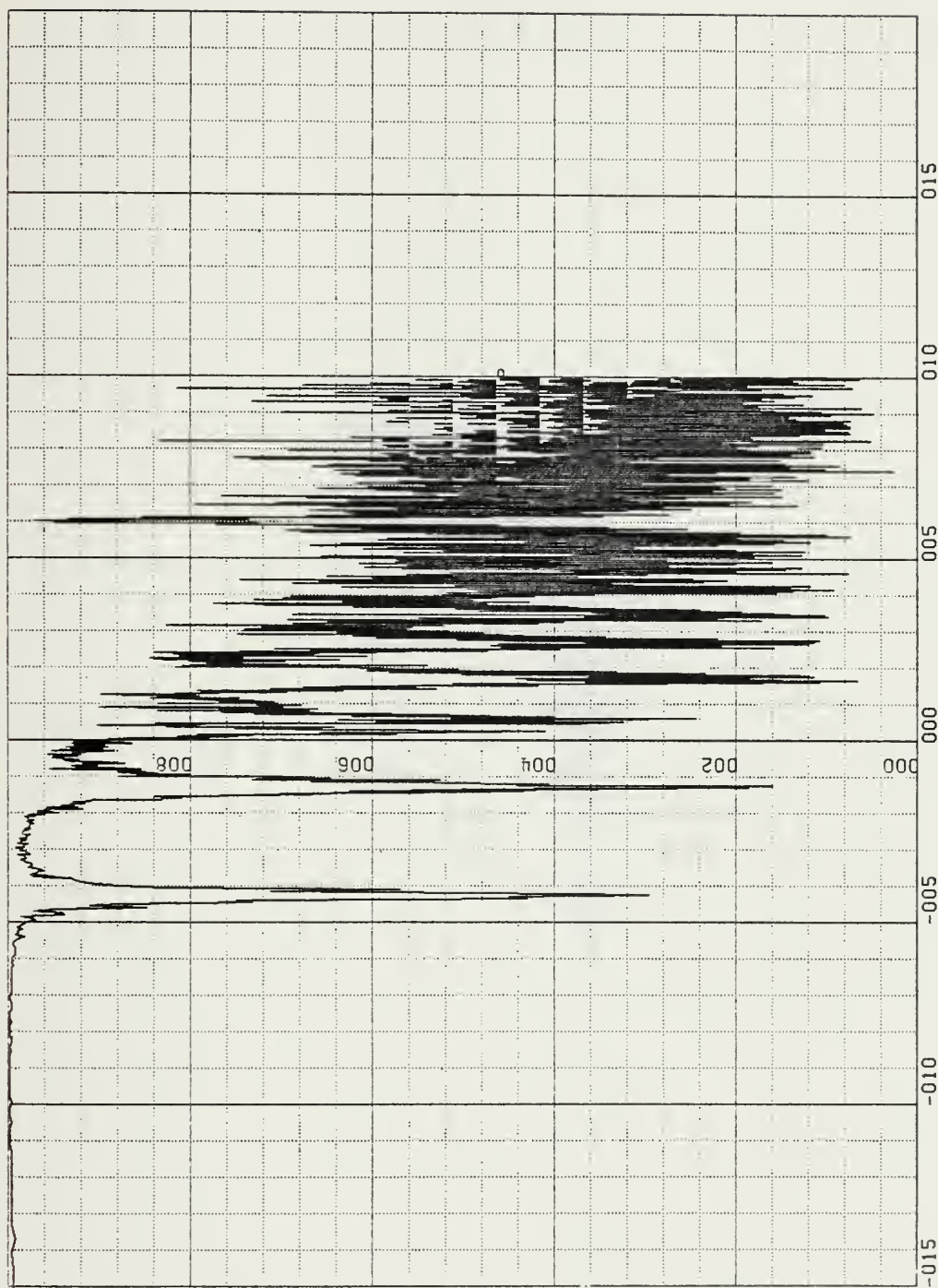


Figure 2.11. Degree of Polarization Z-X Plane, 17 August 82, 2240-2348 Local.  
 Degree of Polarization (0.2 units/in) vs. Log Frequency  
 (Hz) (0.5 units/in) , 16 Averages





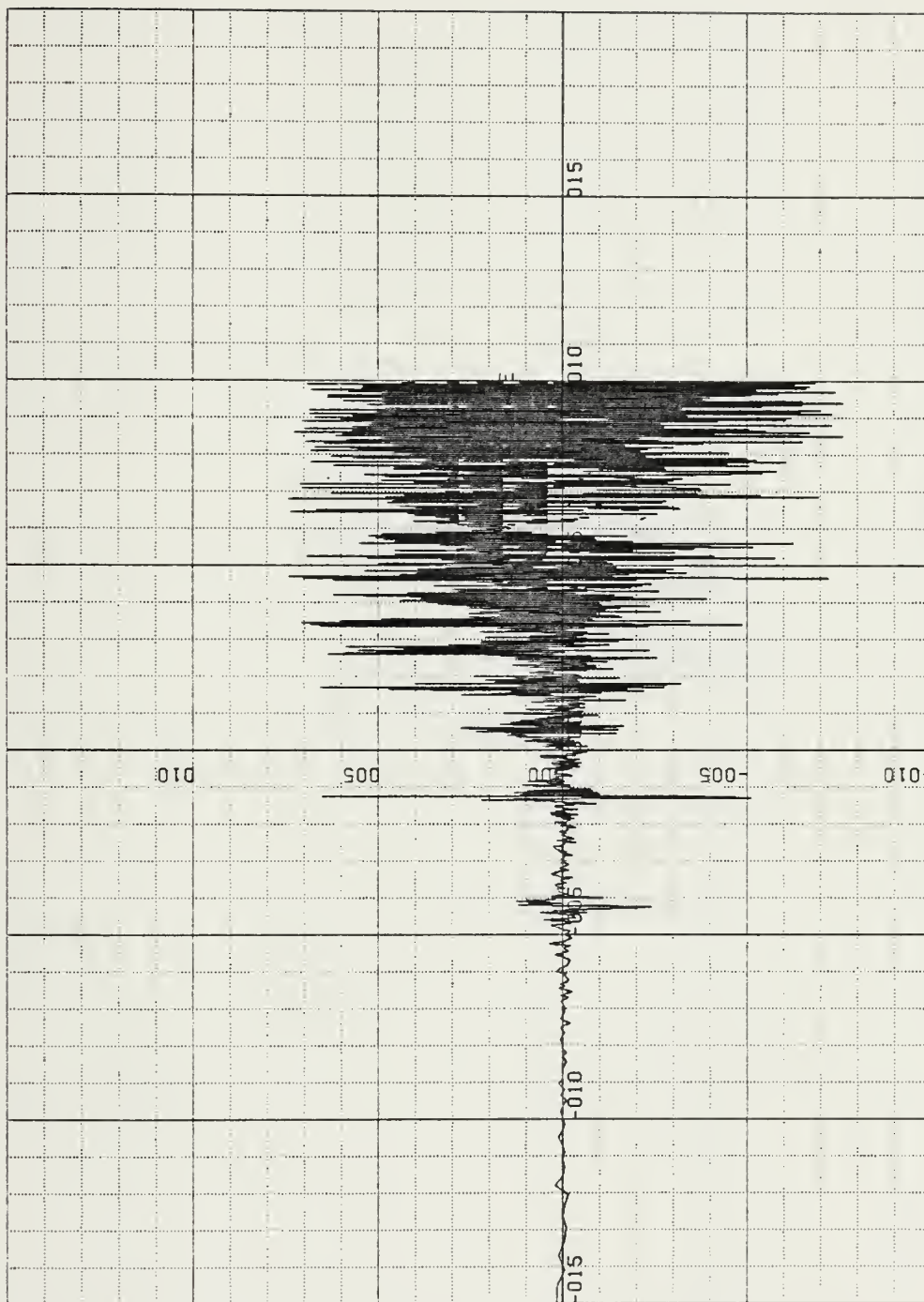


Figure 2.12. Ellipticity X-Y Plane, 17 August 82, 2240-2348 Local.  
 Ellipticity (0.5 unit/in) vs. Log Frequency (Hz) (0.5 unit/in)  
 16 Averages



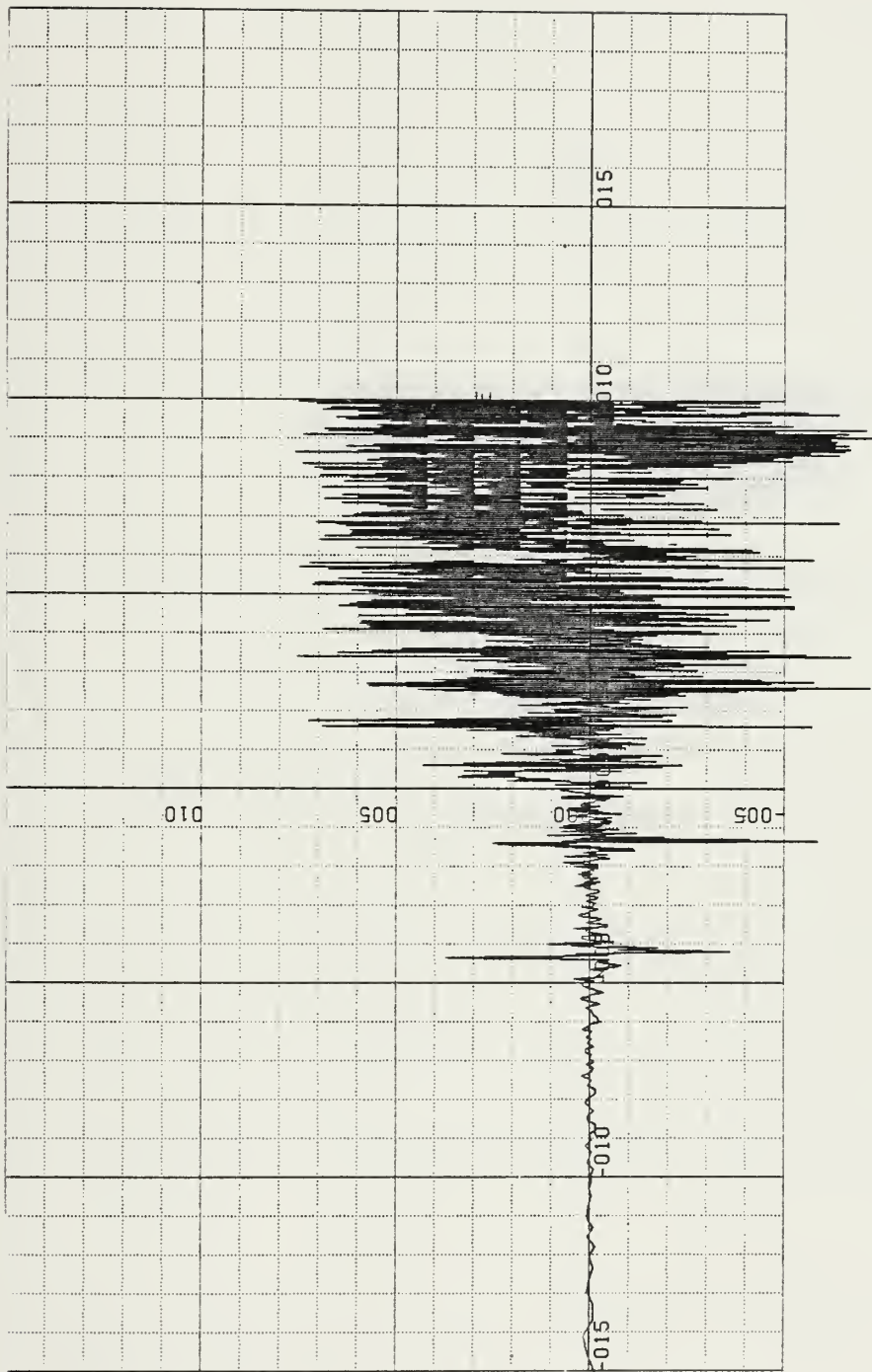


Figure 2.13. Ellipticity Y-Z Plane, 17 August 82, 2240-2348 Local.  
 Ellipticity (0.5 units/in) vs. Log Frequency (Hz) (0.5 units/in)  
 16 Averages



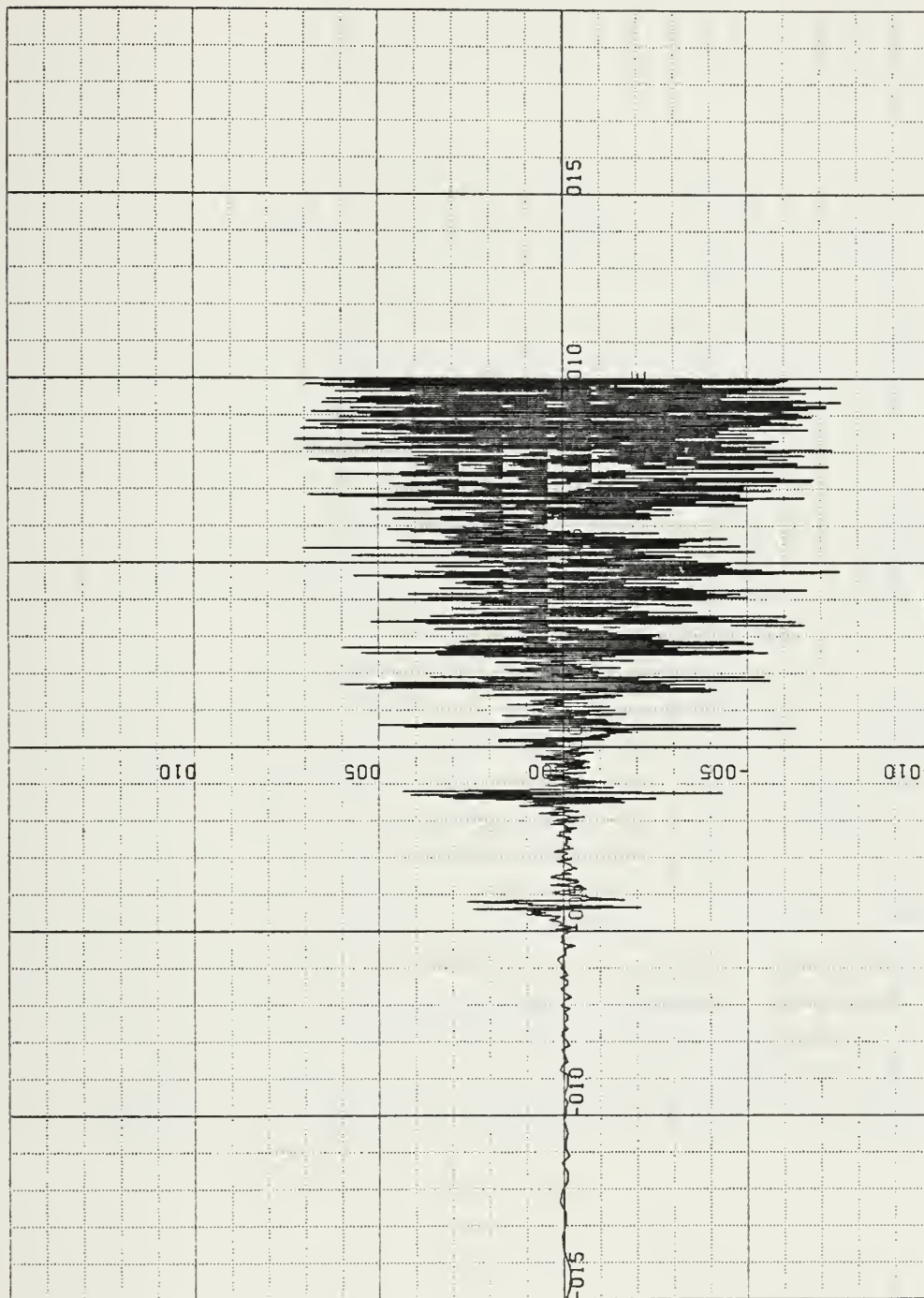


Figure 2.14. Ellipticity Z-X Plane, 17 August 82, 2240-2348 Local.  
 Ellipticity (0.5 units/in) vs. Log Frequency (Hz) (0.5 units/in)  
 16 Averages



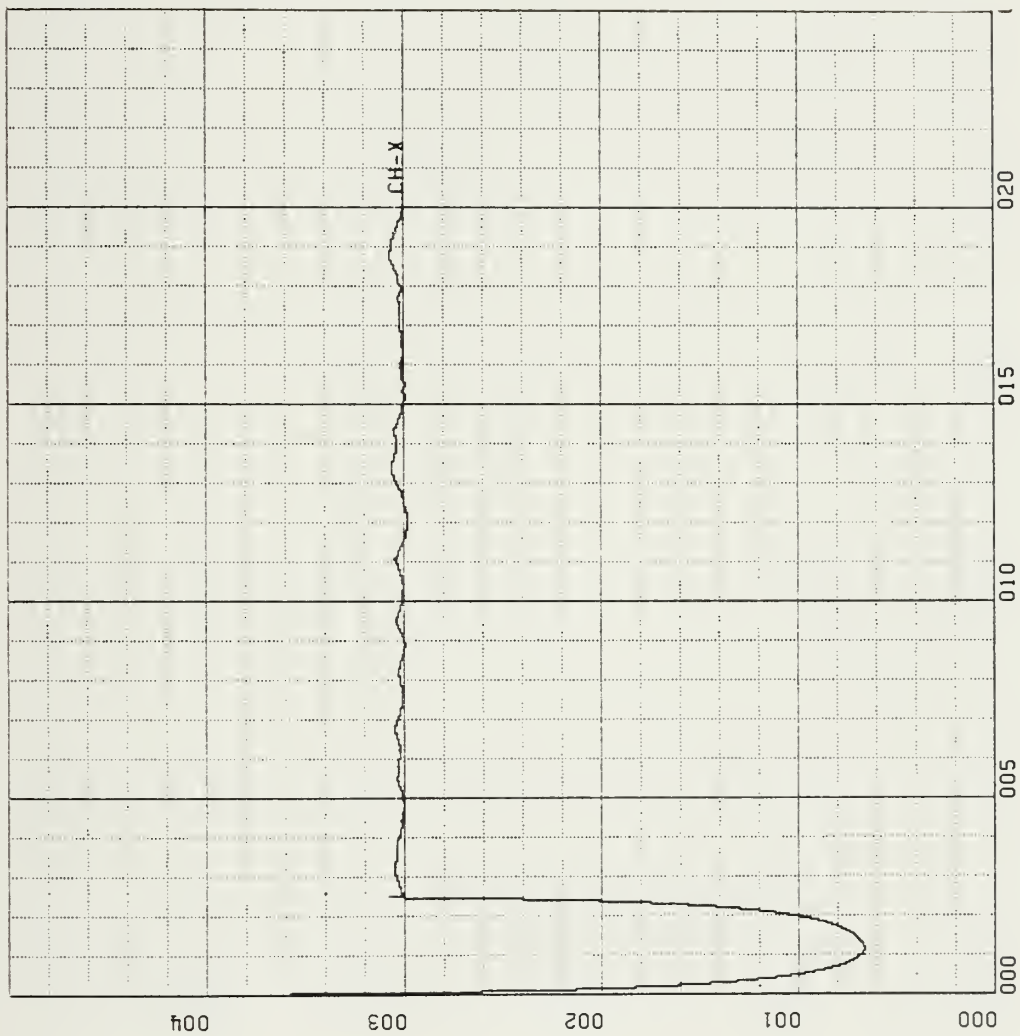


Figure 2.15. X-Coil Magnetic Field, 17 August 82, 2240-2348- Local.  
 Amplitude (nanoteslas : 10 units/in) vs. Time (seconds : 500 units/in)  
 16 Averages





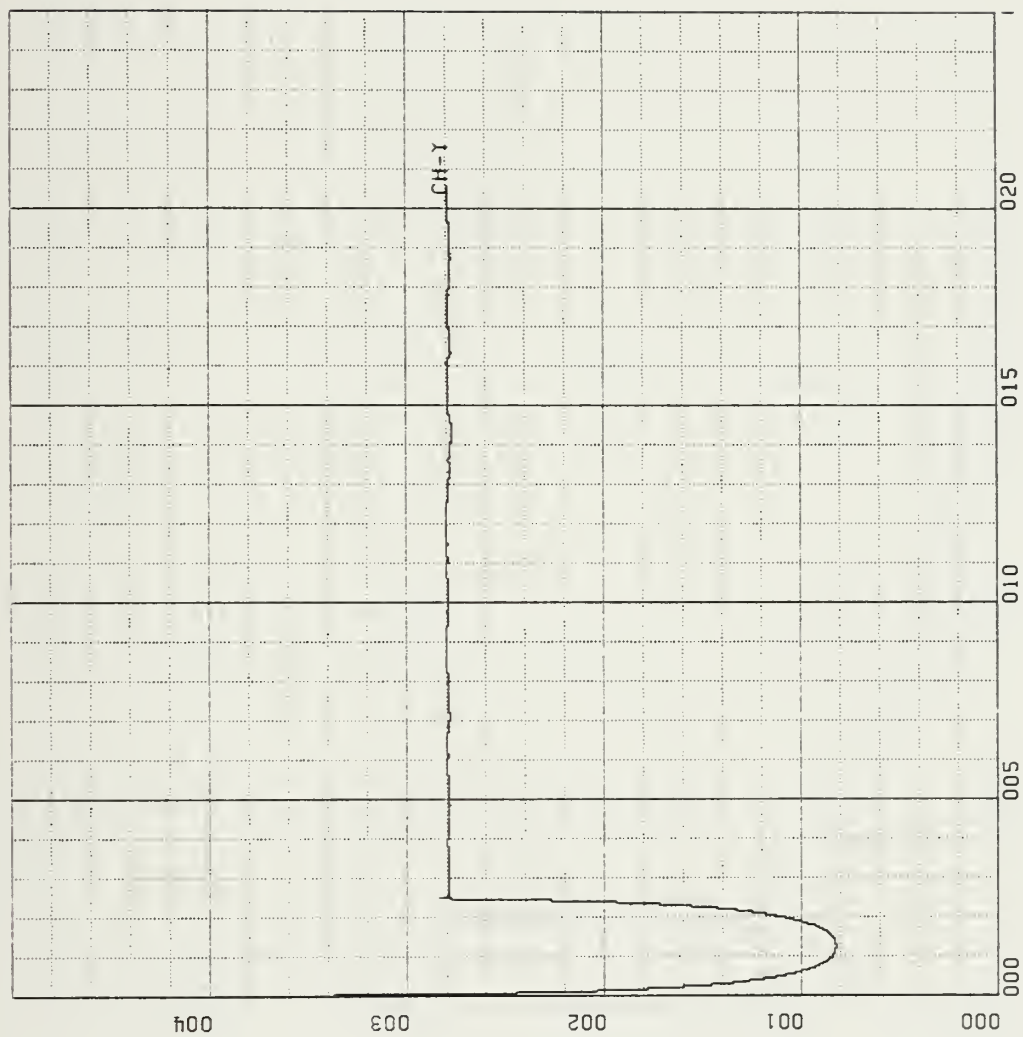


Figure 2.16. Y-Coil Magnetic Field, 17 August 82, 2240-2348 Local.  
 Amplitude (nanoteslas : 10 units/in) vs. Time (seconds : 500 units/in)  
 16 Averages



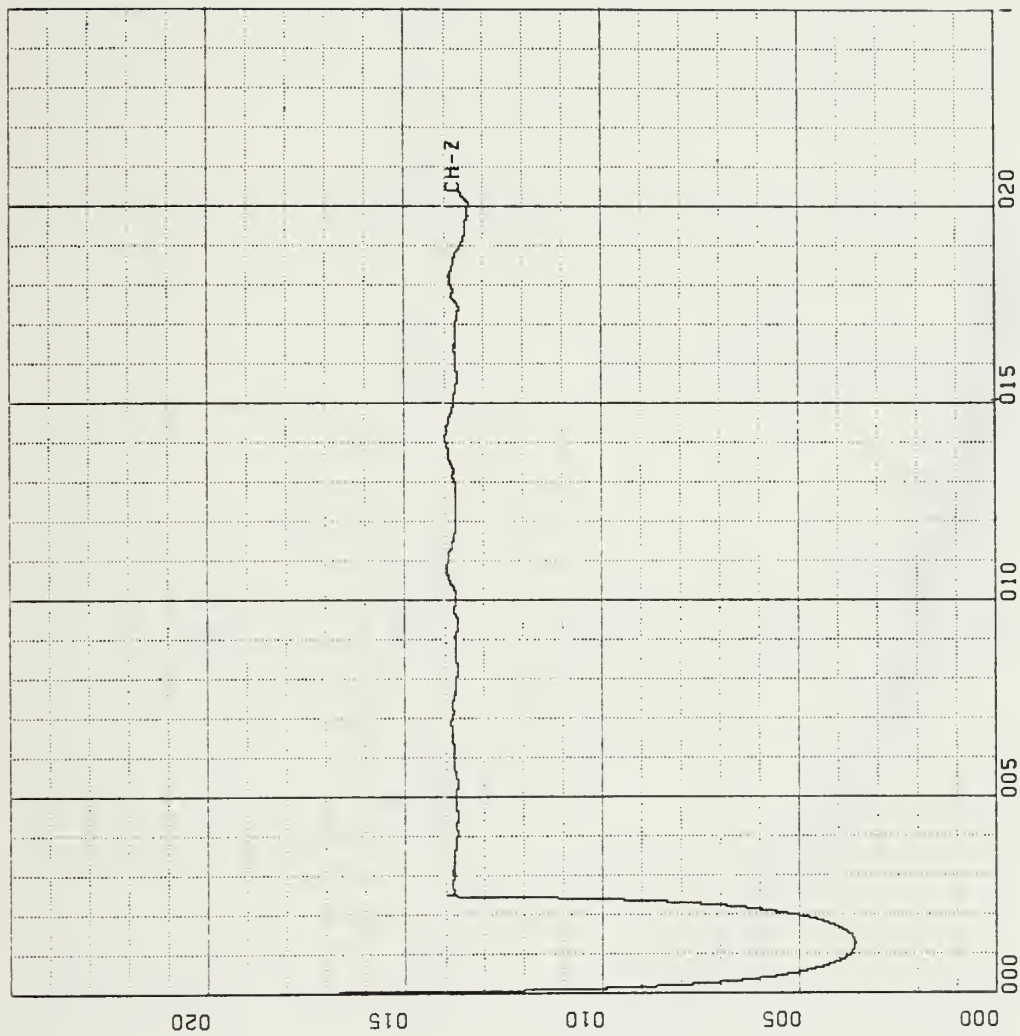


Figure 2.17. Z-Coil Magnetic Field, 17 August 82, 2240-2348 Local.  
 Amplitude (nanoteslas : 5 units/in) vs. Time (seconds : 500 units/in)  
 16 Averages



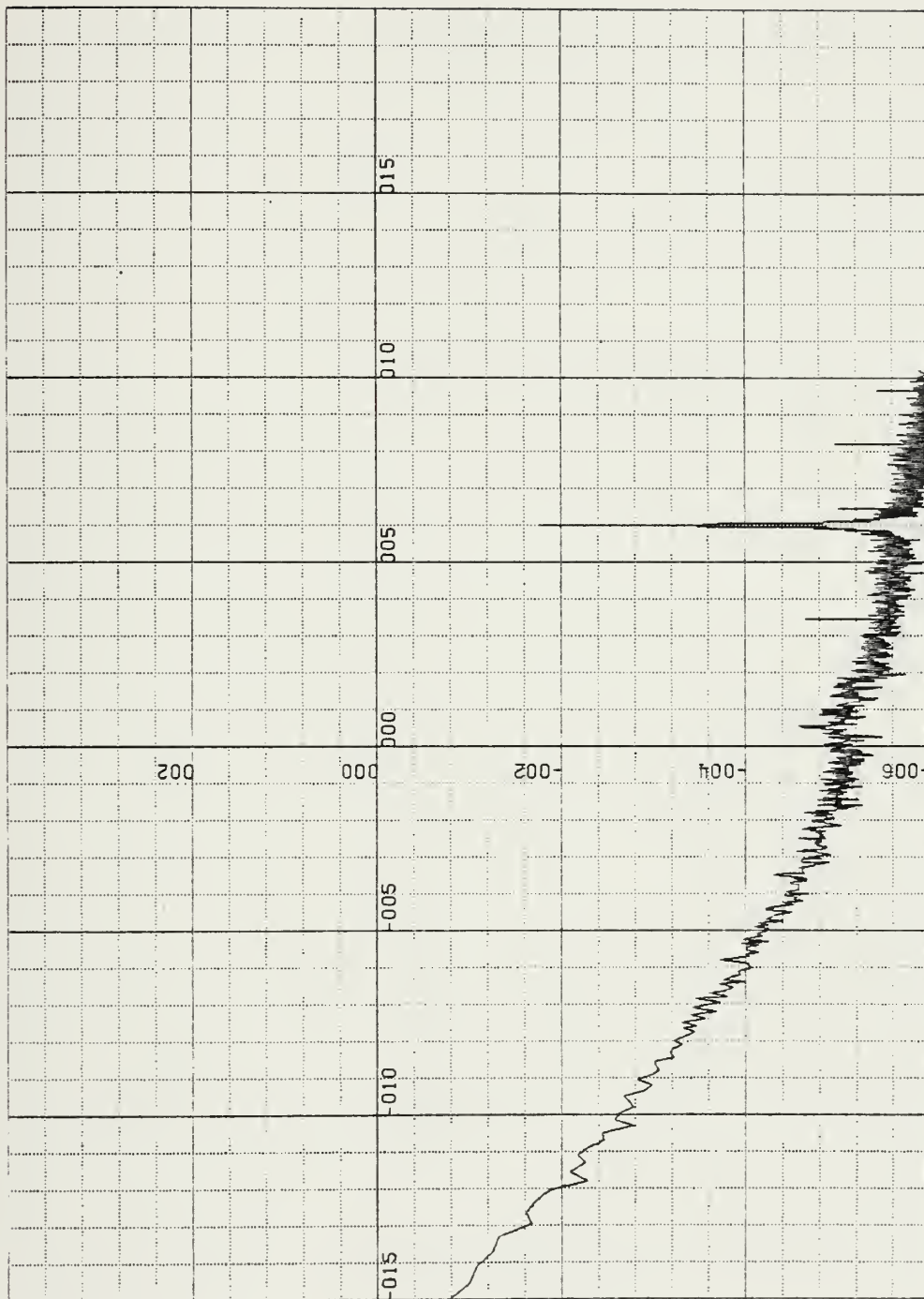


Figure 2.18. PSD X Coil, 17 August 82, 2245-2353 Local.  
 Amplitude in dB (REF nT\*\*2/Hz) (20 units/in) vs. Log  
 Frequency (Hz) (0.5 units/in), 16 Averages



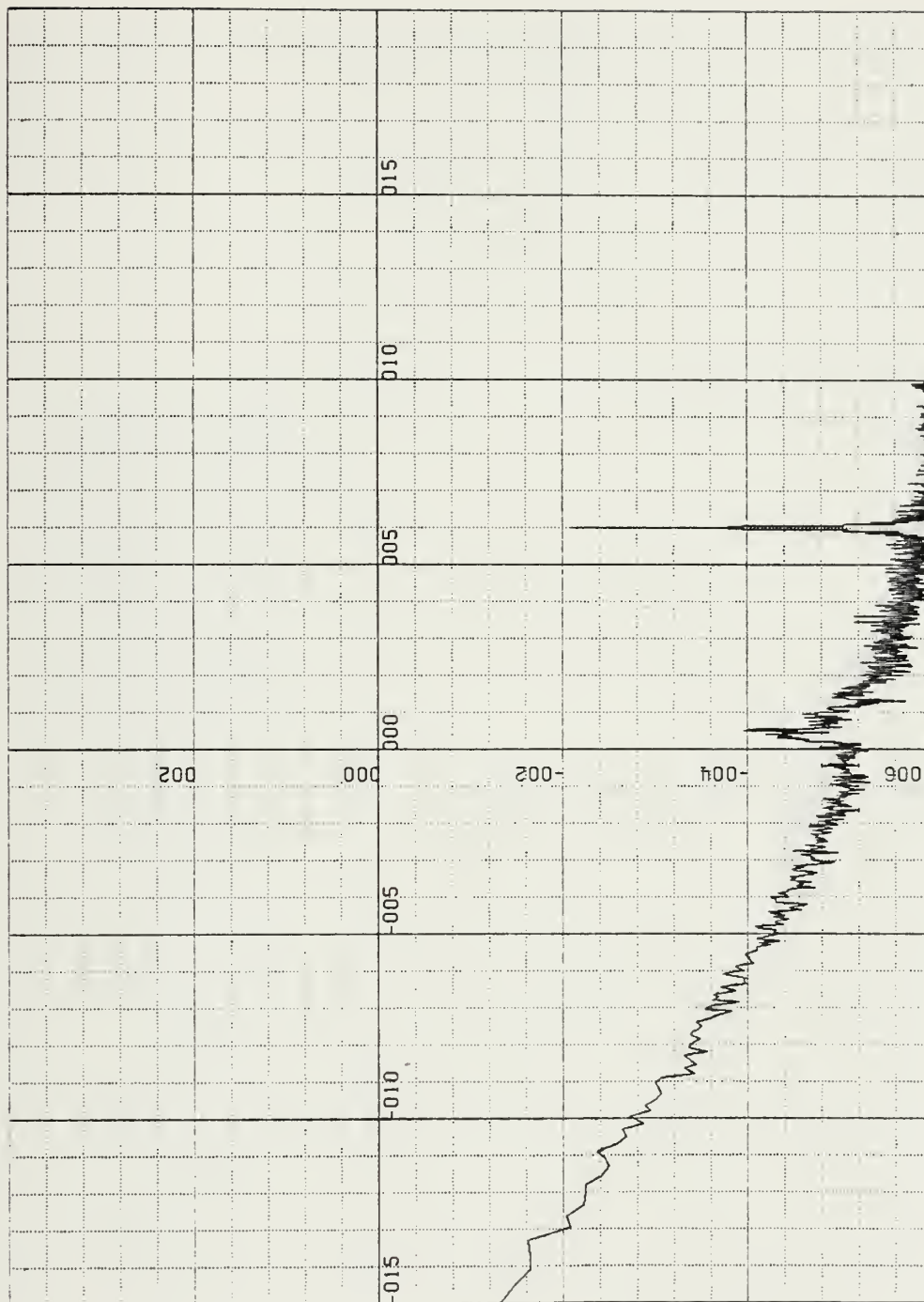


Figure 2.19. PSD Y Coil, 17 August 82, 2245-2353 Local.  
 Amplitude in dB (REF  $nT^{**}2/Hz$ ) (20 units/in) vs. Log  
 Frequency (Hz) (0.5 units/in), 16 Averages





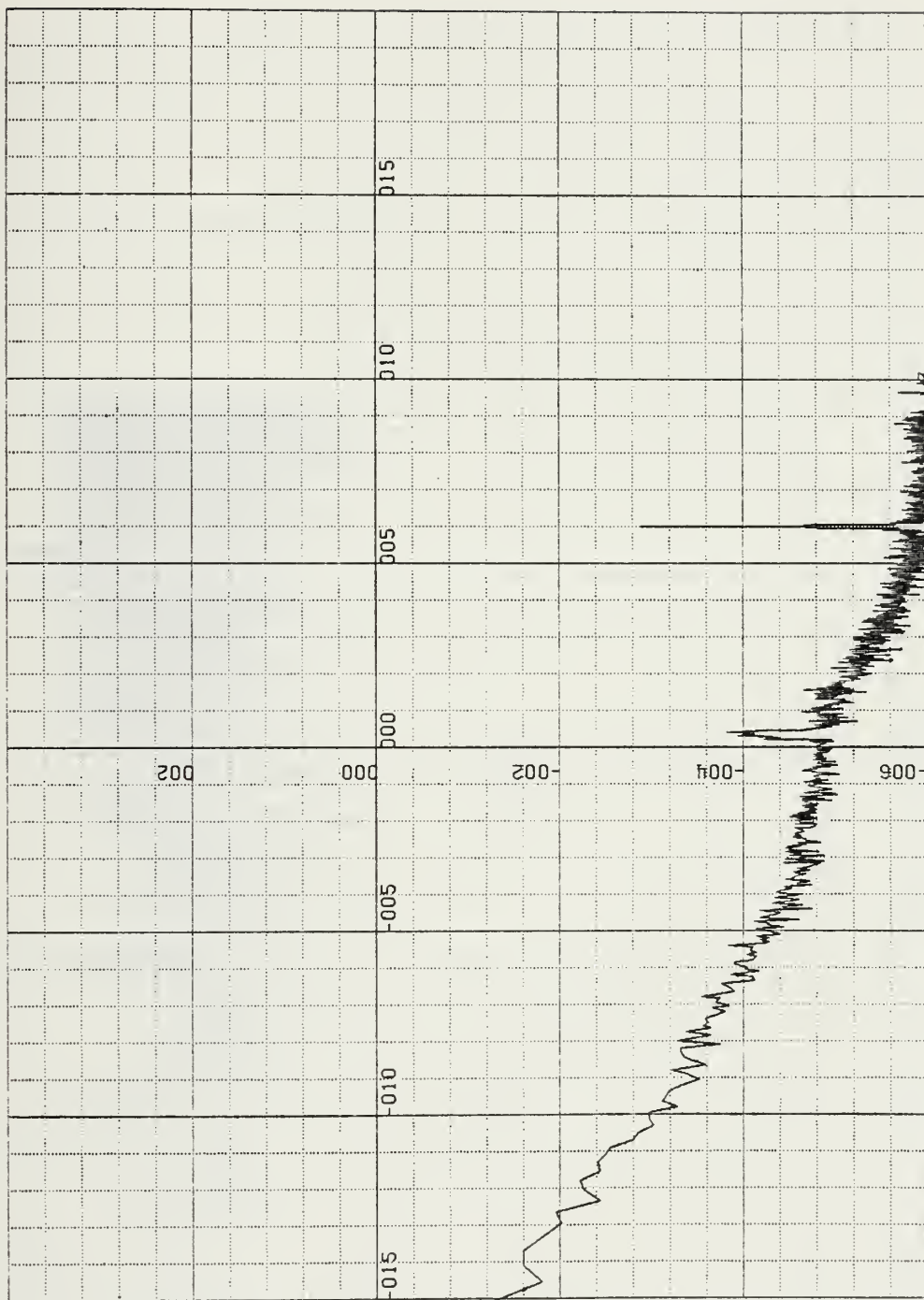


Figure 2.20. PSD Z Coil, 17 August 82, 2245-2353 Local.  
 Amplitude in dB (REF  $nT^{**}2/Hz$ ) (20 units/in) vs. Log  
 Frequency (Hz) (0.5 units/in), 16 Averages



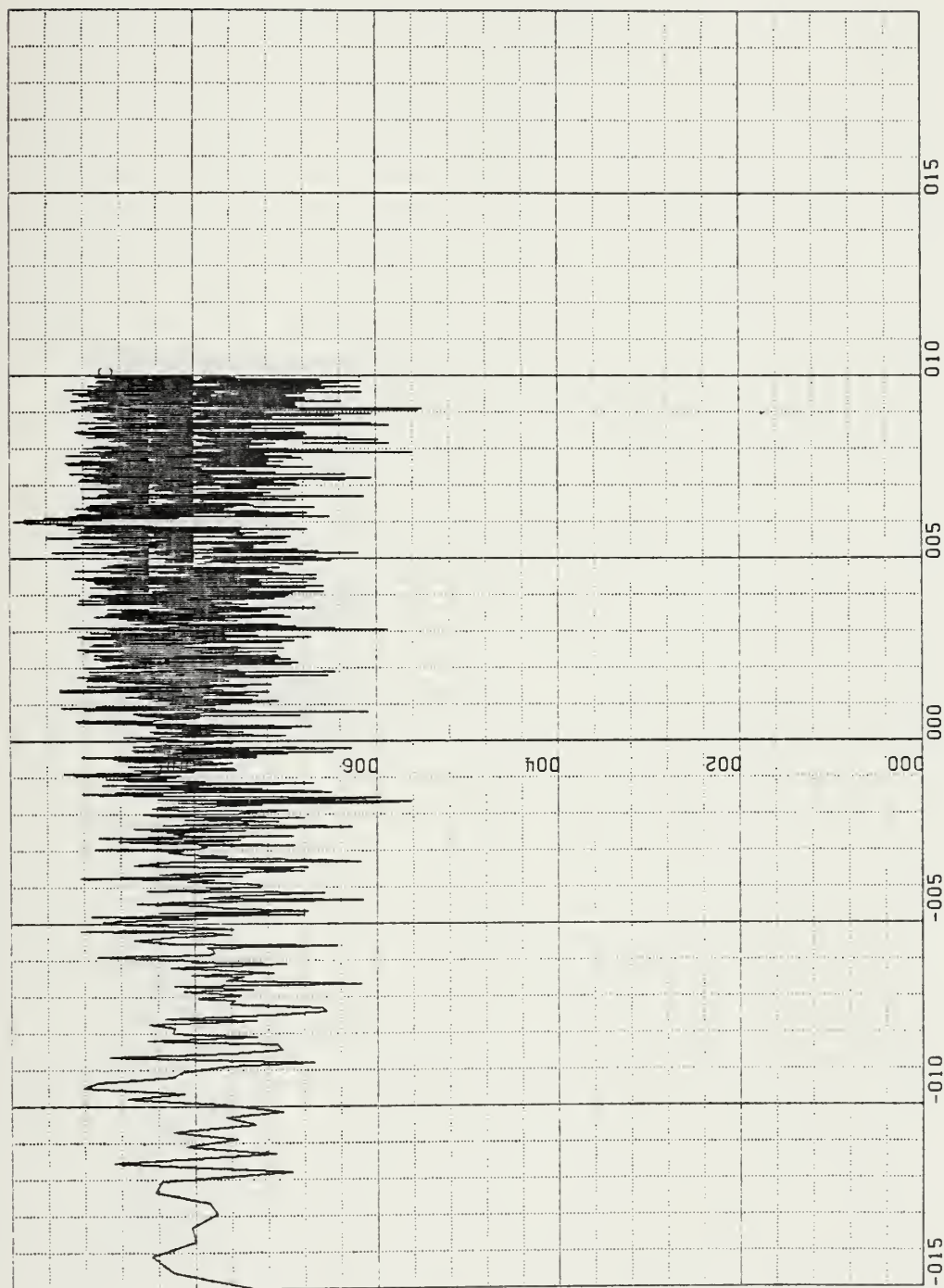


Figure 2.21. Coherence X-Y coils, 17 August 82, 2245-2353 Local.  
 Coherence X-Y Coils (0.2 units/in) vs. Log Frequency (Hz)  
 (0.5 units/in), 16 Averages



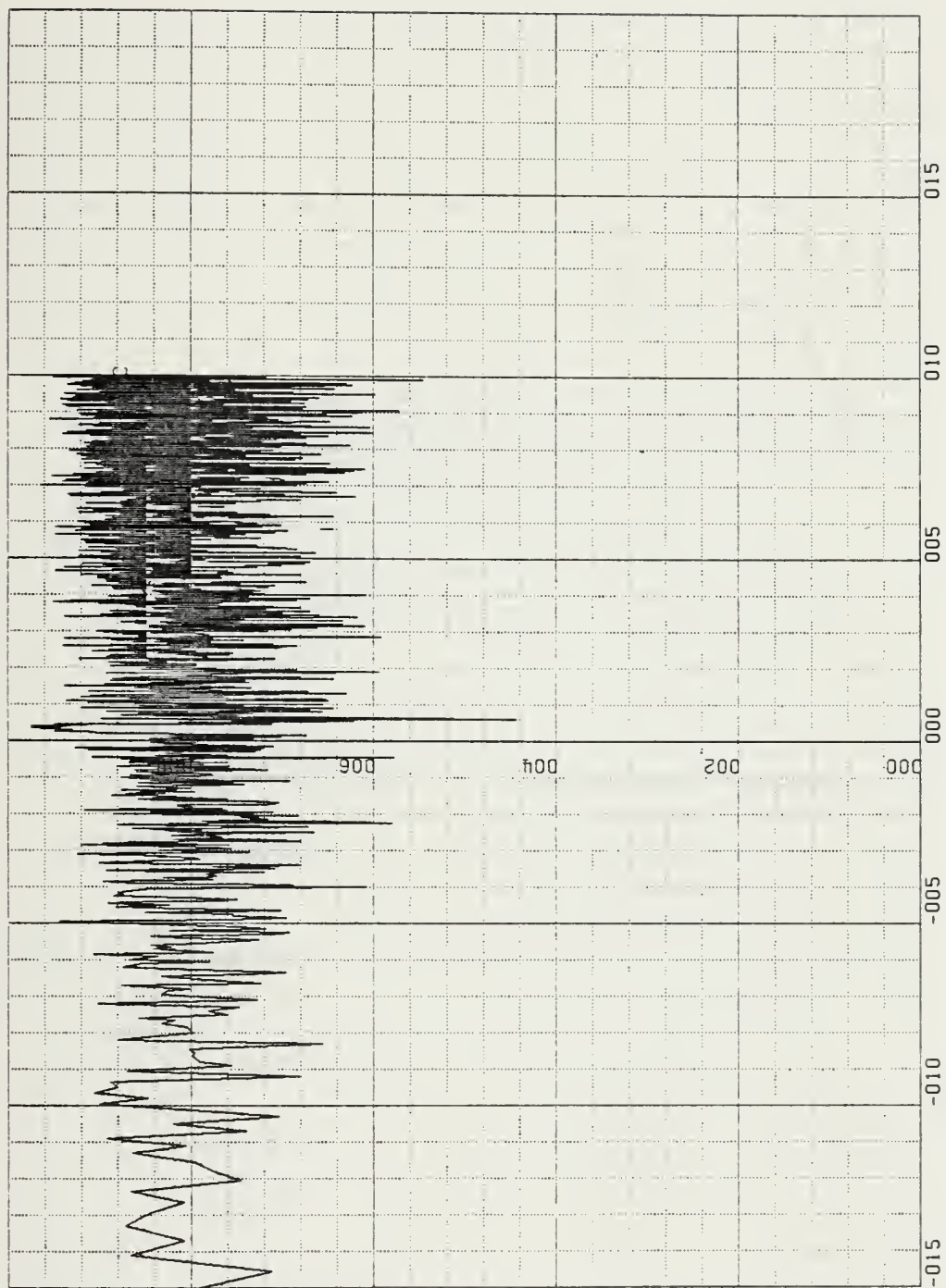


Figure 2.22. Coherence Y-Z Coils, 17 August 82, 2245-2353 Local  
 Coherence X-Y Coils (0.2 units/in) vs. Log Frequency (Hz)  
 (0.5 units/in), 16 Averages





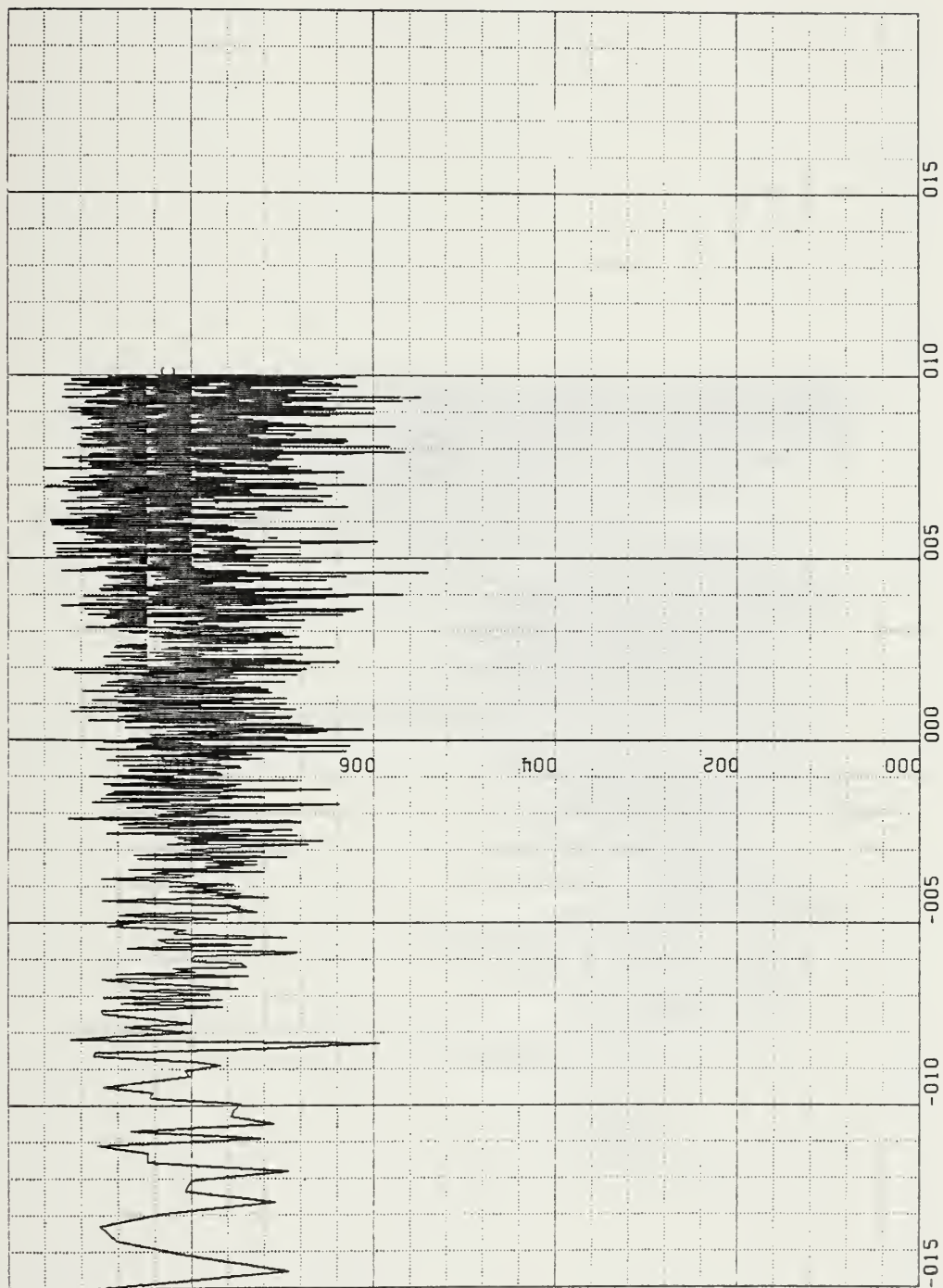


Figure 2.23. Coherence Z-X Coils, 17 August 82, 2245-2353 Local.  
Coherence Z-X Coils (0.2 units/in) vs. Log Frequency (Hz)  
(0.5 units/in), 16 Averages





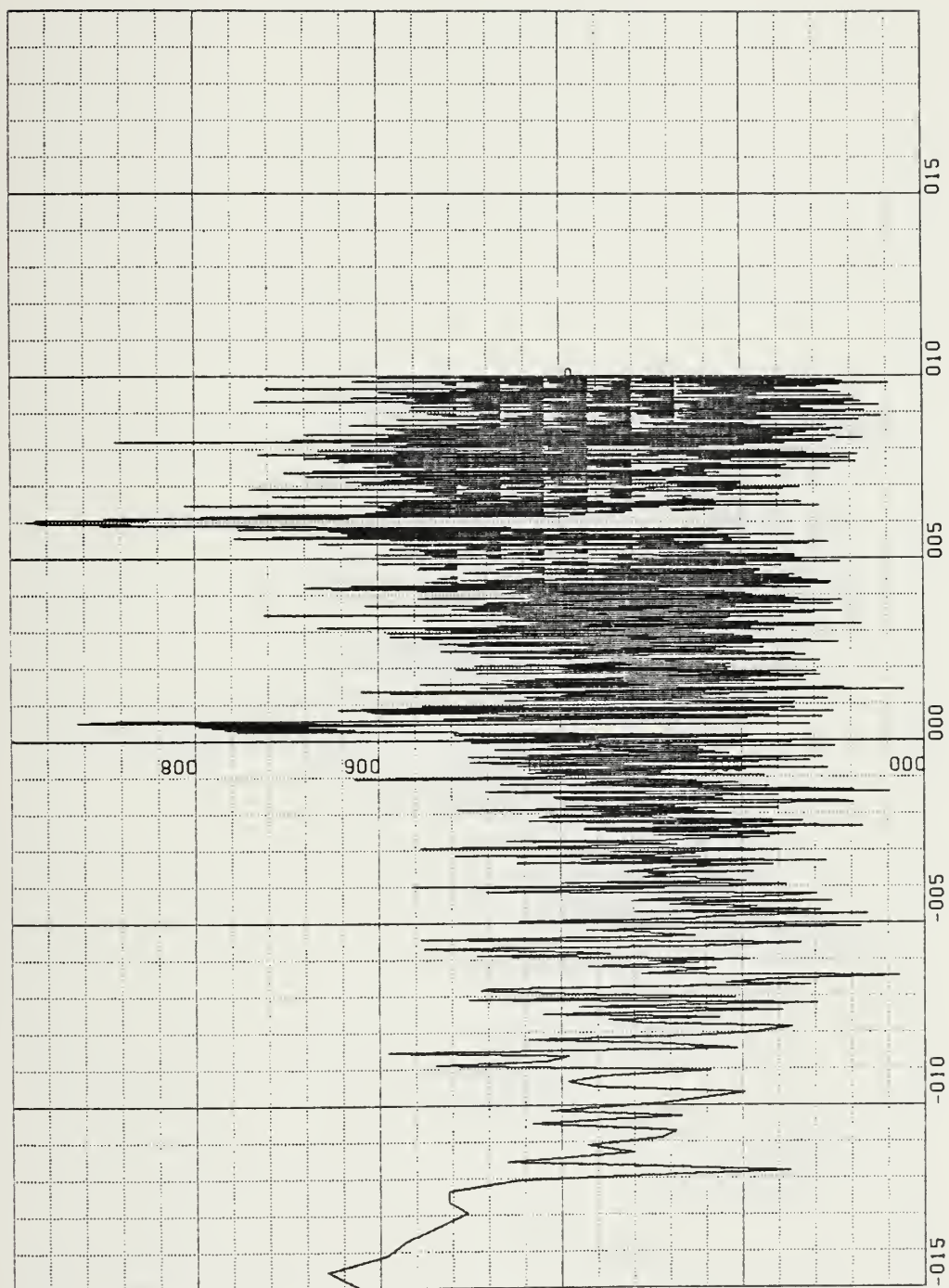


Figure 2.24. Degree of Polarization X-Y Plane, 17 August 82, 2245-2353 Local.  
 Degree of Polarization (0.2 units/in) vs. Log Frequency (Hz)  
 (0.5 units/in), 16 Averages



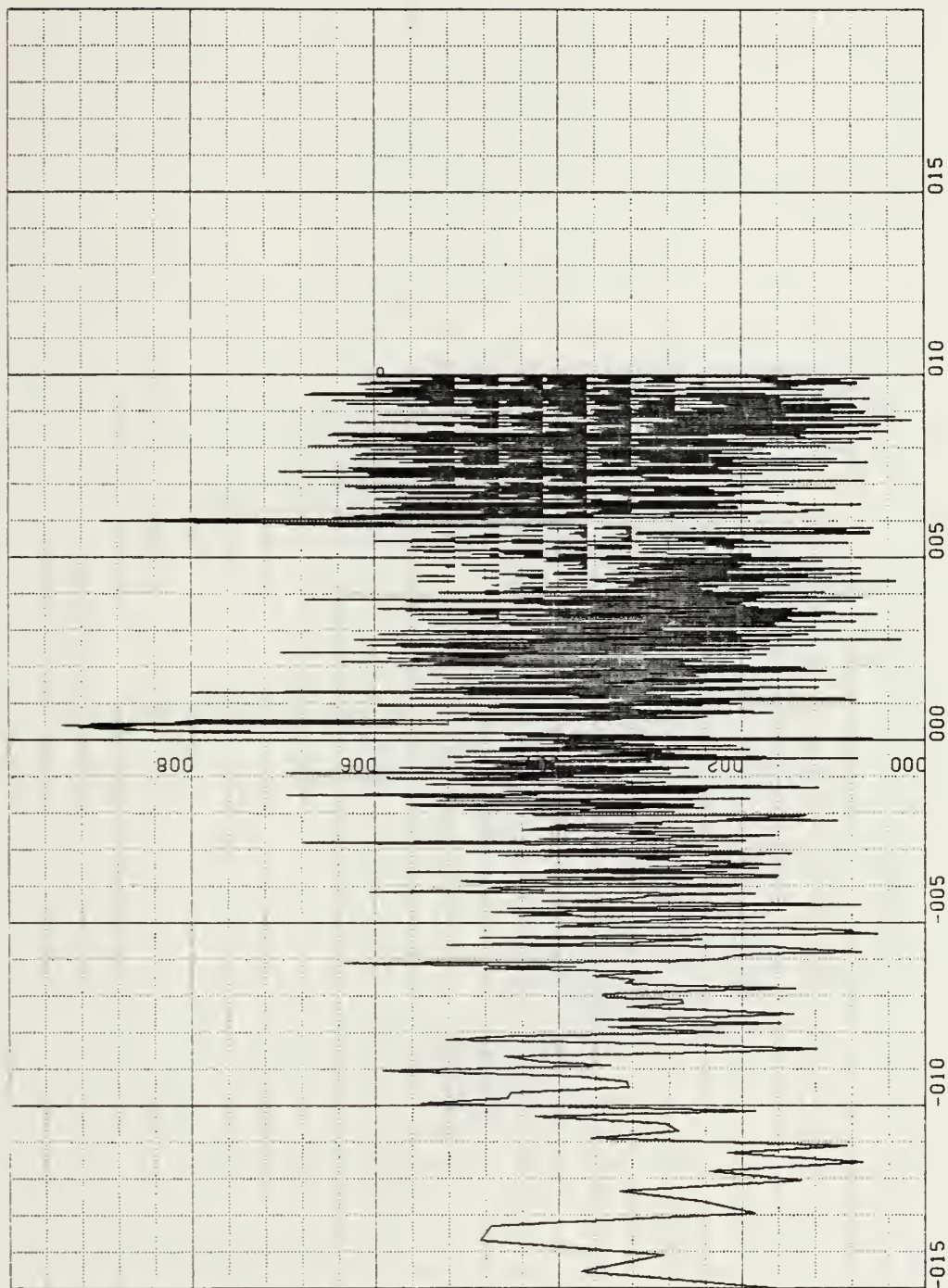


Figure 2.25. Degree of Polarization Y-Z Plane, 17 August 82, 2245-2353 Local.  
 Degree of Polarization (0.2 units/in) vs. Log Frequency (Hz)  
 (0.5 units/in), 16 Averages



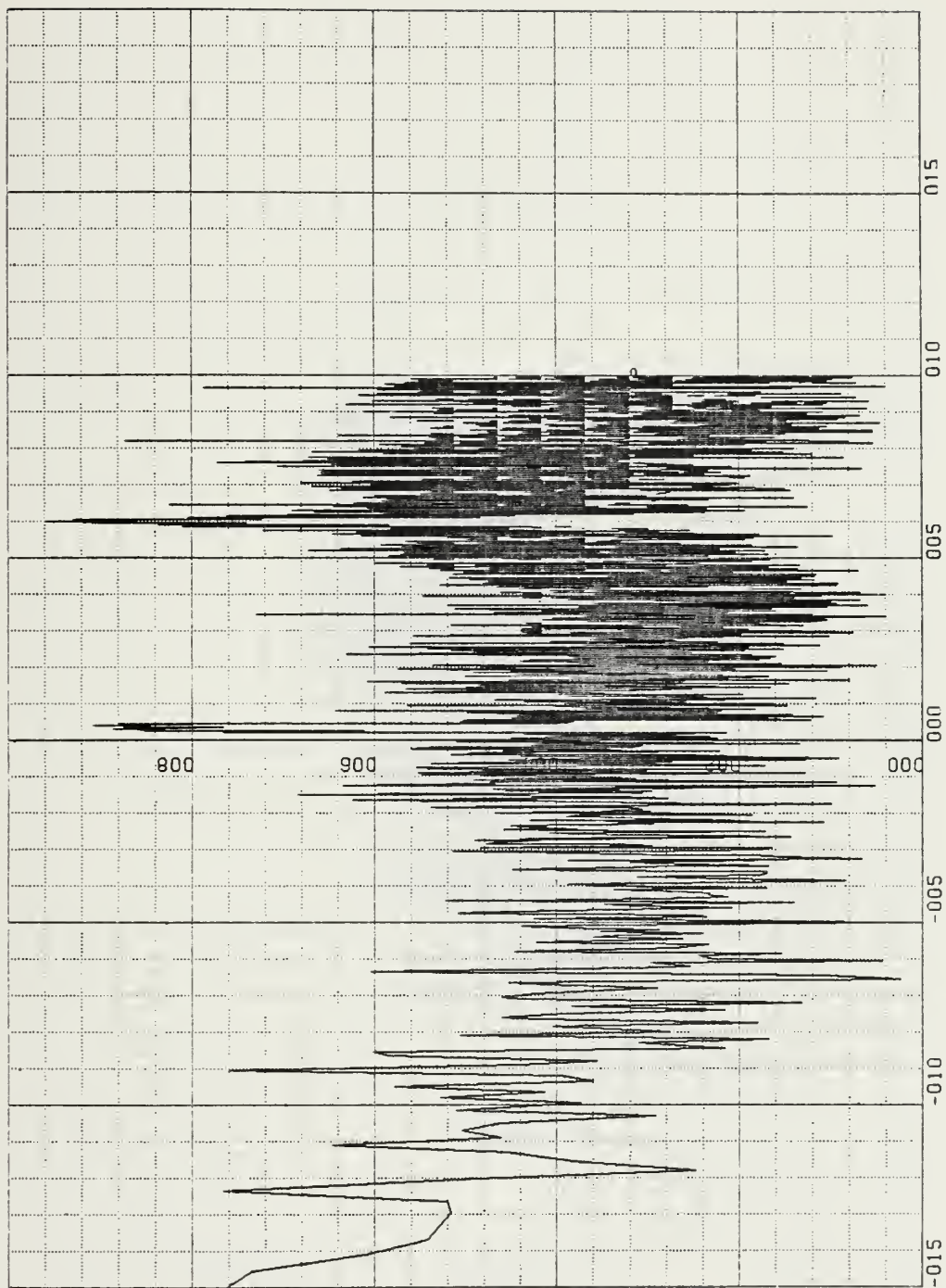


Figure 2.26. Degree of Polarization Z-X Plane, 17 August 82, 2245-2353 Local.  
Degree of Polarization (0.2 units/in) vs. Log Frequency (Hz)  
(0.5 units/in), 16 Averages





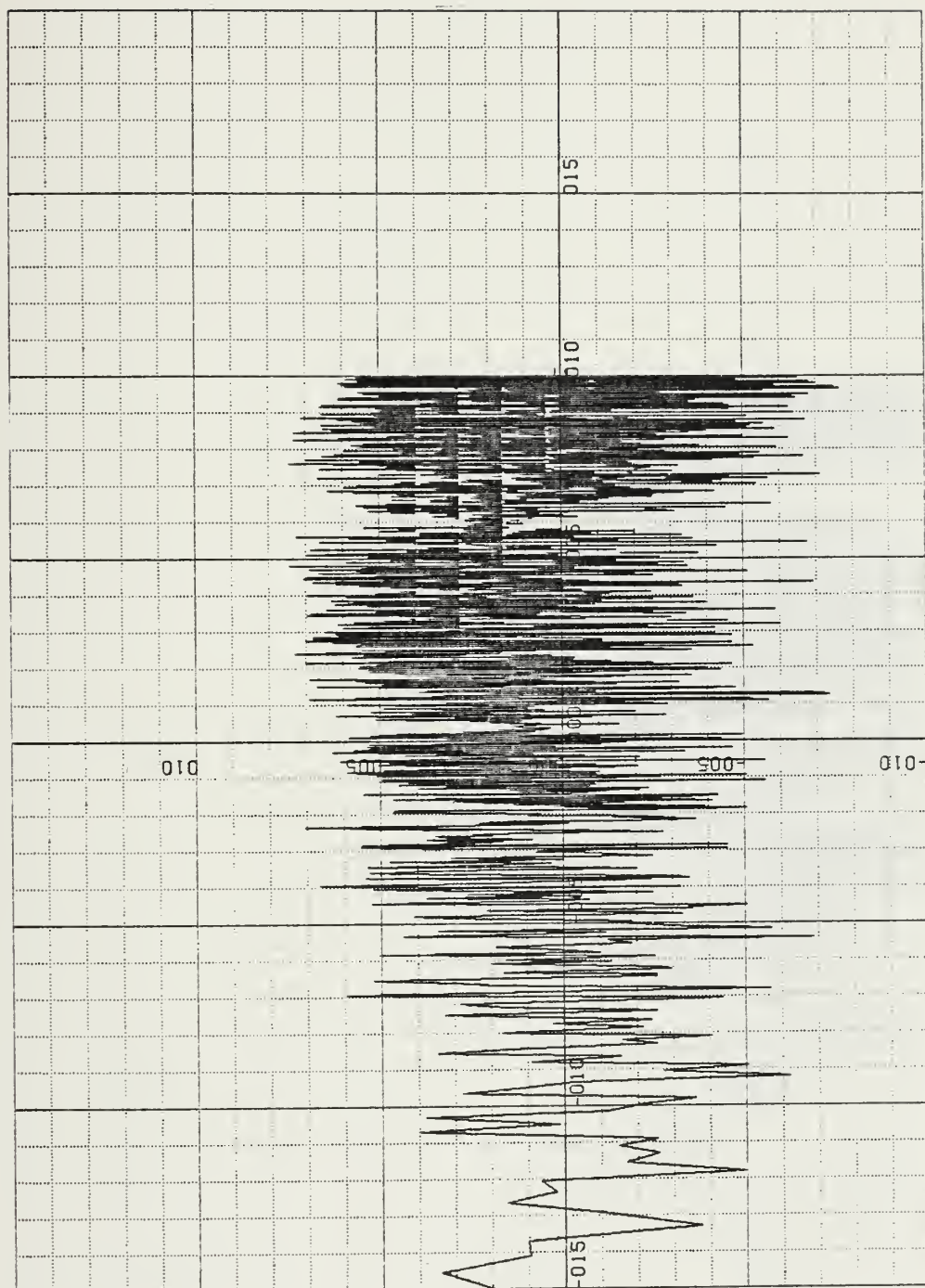


Figure 2.27. Ellipticity X-Y Plane, 17 August 82, 2245-2353 Local.  
 Ellipticity (0.5 units/in) vs. Log Frequency (Hz)  
 (0.5 units/in), 16 Averages





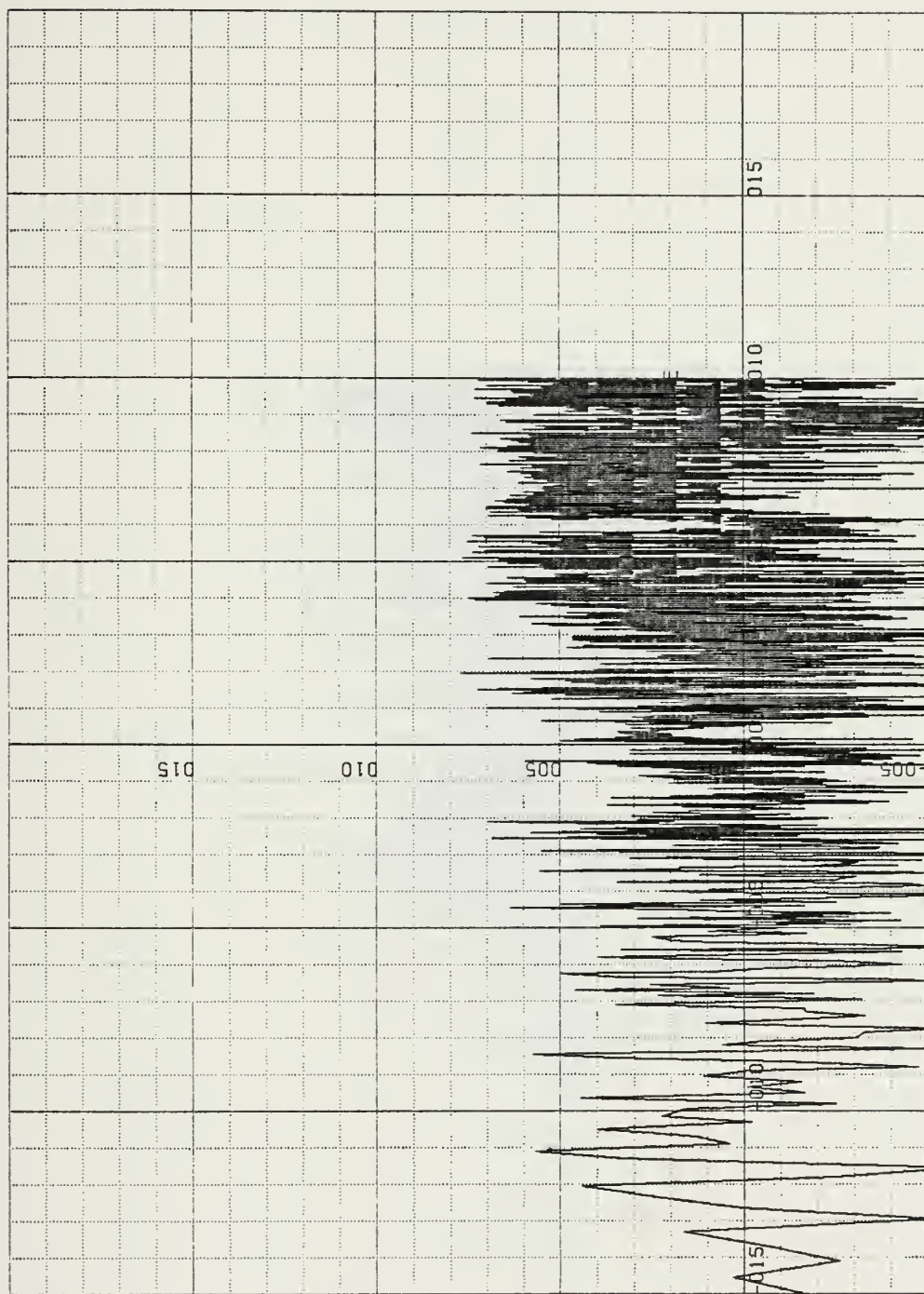


Figure 2.28. Ellipticity Y-Z Plane, 17 August 82, 2245-2353 Local.  
 Ellipticity (0.5 units/in) vs. Log Frequency (Hz) (0.5 units/in)  
 16 Averages



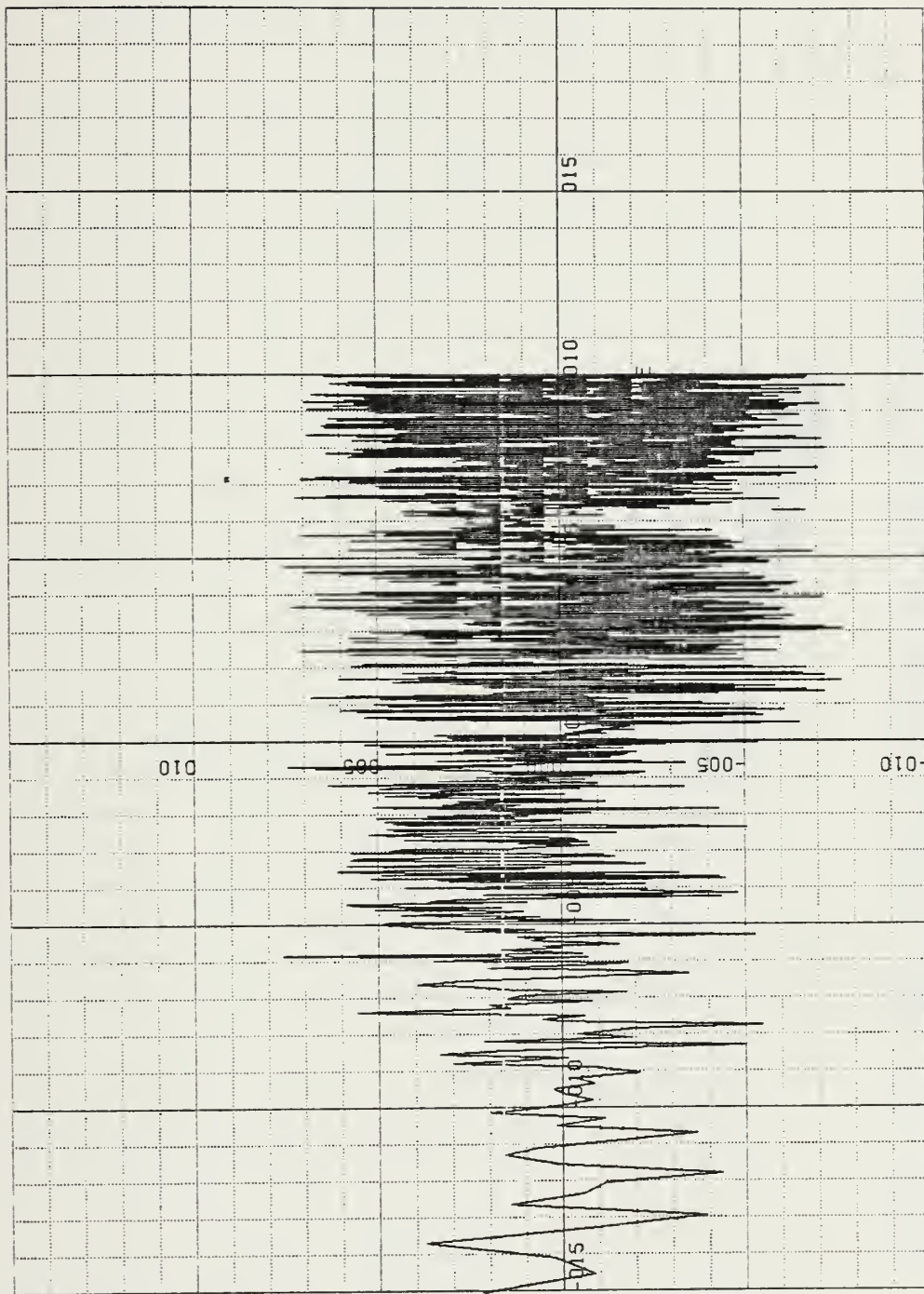


Figure 2.29. Ellipticity Z-X Plane, 17 August 82, 2245-2353 Local.  
 Ellipticity (0.5 units/in) vs. Log Frequency (Hz)  
 (0.5 units/in), 16 Averages



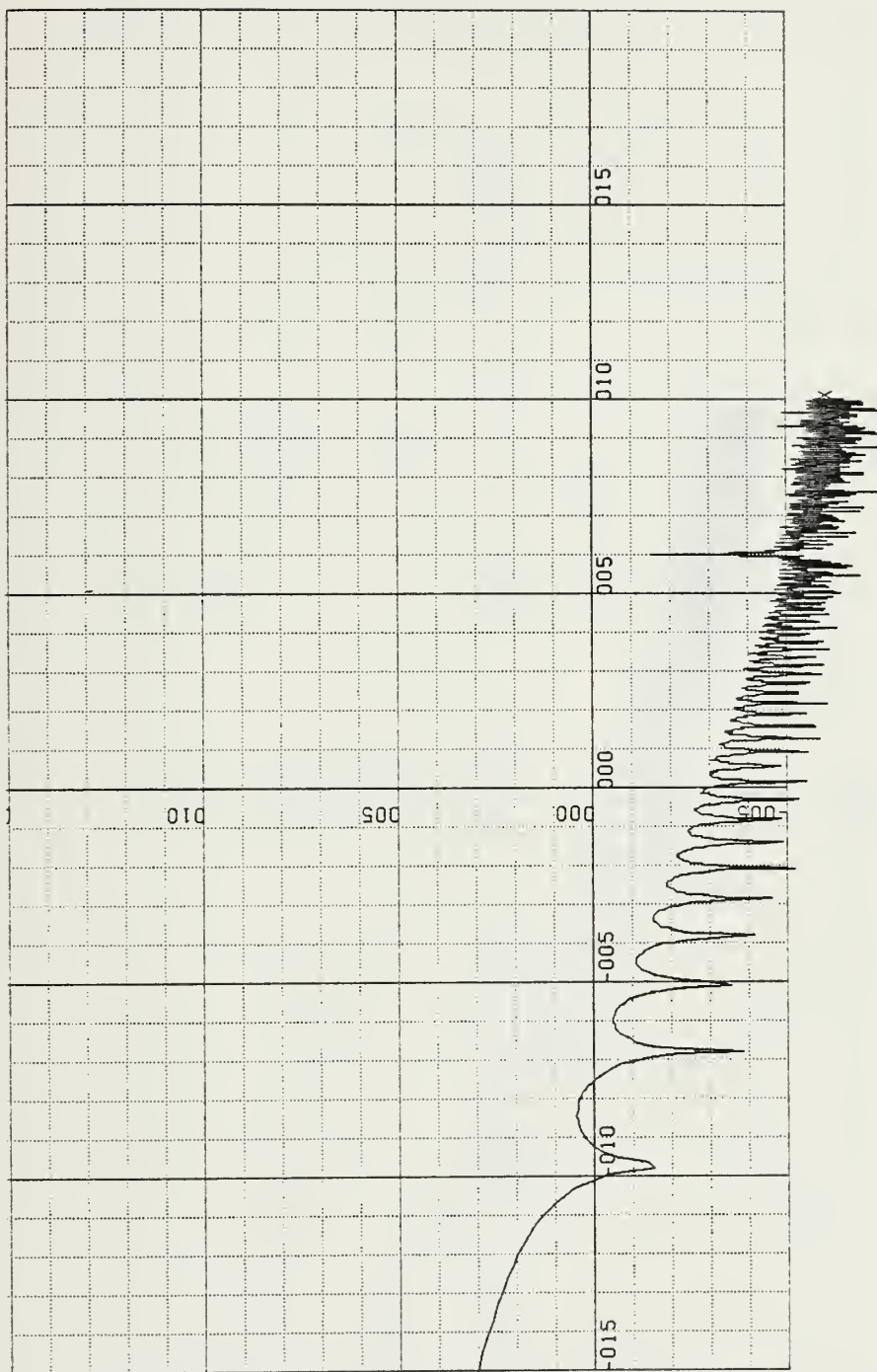


Figure 2.30. PSD X Coil, 17 August 82, 2240-2250 Local.  
 Amplitude in dB (REF  $nT^{**}2/Hz$ ) (50 units/in) vs. Log  
 Frequency (Hz) (0.5 units/in), 2 Averages





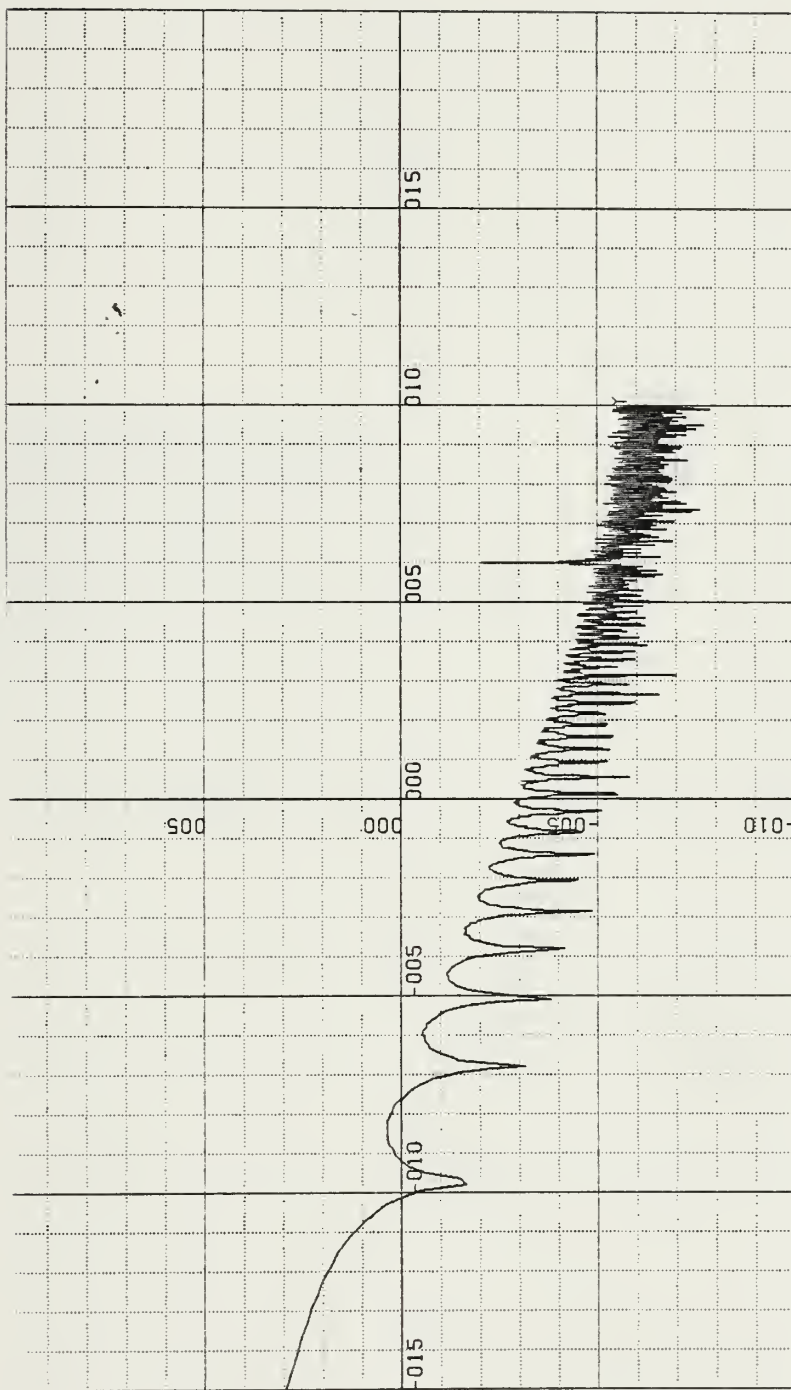


Figure 2.31. PSD Y Coil, 17 August 82, 2240-2250 Local.  
 Amplitude in dB (REF  $nT^{**2}/Hz$ ) (50 units/in) vs. Log  
 Frequency (Hz) (0.5 units/in), 2 Averages





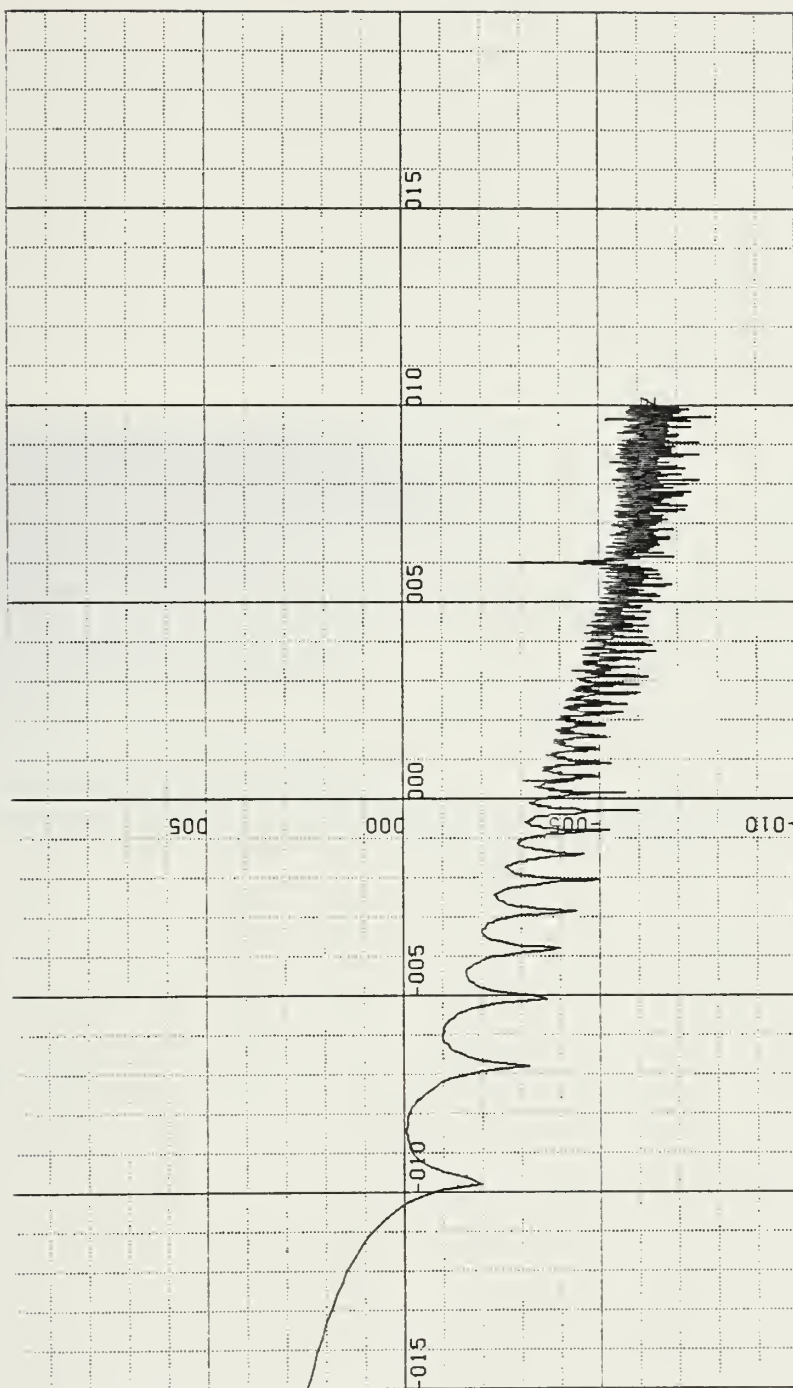


Figure 2.32. PSD Z Coil, 17 August 82, 2240-2250 Local.  
 Amplitude in dB (REF nT\*\*2/Hz) (50 units/in) vs. Log  
 Frequency (Hz) (0.5 units/in), 2 Averages



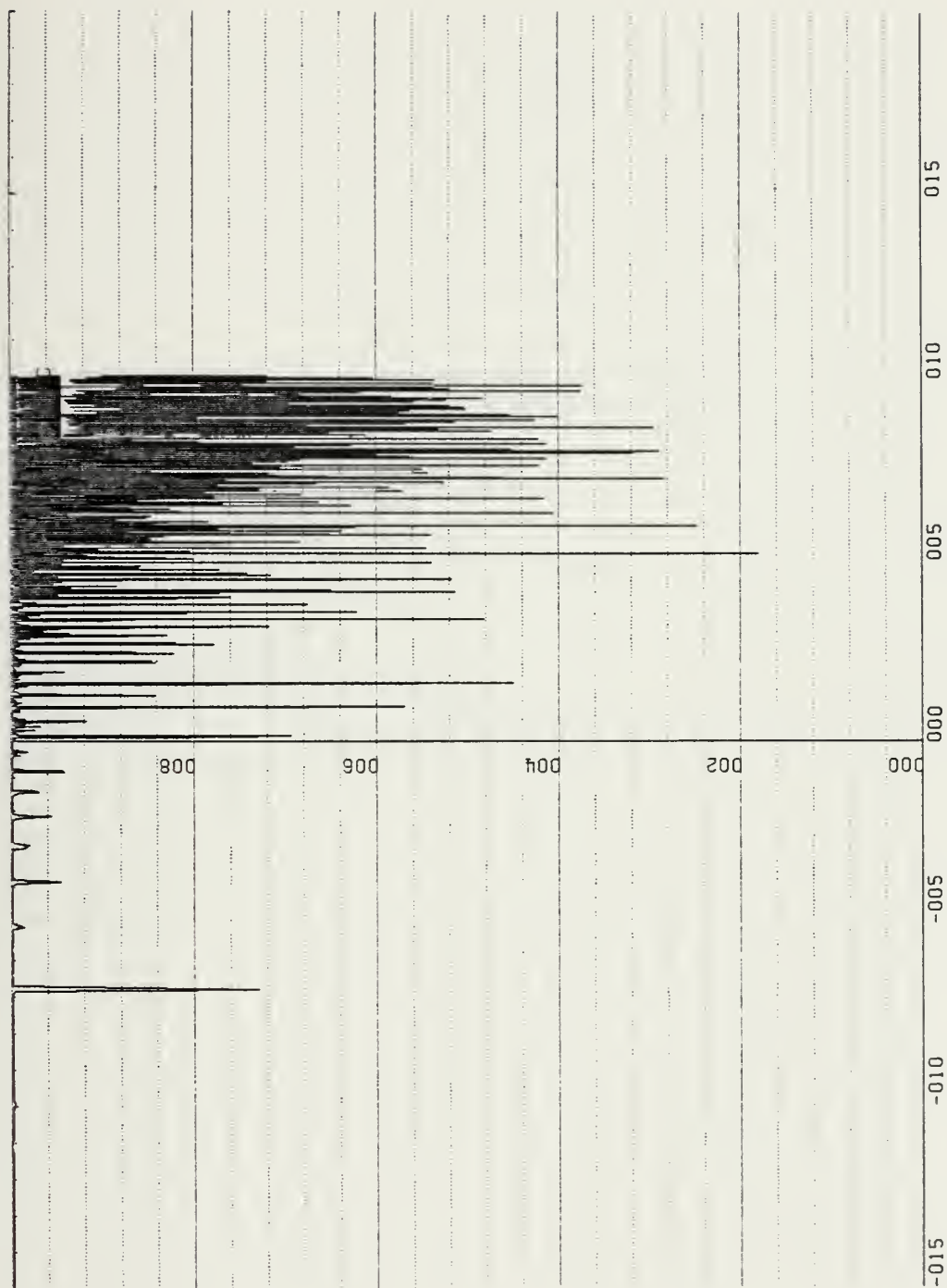


Figure 2.33. Coherence X-Y Coils, 17 August 82, 2240-2250 Local.  
 Coherence X-Y Coils (0.2 units/in) vs. Log Frequency (Hz)  
 (0.5 units/in), 2 Averages



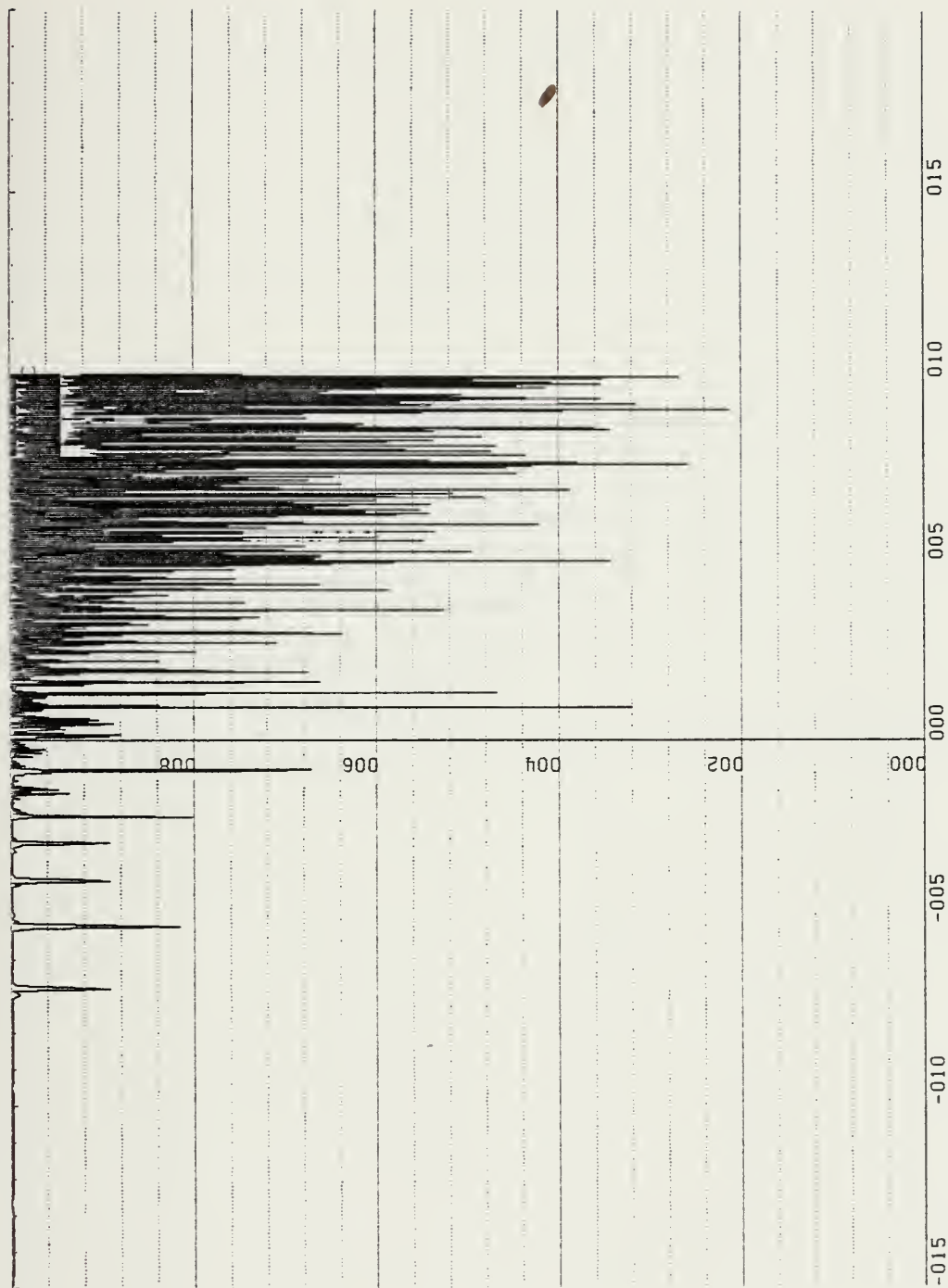


Figure 2.34. Coherence Y-Z Coils, 17 August 82, 2240-2250 Local.  
 Coherence Y-Z Coils (0.2 units/in) vs. Log Frequency (Hz)  
 (0.5 units/in), 2 Averages



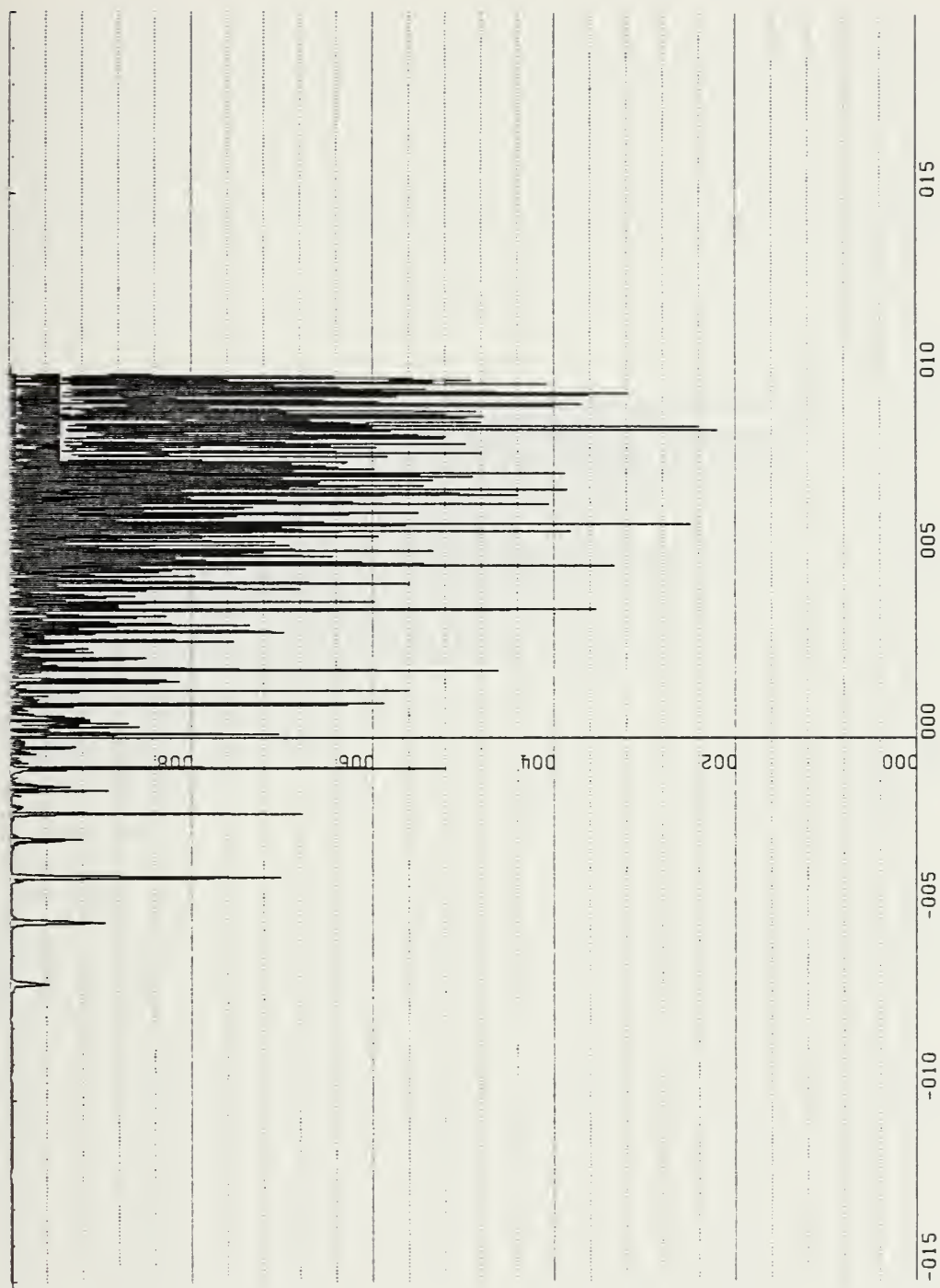


Figure 2.35. Coherence Z-X Coils, 17 August 82, 2240-2250 Local.  
 Coherence Z-X Coils (0.2 units/in) vs. Log Frequency (Hz)  
 (0.5 units/in), 2 Averages





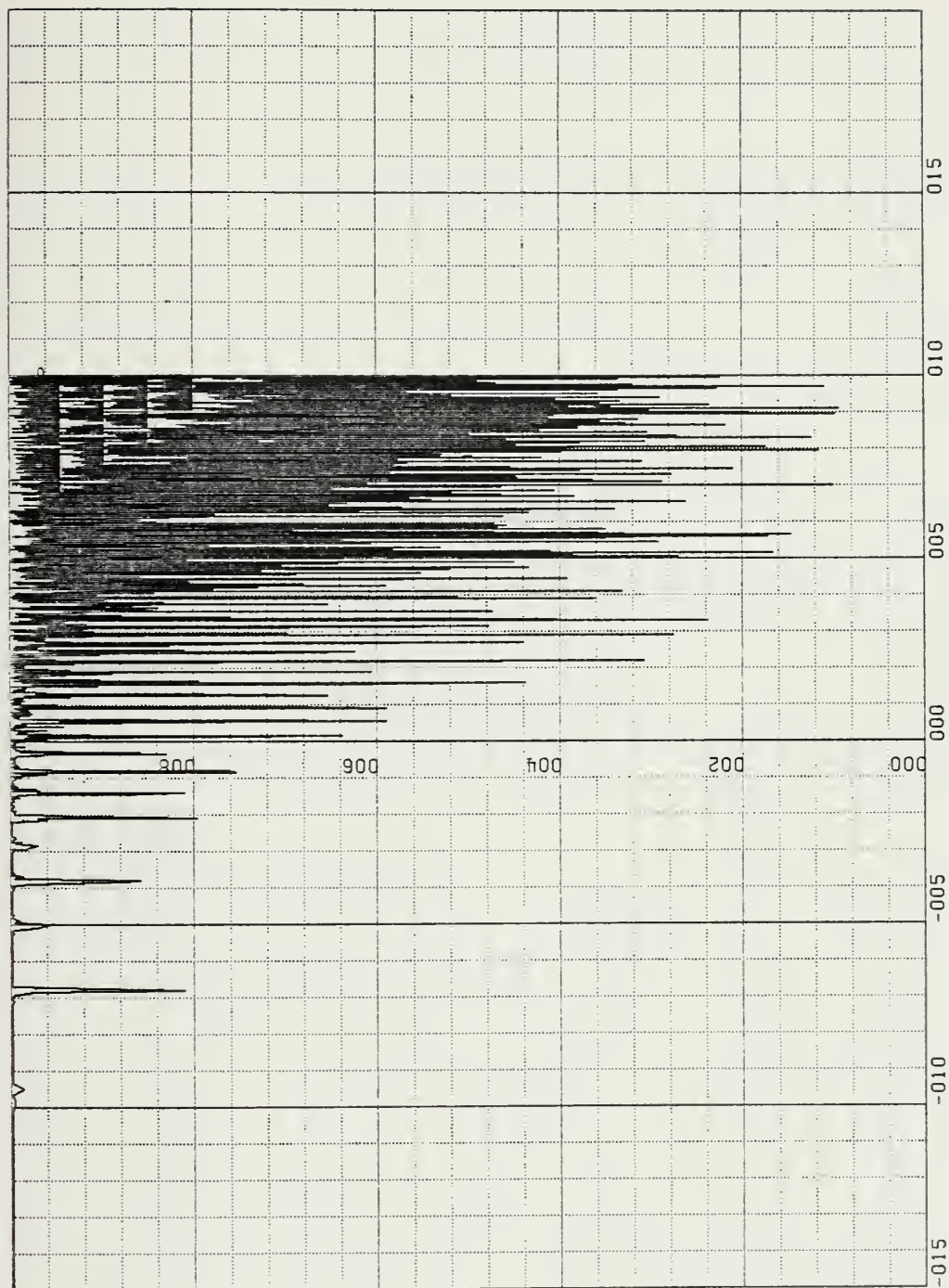


Figure 2.36. Degree of Polarization X-Y Plane, 17 August 82, 2240-2250 Local.  
 Degree of Polarization (0.2 units/in) vs. Log Frequency (Hz)  
 (0.5 units/in), 2 Averages



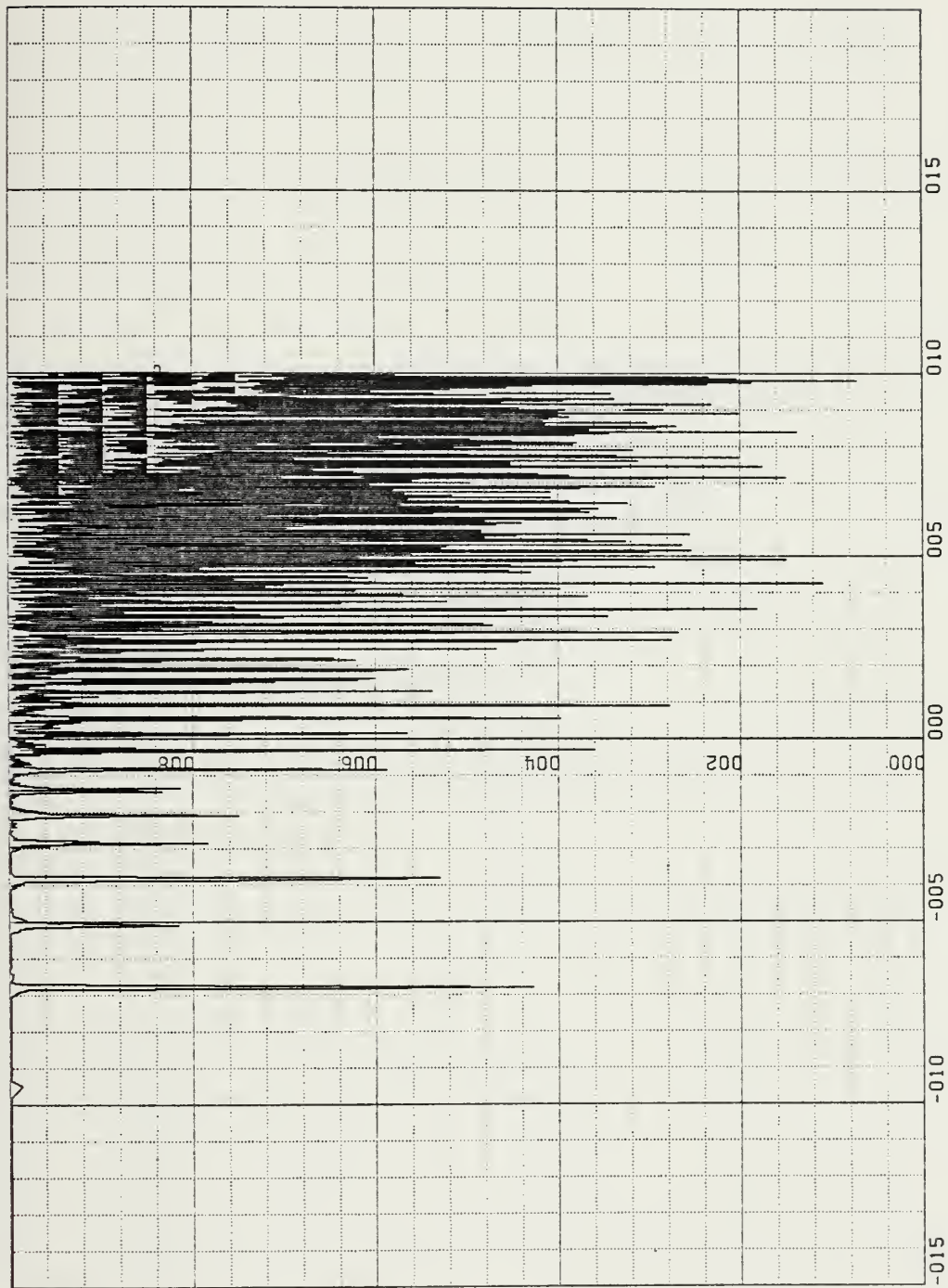


Figure 2.37. Degree of Polarization Y-X Plane, 17 August 82, 2240-2250 Local.  
Degree of Polarization (0.2 units/in) vs. Log Frequency (Hz)  
(0.5 units/in), 2 Averages



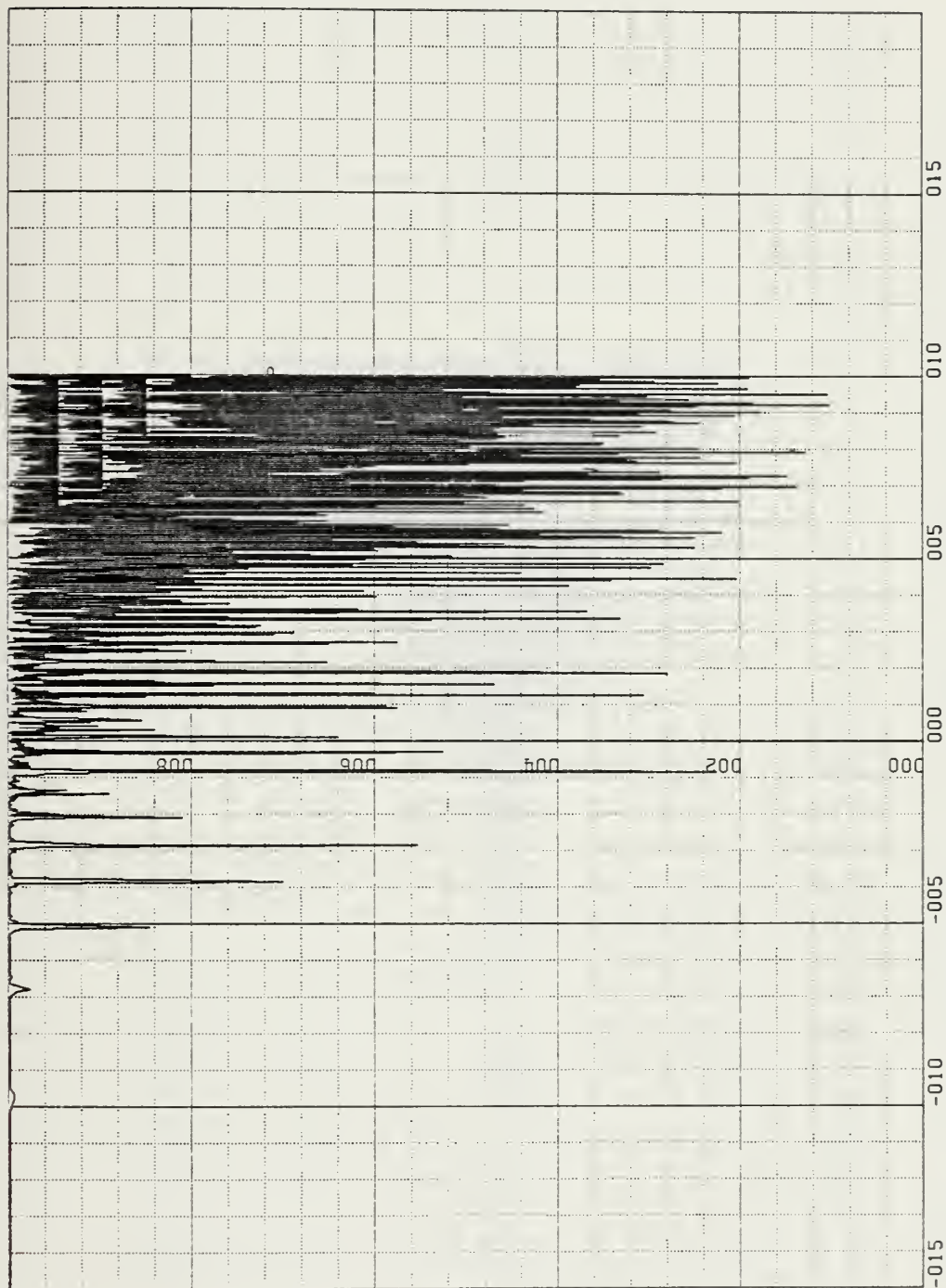


Figure 2.38. Degree of Polarization Z-X Plane, 17 August 82, 2240-2250 Local.  
 Degree of Polarization (0.2 units/in) vs. Log Frequency (Hz)  
 (0.5 units/in), 2 Averages





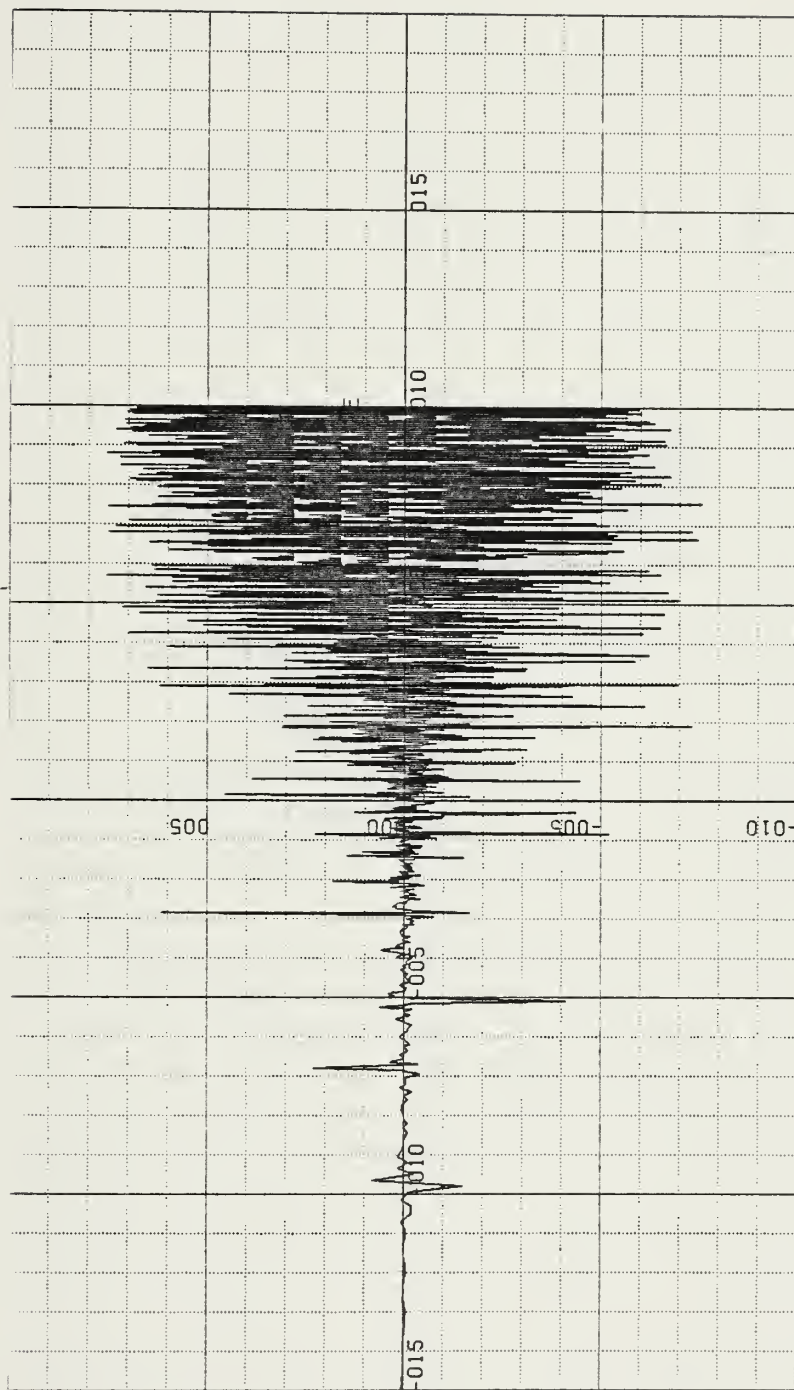


Figure 2.39. Ellipticity X-Y Plane, 17 August 82, 2240-2250 Local.  
 Ellipticity (0.5 units/in) vs. Log Frequency (Hz) (0.5 units/in)  
 2 Averages





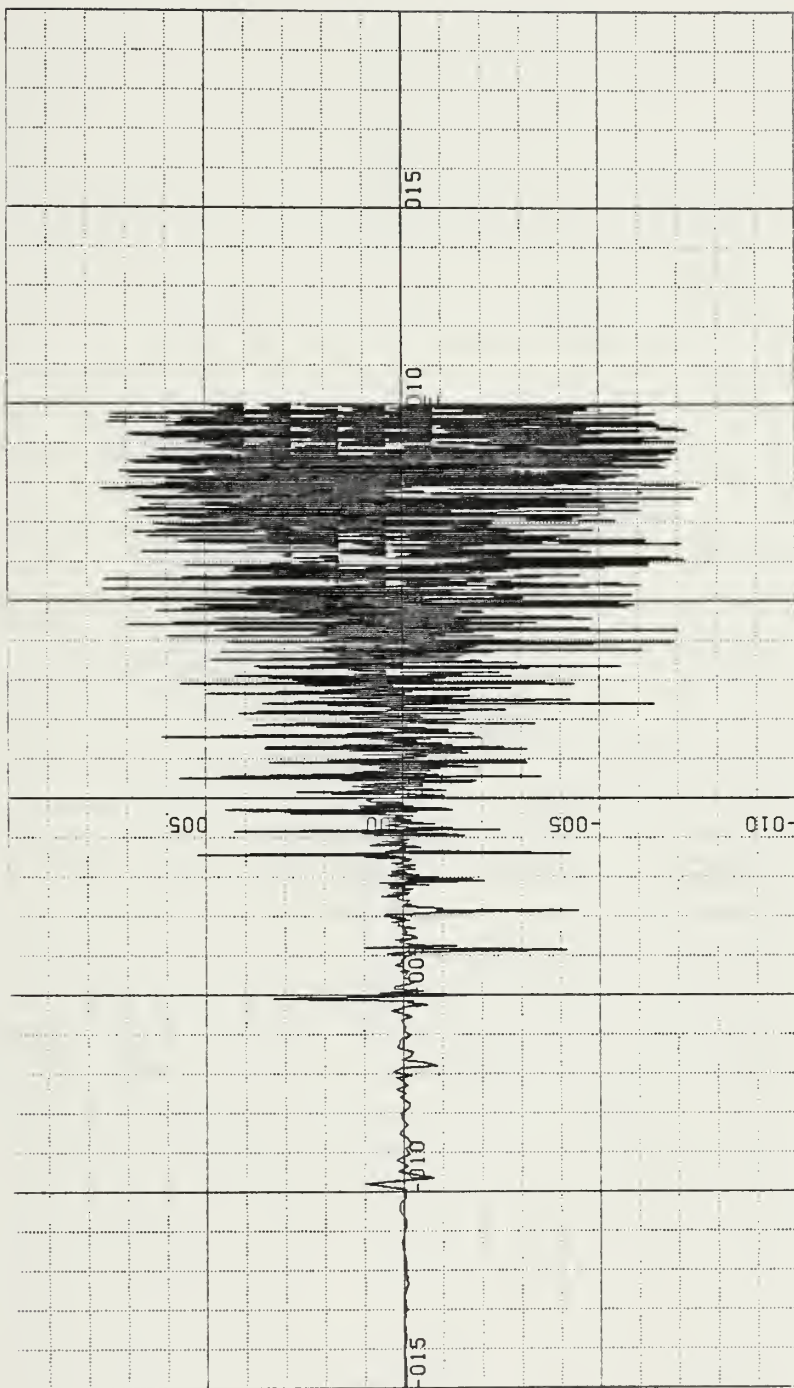


Figure 2.40. Ellipticity Y-Z Plane, 17 August 82, 2240-2250 Local.  
 Ellipticity (0.5 units/in) vs. Log Frequency (Hz) (0.5 units/in)  
 2 Averages



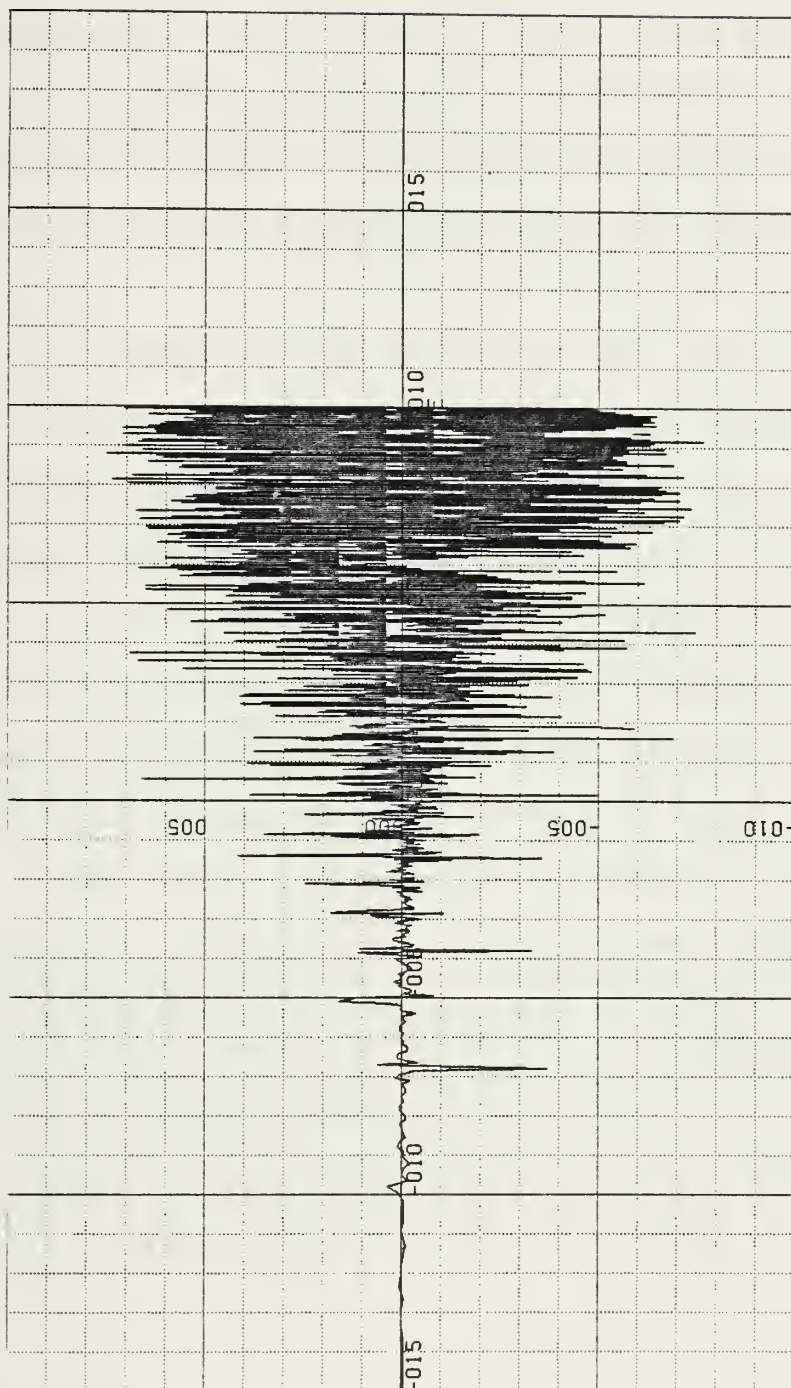


Figure 2.41. Ellipticity Z-X Plane, 17 August 82, 2240-2250 Local.  
 Ellipticity (0.5 units/in) vs. Log Frequency (Hz)  
 (0.5 units/in), 2 Averages



recommended at the beginning of the programs producing the above mentioned plots. Time series plots should also be made to provide a further check.

An explanation of the source of the large fluctuations is that the PCM to digital conversion begins before the actual PCM data starts on the tape. The decoding equipment considers the noise on the section of tape before the PCM data starts as signal.

The above analysis clearly proves that the "hump" like structure in the PSD's and the "nice" behavior observed in the corresponding coherence, ellipticity and degree of polarization are artificial and do not represent any real phenomena in the geomagnetic field. Thus, the data in Figures 2.3-2.14 and Figures 2.30-2.41 does not appear to be reliable. Unfortunately, this artificially induced, and therefore unphysical, behavior of the polarization has been published recently [Ref. 7]. The conclusion found in Reference 7 that

Geomagnetic fluctuations in land are well polarized below 1.0 Hz and that the polarization is quite frequently, though not consistently, linear. The situation under the sea is similar. Furthermore, a land-sea coherence study in the horizontal plane showed very high coherence below 1.0 Hz.

are not substantiated by the physical data. Plots of the artificially induced behavior are published in References 1, 2, and 3.



The 4 Hz peak present in the PSD's shown in Figures 2.18-2.20 is the result of 60 Hz aliasing. 60 Hz magnetic fields generated by local power lines exist at the measurement site. Digitization at a 32 Hz or 64 Hz rate of the analog voltages from the sensing coils shifts the true frequency of the power line signals down at 4 Hz. The 60 Hz aliasing results in the anomalous behavior at 4 Hz seen in the coherence, degree of polarization and ellipticity plots shown in Figures 2.21-2.29.

Another peak is present at about 1.2 Hz for the PSD's in Figures 2.18-2.20. For this data set, the 1.2 Hz signal correlates with a 1.2 Hz signal identified in the time series data. The origin of the 1.2 Hz signal is unknown. The 4 Hz and 1.2 Hz peaks are of little concern in this study since both are well above the frequency of the micropulsation analyzed.

Another "suspicious" feature of the PSD's is the large amount of hash appearing from 2 to 10 hertz. We will gain further insight into this problem in analyzing the time series voltage data.

From the analysis of the abnormal behavior in the PSD's, coherence, etc., future coil data sets should receive a balanced treatment between the time domain and the frequency domain to avoid misinterpretation.





### III. TIME SERIES DATA

#### A. TIME SERIES VOLTAGE DATA

##### 1. Voltage Software

The importance of time series data as a check became evident when we uncovered the problem with the initial PSD's, coherences, etc. Computer code was developed to produce both unsmoothed and smoothed times series voltage plots. The reason for producing both smoothed and unsmoothed voltage plots will become apparent in the time series voltage analysis section. Time series voltage plots could provide a means of monitoring the data for system "glitches" which might later produce erroneous PSD's, etc., and suspicious features on time series magnetic field plots.

The Fortran computer program that produces the voltage plots is compiled and run on the Naval Postgraduate School IBM 3033 VM or "batch" system. Both the unsmoothed voltage program (VOLTR) and the smoothed voltage program (VOLTS) require 2.048 megabytes of core memory and approximately 15 minutes of central processor unit (CPU) time to run. These figures provide a comfortable margin to insure that the program does not "bomb" due to lack of core or run time.

The design of both VOLTR and VOLTS is the same with the exception that a smoothing algorithm is applied to the data in the case of VOLTS. Both programs have incorporated in them the digital tape advance package using ISEC as the number of



seconds one wishes to advance the tape. Data is read off the digital tape in blocks of 8192 frames by the subroutine RD referenced earlier. As before, this data is in integer form and represents voltages between  $\pm 5$  volts by numbers between 0 and 4096. The integer representing 0 volts is ideally 2048, however, I found that the "real" zero values wander. The reason for this "wander" is not understood. For good results, the following values worked well for the respective coils.

X-coil : zero = 1966

Y-coil : zero = 2085

Z-coil : zero = 2539

The voltage values normalized to  $\pm 5$  volts are placed in new real arrays. At this point the next block of data is read off the digital tape and goes through the same process. VOLTR and VOLTS analyze eight blocks or 34 minutes of data. The linear arrays holding the voltage data are dimensioned to 65,536 elements given a sampling rate of 32 samples/second. For every one of the 65,536 voltage values there is a time value in another array. Thus four arrays are required to handle the data, three arrays containing voltage data and one that contains the respective times for each of the measurements. At this point, the VOLTR program calls the NONIMSL subroutine DRAWP to plot the data. The VOLTS program uses a smoothing algorithm to reduce the amount of high frequency hash.

The smoothing algorithm is a double running point average executed on all three axes of data. Since I was



interested in periods of approximately 10-45 seconds, I averaged over 144 points. With a running average over 23 percent of the oscillation, the unwanted background can be removed without destroying the oscillations. Averages greater than 50 percent of the period would partially remove the oscillation of interest. The construction of the algorithm makes changing the number of points averaged over trivial. One need only change a loop index and three divisors to obtain a different average. The smoothing algorithm is provided as Table 3.1. The computer code for both VOLTR and VOLTS is attached in Appendix A and Appendix B.

## 2. Time Series Voltage Data Analysis

One can gain a great deal of insight into the contents of the data by looking at the smoothed and unsmoothed voltage products. Figures 3.1-3.3 are unsmoothed voltage plots representing the first 34 minutes of the digital data tape GMDT 11 recorded 17 August 82, 1301-1408 local time. A one minute tape advance was used in producing this data. Immediately one notices the large amount of 60 hertz aliasing in the time series unsmoothed voltage. The 60 hertz aliasing appears as 4 hertz because of the 32 sample/second sampling rate. The sensing system has a low pass filter that should be improved to remove the aliasing problem. The 4 hertz background can be seen more clearly in Figures 3.4-3.6. Above the 60 hertz aliasing background, we see voltage spikes ranging in magnitude from 1 volt to over 4 volts. Expanding the time scale to 50



Table 3.1. Smoothing Algorithm

```

DC 73 L2=1,2
Q=0
DC 74 IS=1,65318
SUMX=0.0
SUMY=0.0
SUMZ=0.0
DC 75 J=1,144
SUMX=ZZX1(Q+J)+SUMX
SUMY=ZZY1(Q+J)+SUMY
SUMZ=ZZV1(Q+J)+SUMZ
75 CCNTINUE
ZZX1(IS)=SUMX/144.
ZZY1(IS)=SUMY/144.
ZZV1(IS)=SUMZ/144.
Q=Q+1
74 CCNTINUE
73 CCNTINUE

```





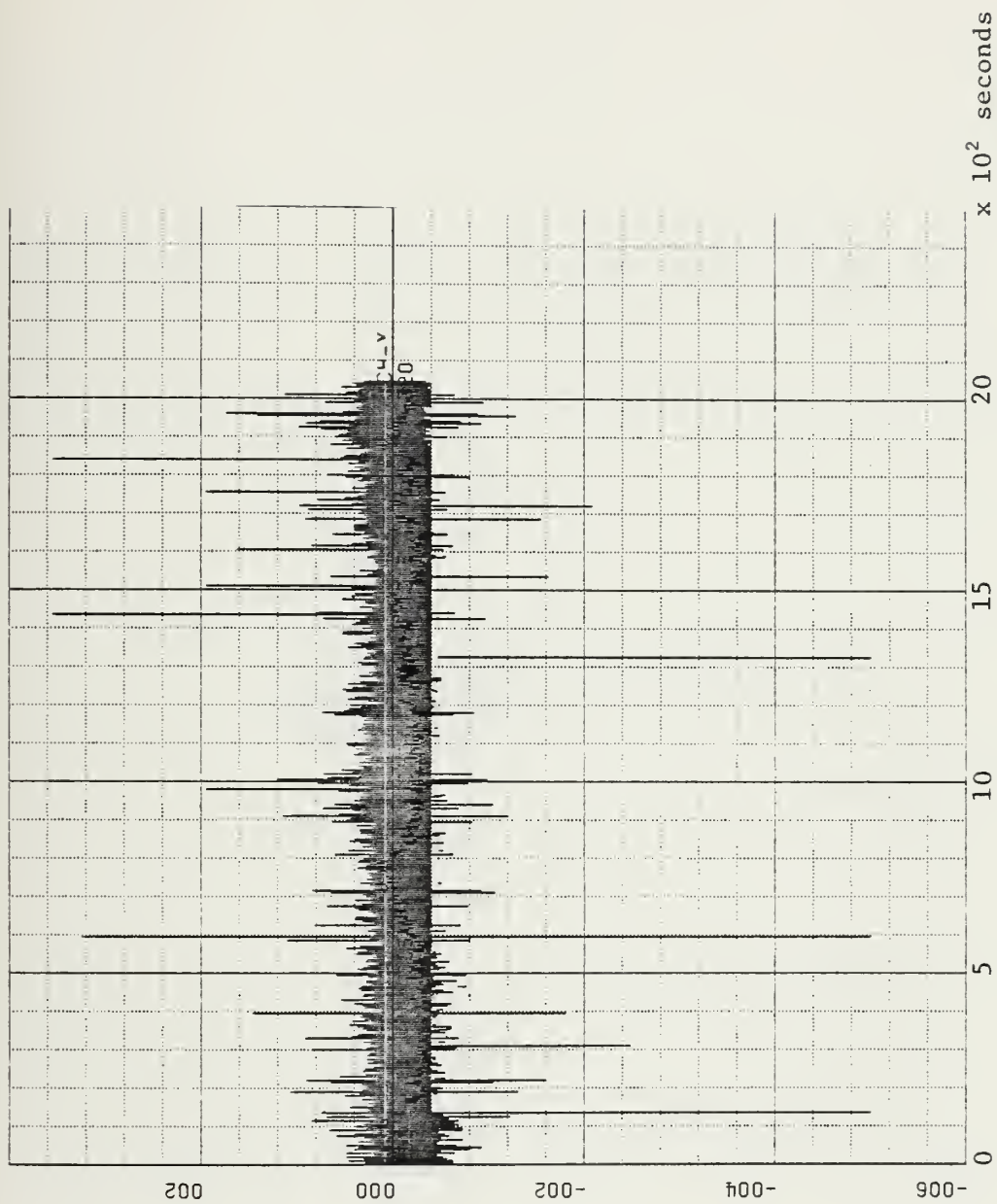


Figure 3.1. X Coil Voltage, 17 August 82, 1302-1336 Local.  
Amplitude (volts : 2 units/in) vs. Time (seconds : 500 units/in)



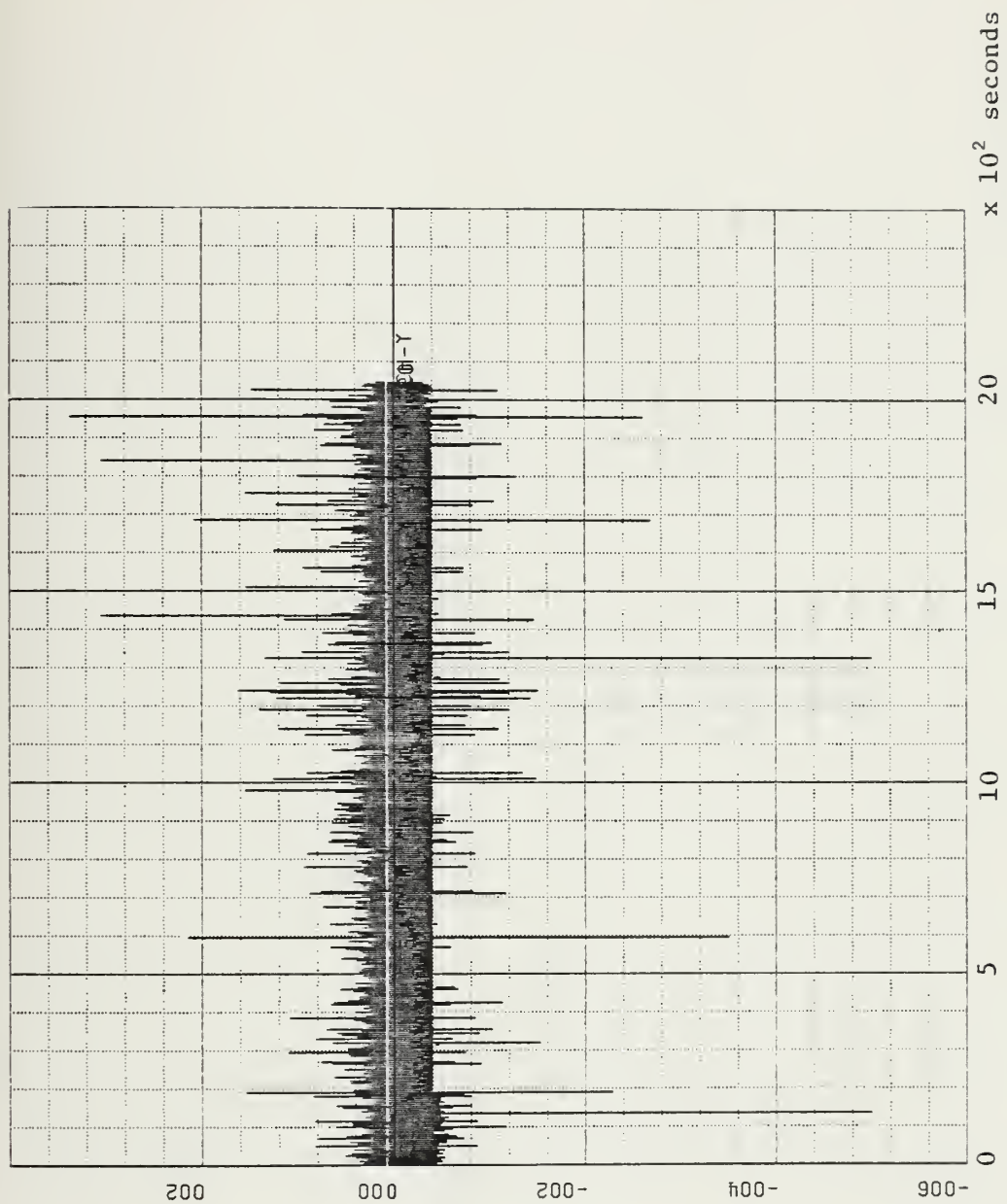


Figure 3.2. Y Coil Voltage, 17 August 82, 1302-1336 Local.  
Amplitude (volts : 2 units/in) vs. Time (seconds : 500 units/in)



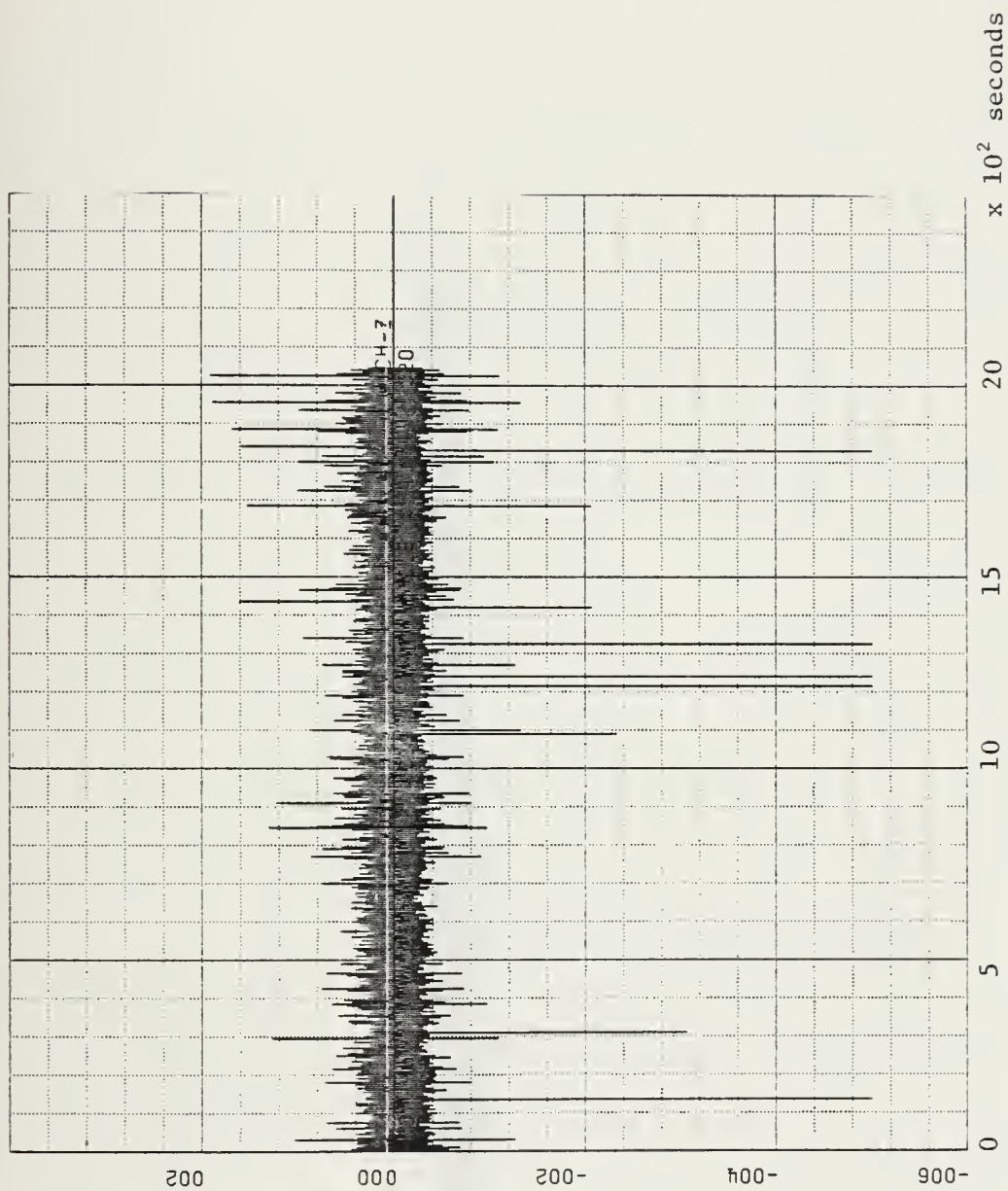


Figure 3.3. Z Coil Voltage, 17 August 82, 1302-1336 Local.  
Amplitude (volts : 2 units/in) vs. Time (seconds : 500 units/in)



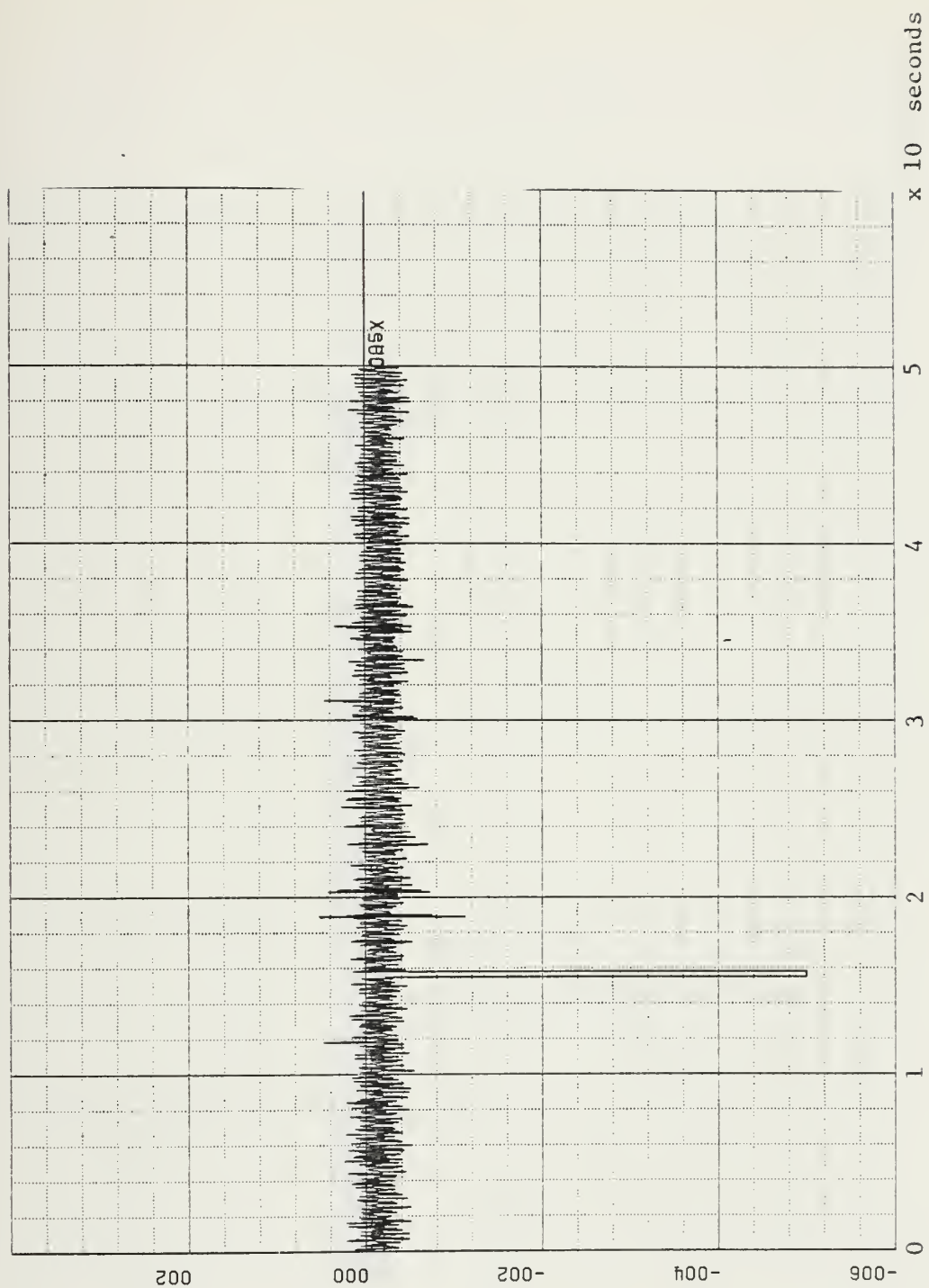


Figure 3.4. X-Coil Voltage, 17 August 82, 1322-1323 Local.  
Amplitude (Volts: 2 units/in) vs. Time (seconds : 10 units/in)





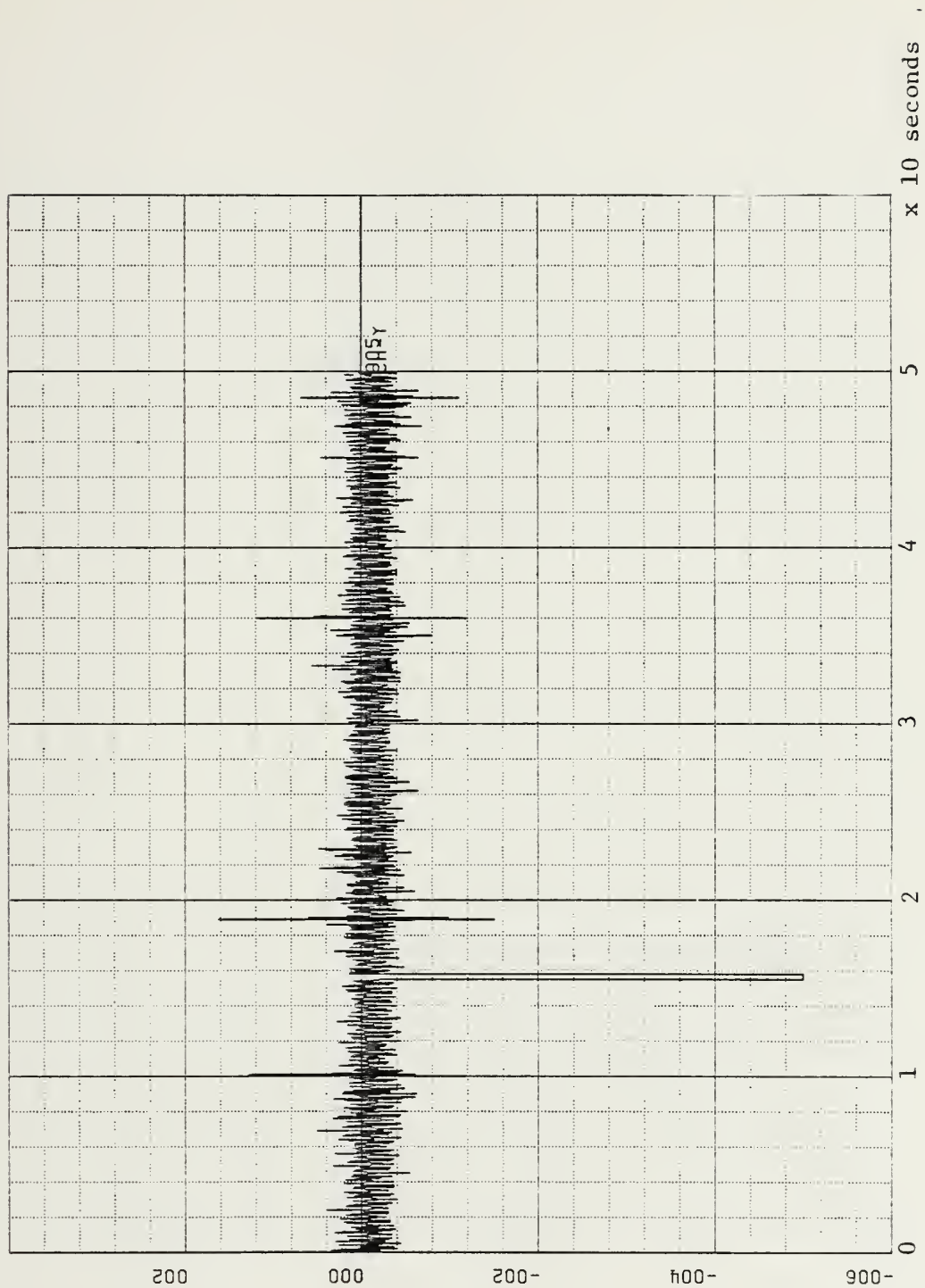


Figure 3.5. Y-Coil Voltage, 17 August 82, 1322-1323 Local.  
Amplitude (volts : 2 units/in) vs. Time (seconds : 10 units/in)



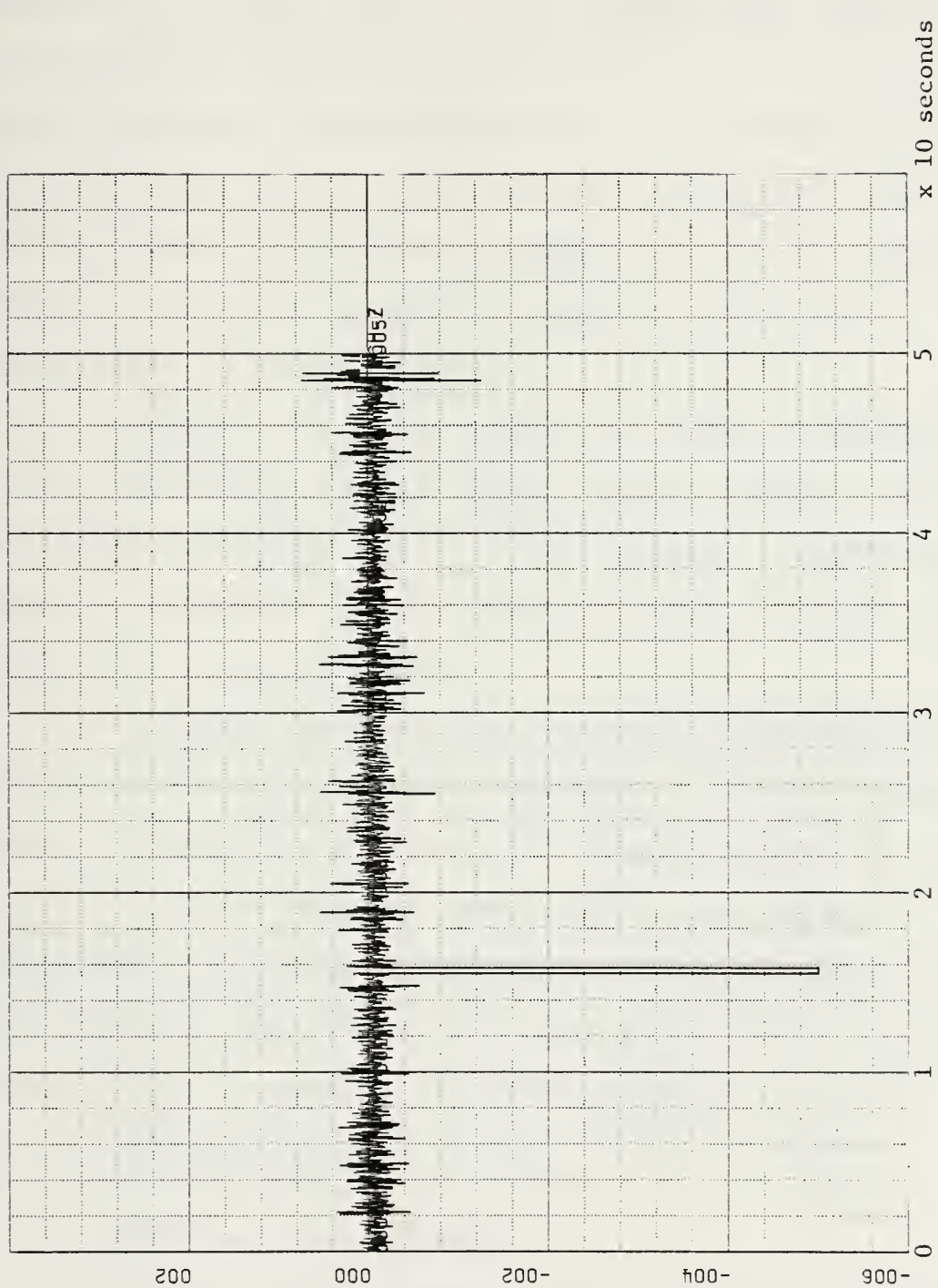


Figure 3.6. Z-Coil Voltage, 17 August 82, 1322-1323 Local.  
Amplitude (volts : 2 units/in) vs. Time (seconds : 10 units/in)



seconds of data, the structure of the voltage spikes becomes apparent in Figures 3.4-3.6. The "square well" shape is characteristic of PCM dropouts or instances during the PCM to digital conversion synchronization is lost between the tape recorder containing the PCM tape and the decoding unit. We do not know whether PCM dropouts always occur on all three channels, but current evidence suggests dropouts are simultaneous on all channels.

Figures 3.7-3.9 again show the first 34 minutes of GMDT 11 only smoothed by the 144 point running average. The smoothing algorithm removes the 60 hertz aliasing. The PCM dropouts appear as "glitches" in the otherwise quasi sinusoid characteristic of a micropulsation.

We should note that the unusually large amount of hash present between 2 hertz and 10 hertz in the PSD's and the average slope of the PSD curve for those frequencies may in part be due to the PCM dropouts that occur on the tapes. A "deglitching" algorithm could be developed to remove the sudden large amplitude structures injected by the system into the voltage data if hardware modifications fail.

## B. TIME SERIES MAGNETIC FIELD DATA

### 1. Magnetic Field Software

The time series magnetic field software is basically the same as that which produces the PSD's, etc. [Ref. 1 and Ref. 3]. The differences begin after the forward Fourier transform and the application of the transfer function. We



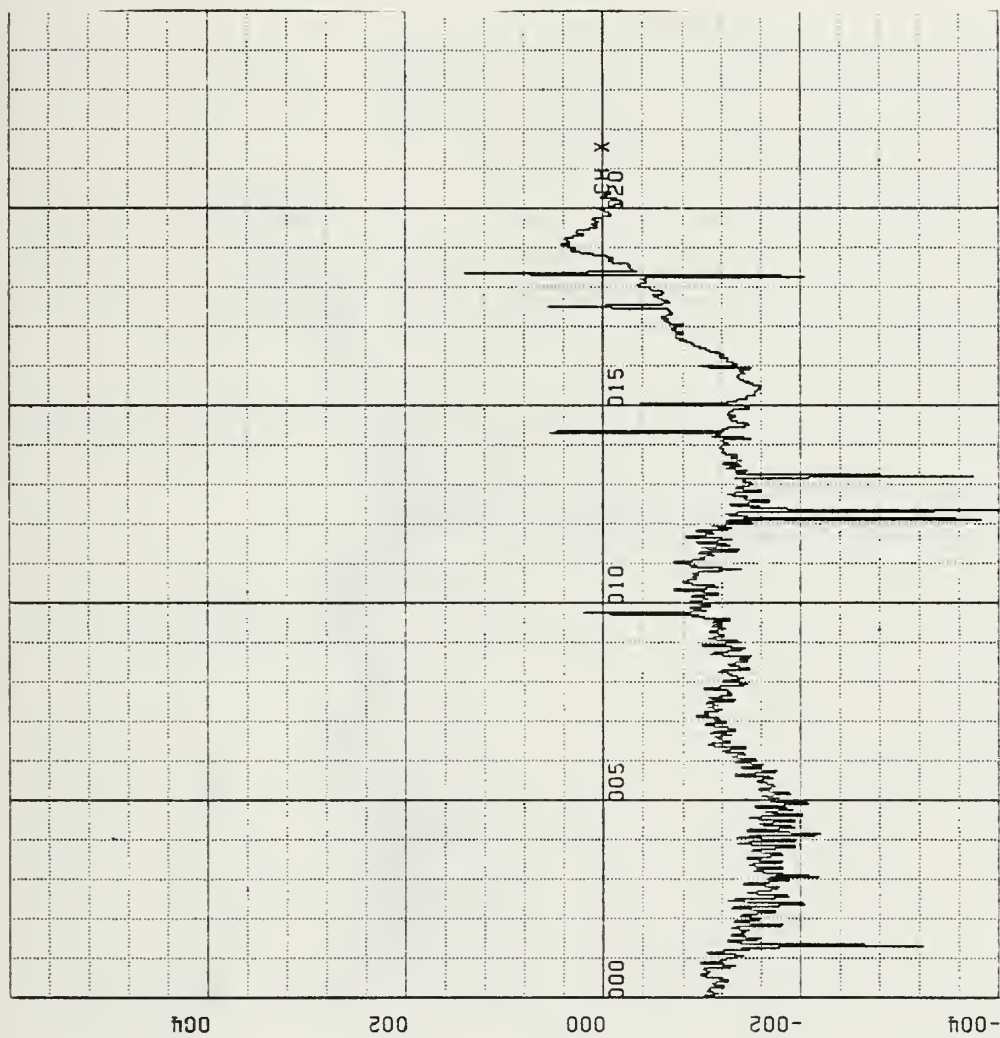


Figure 3.7. X Coil Voltage, 17 August 82, 1302-1336 Local.  
Amplitude (volts : 0.2 units/in) vs. Time (seconds : 500 units/in)





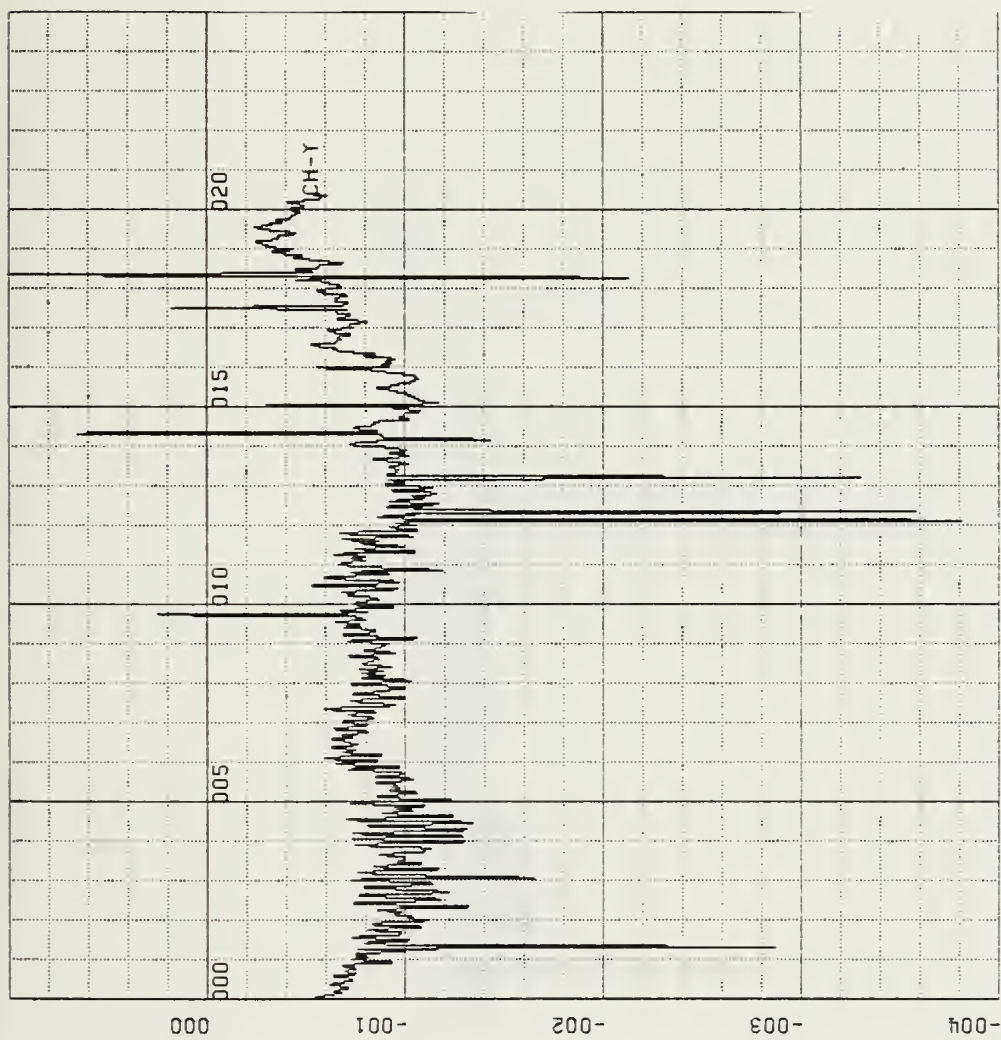


Figure 3.8. Y Coil Voltage, 17 August 82, 1302-1336 Local.  
Amplitude (volts : 0.1 units/in) vs. Time (seconds : 500 units/in)



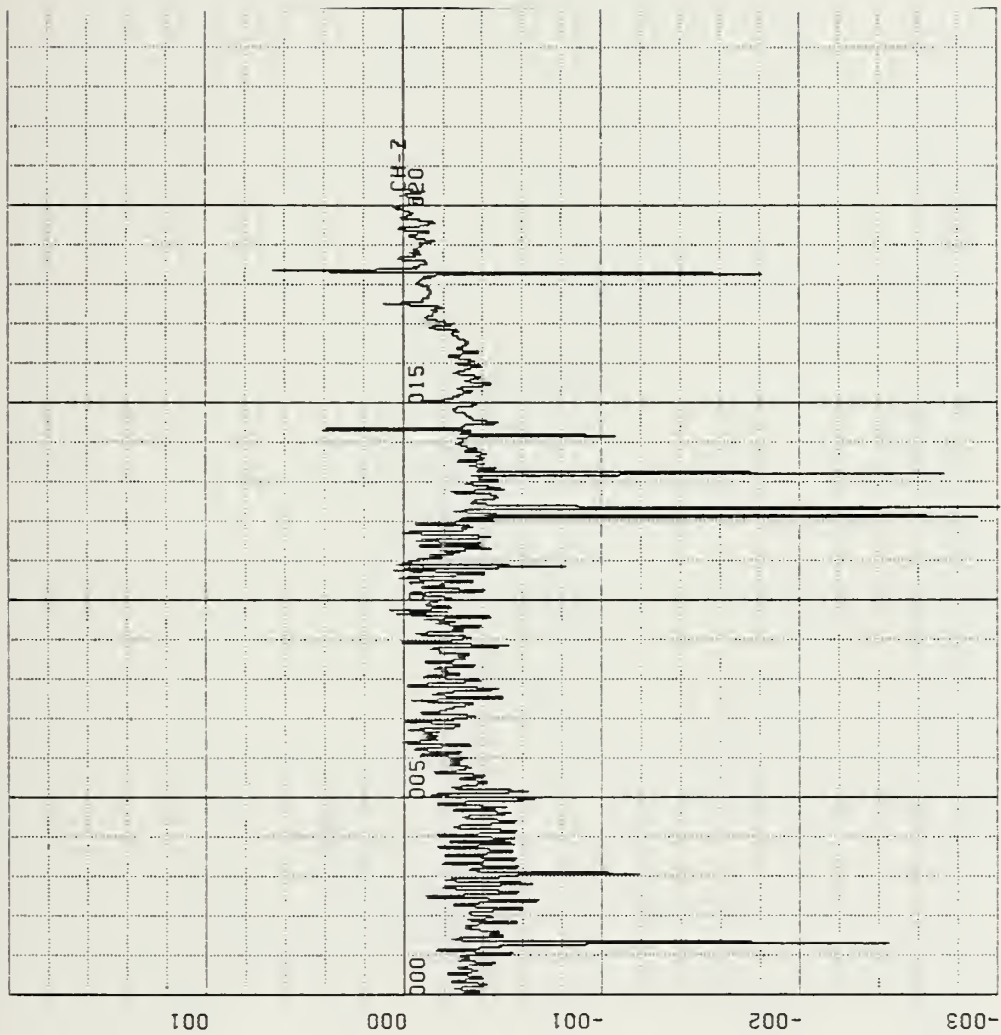


Figure 3.9. Z Coil Voltage, 17 August 82, 1302-1336 Local.  
Amplitude (volts : 0.1 units/in) vs. Time (seconds : 500 units/in)



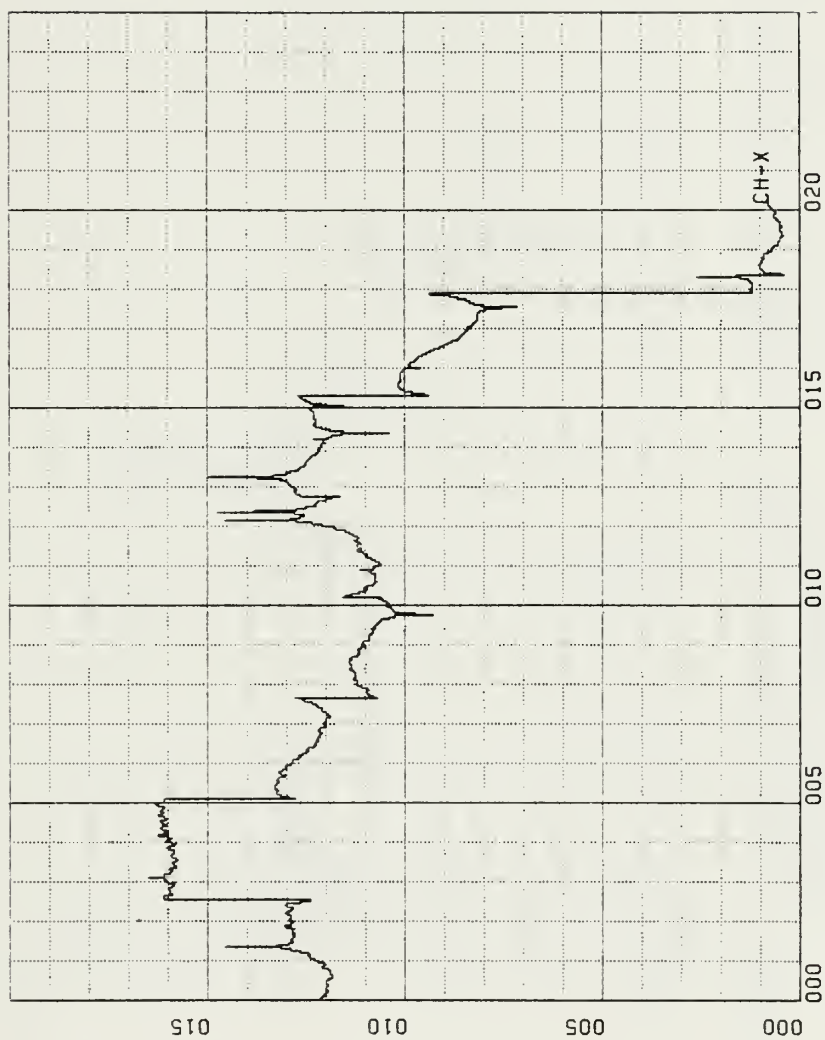


Figure 3.10a. X-Coil Magnetic Field, 17 August 82, 1302-1336 Local.  
 Amplitude (nanoteslas : 5 units/in) vs. Time (seconds : 500 units/in)  
 8 point smoothing



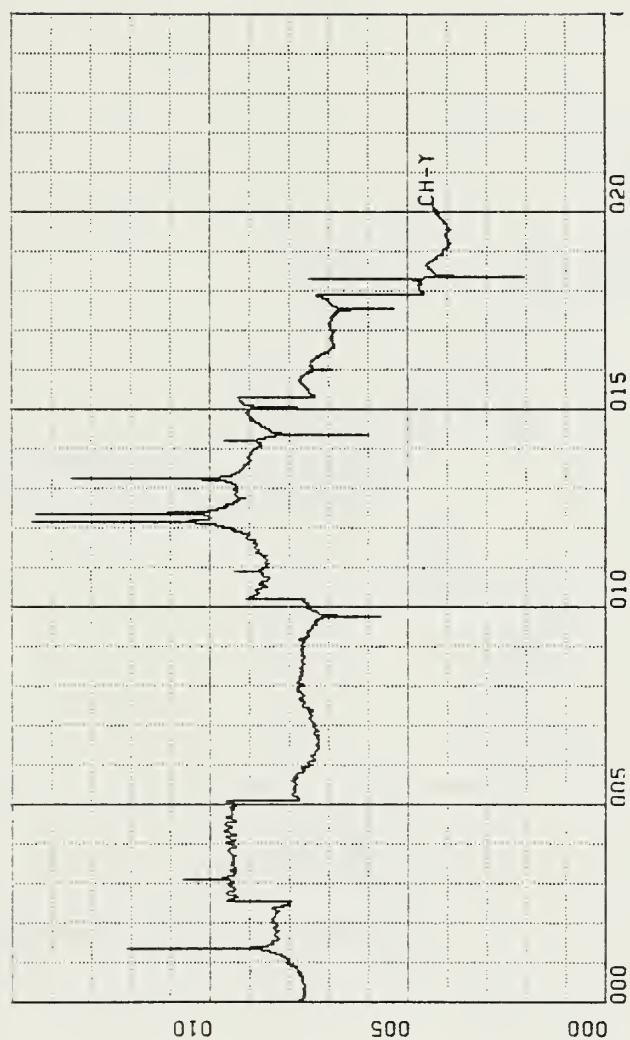


Figure 3.11a. Y-Coil Magnetic Field, 17 August 82, 1302-1336 Local.  
 Amplitude (nanoteslas : 5 units/in) vs. Time (seconds : 500 units/in)  
 8 point smoothing





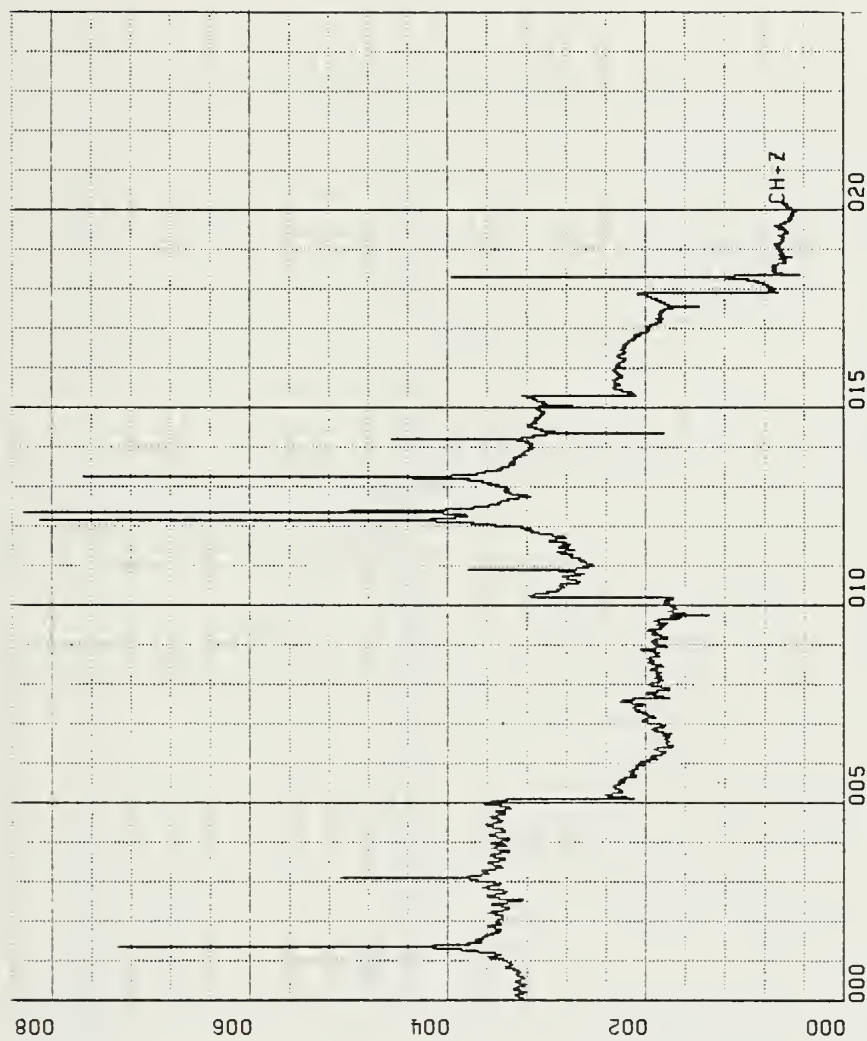


Figure 3.12a. Z-Coil Magnetic Field, 17 August 82, 1302-1336 Local.  
 Amplitude (nanoteslas : 2 units/in) vs. Time (seconds : 500 units/in)  
 8 point smoothing



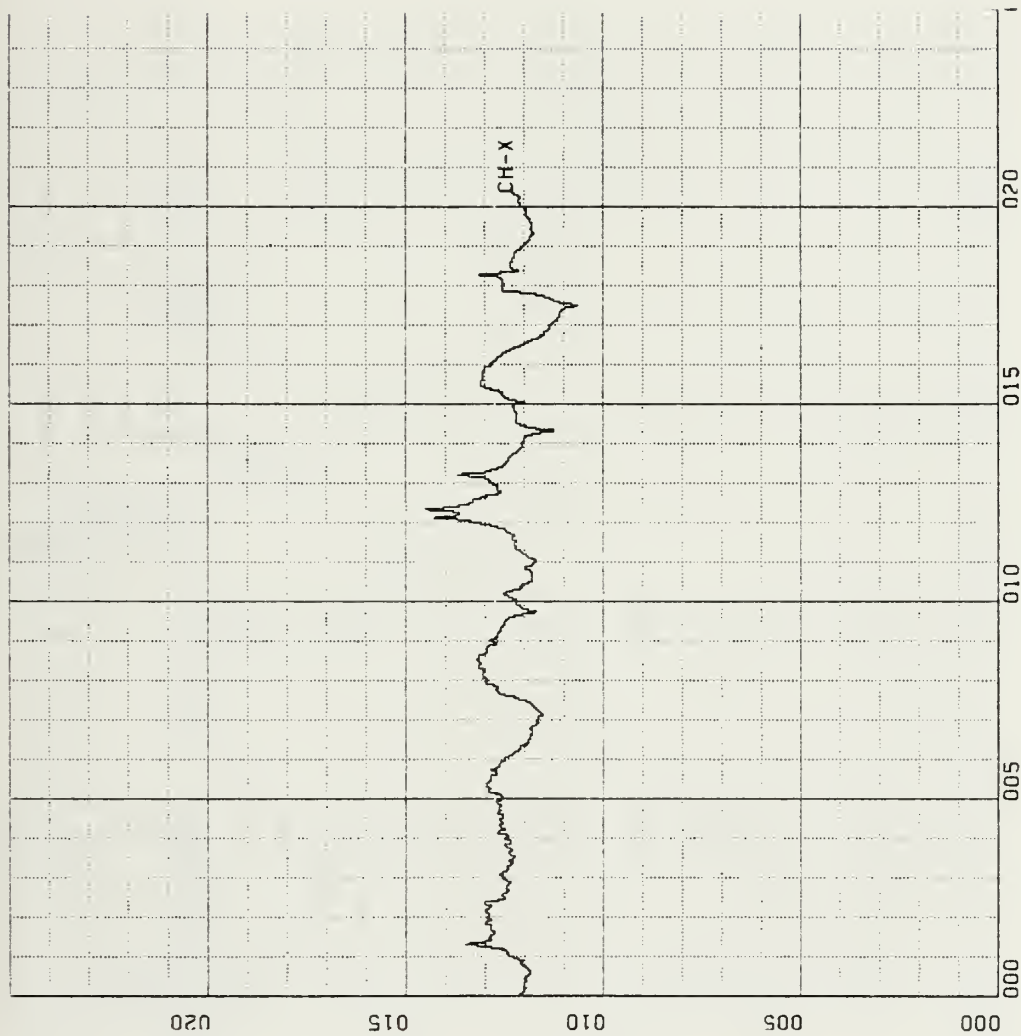


Figure 3.10b. X Coil Magnetic Field, 17 August 82, 1302-1336 Local.  
Amplitude (nanoteslas : 5 units/in) vs. Time (seconds : 500 units/in)  
144 point smoothing



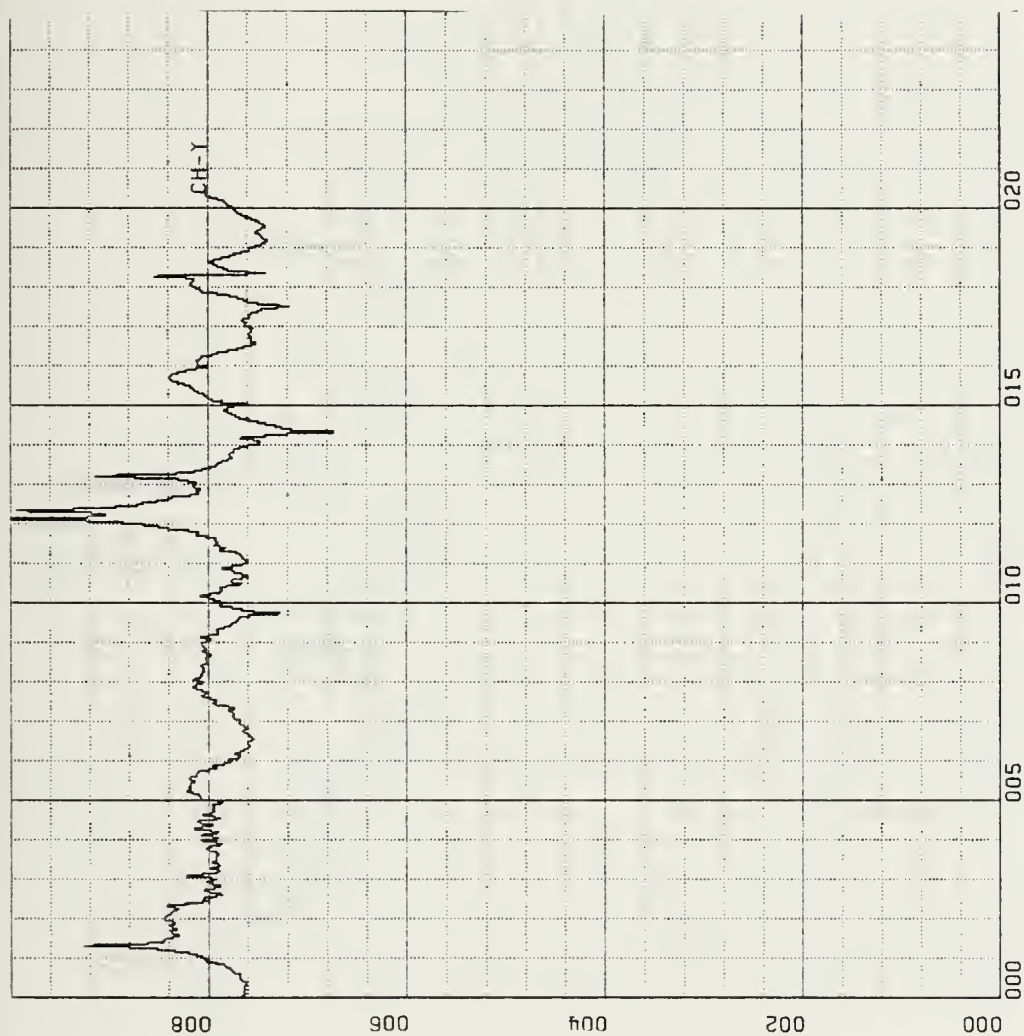


Figure 3.11b. Y Coil Magnetic Field, 17 August 82, 1302-1336 Local.  
 Amplitude (nanoteslas : 1 unit/in) vs. Time (seconds : 500 units/in)  
 144 point smoothing



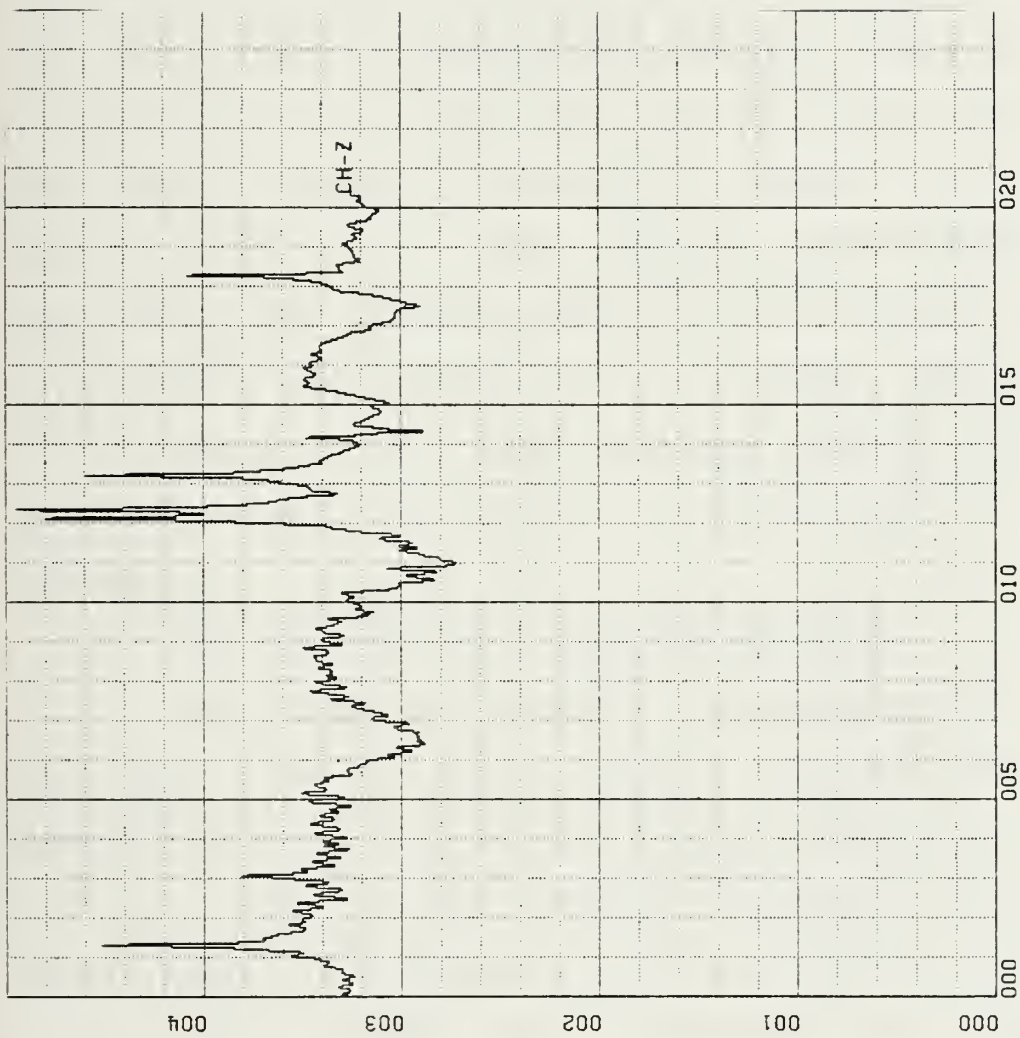


Figure 3.12b. Z Coil Magnetic Field, 17 August 82, 1302-1336 Local,  
 Amplitude (nanoteslas : 1 unit/in) vs. Time (seconds : 500 units/in)  
 144 point smoothing





should note that the transfer function as designed ignores phase information since it is just a least squares fit to data like that of Figure 2.2. Once the transfer function is applied, the reverse transform is performed. We obtain the complex absolute values of the magnetic field data (in nanoteslas) and place the data in new real arrays. To insure that there are no discontinuities between blocks of data, Figures 3.10a, 3.11a and 3.12a, all the blocks are connected to the first by adding or subtracting a constant to each element, Figures 3.10b, 3.11b, 3.12b. The data now undergoes the same 144 point double running average as the voltage to bring out fluctuations with periods of 10-45 seconds. Again DRAWP is used to plot the data. The computer program LVFTCl produces the smoothed magnetic field plots. It is provided in Appendix C.

## 2. Smoothed Magnetic Field Data Analysis

Again looking at the first 34 minutes of digital data tape GMDT 11, we see in the magnetic field data the same exceptional structures as seen in the voltage data, Figures 3.10-3.12. The glitches, however, do highlight one problem rather well. From Figures 3.7-3.9 we note that positive voltage spikes produce negative magnetic field spikes. This would indicate a  $\pi$  phase shift is introduced either in the transfer functions or in the digital Fourier transform. After investigating another digital tape GMDT 3A, 18 August 82, 0121-0251 local, we see another behavior. Figures 3.13-3.15



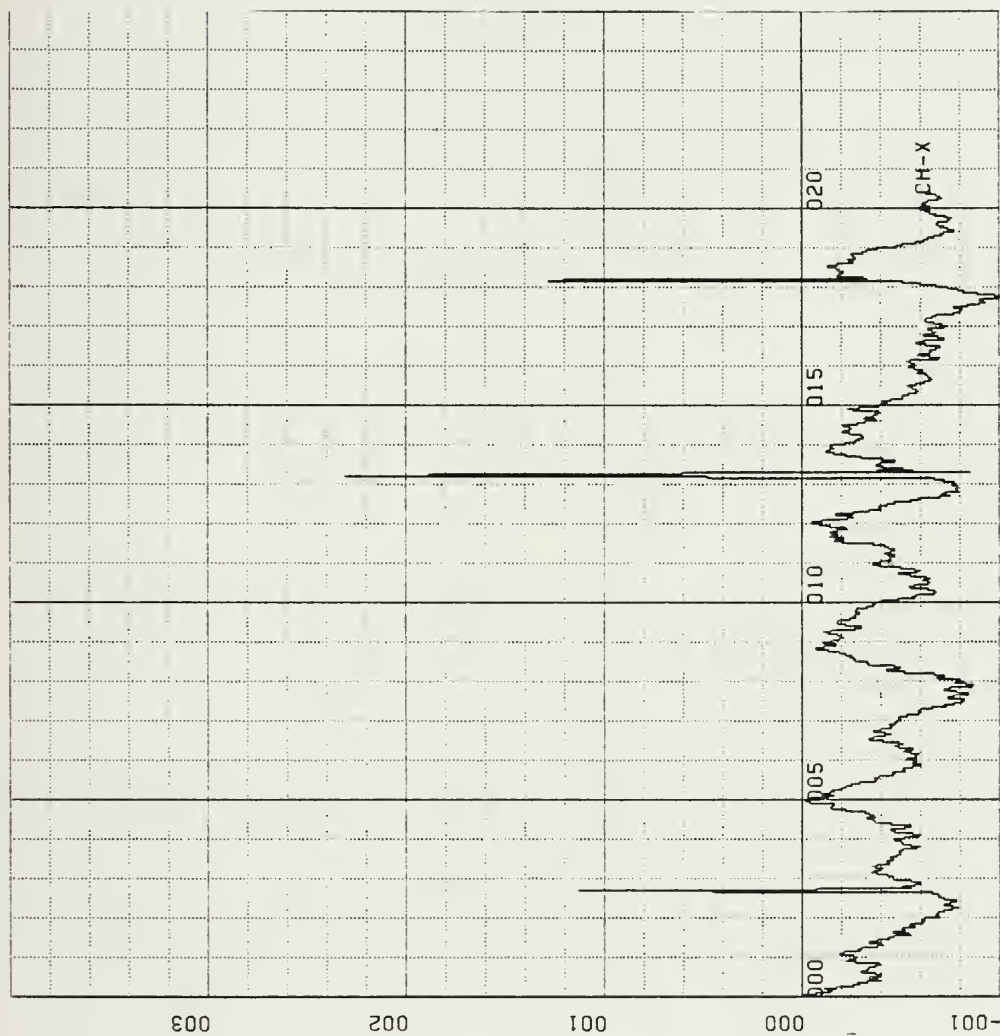


Figure 3.13. X Coil Voltage, 17 August 82, 2241-2315 Local.  
Amplitude (volts : 0.1units/in) vs. Time (seconds : 500 units/in)



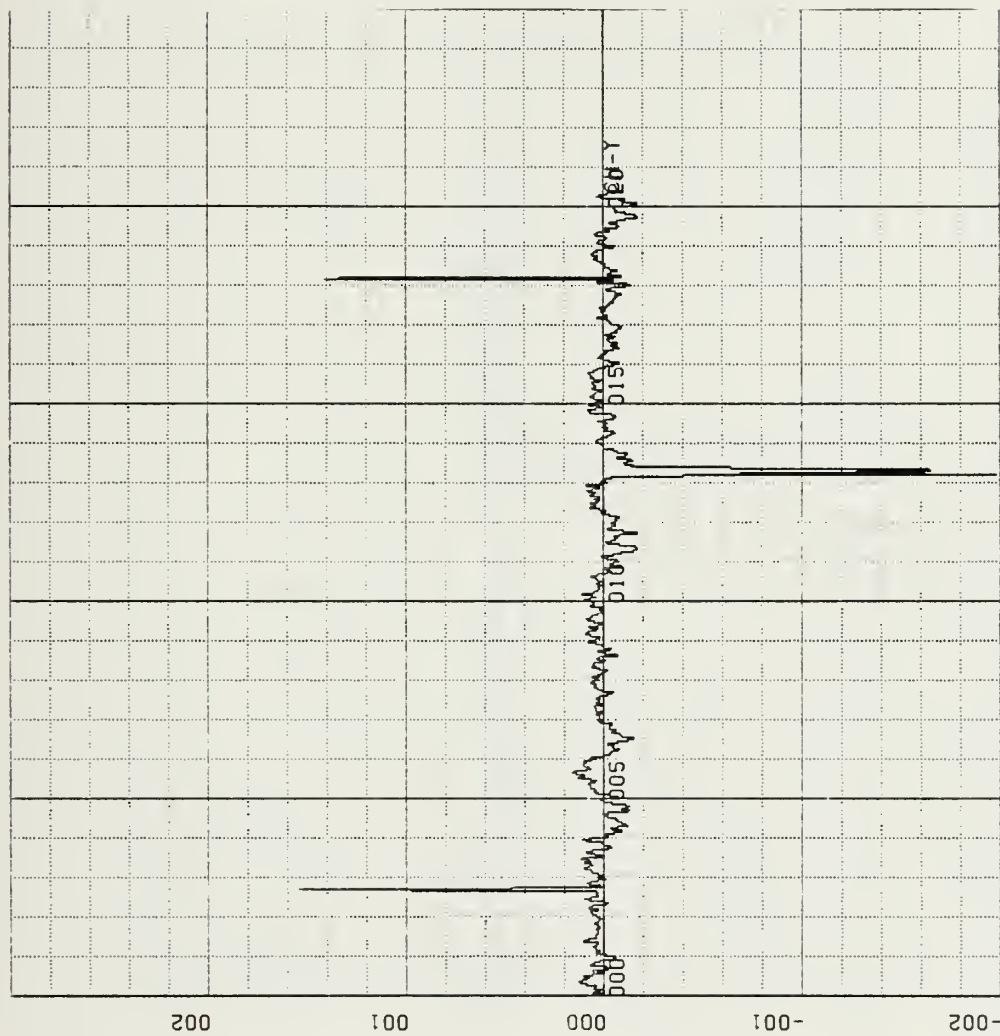


Figure 3.14. Y Coil Voltage, 17 Voltage 82, 2241-2315 Local.  
Amplitude (volts : 0.1 units/in) vs. Time (seconds : 500 units/in)



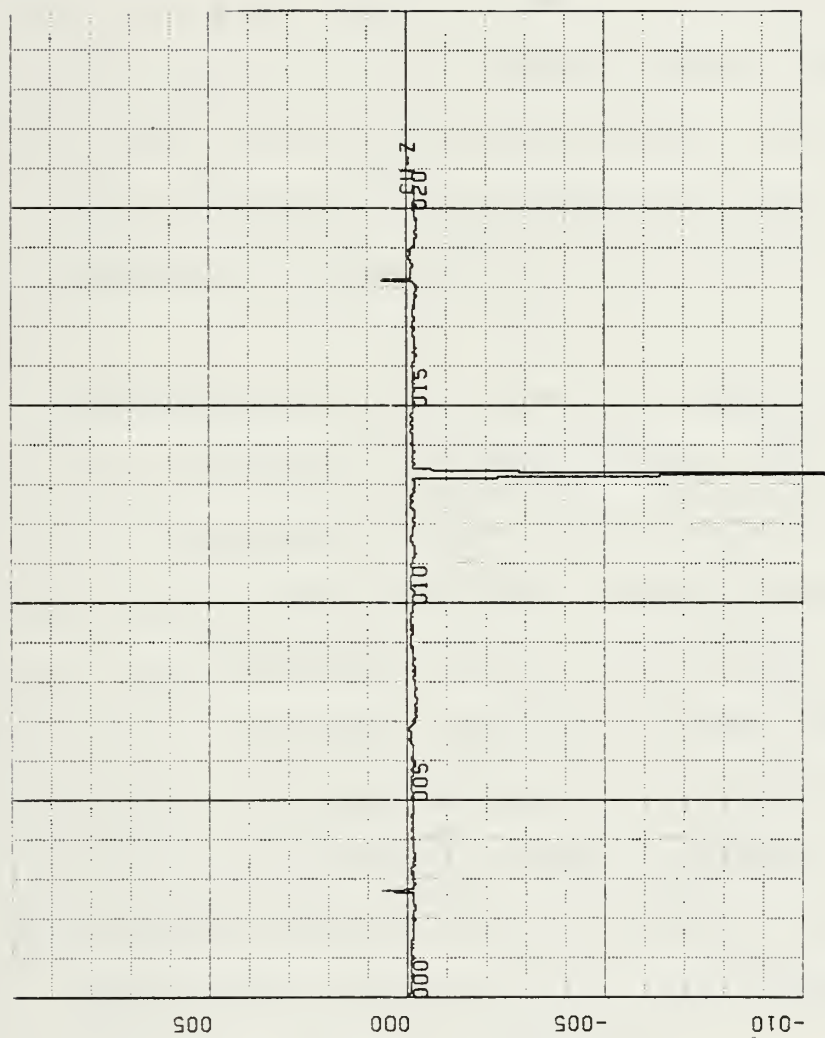


Figure 3.15. Z Coil Voltage, 17 August 82, 2241-2315 Local.  
Amplitude (volts : 0.5 units/in) vs. Time (seconds : 500 units/in)





are the smoothed voltages for the first 34 minutes of data on GMDT3A after a one minute tape advance. Figures 3.16-3.18 are the smoothed magnetic fields for the same time period. The X-coil voltages show three positive spikes while the X-coil magnetic field shows three negative spikes. This supports the theory of a  $\pi$  phase shift. However, the Y-coil voltage shows two positive spikes and one negative spike, while the Y-coil magnetic field has three positive spikes. Thus it appears we have a rather arbitrary phase problem that may find its origin in the transfer functions that do not maintain the correct phase.

From Figures 3.16-3.18 we note exceptional features that do not correspond to voltage spikes. The exceptional features are separated by time periods of 256 seconds which is the size of the blocks analyzed. These features persist with the data block connection scheme and 144 point smoothing. Their origin is not understood. Some data blocks look like Figure 3.19 with the end points having about the same value. However, some have end points as illustrated in Figure 3.20. The varying end point values are also shown in Figures 3.10a, 3.11a and 3.12a. This may be a source of the large amount of hash between 2 hertz and 10 hertz seen in the PSD's.

After looking at the magnetic field data it was obvious a validation experiment was needed for the sensing system and software.



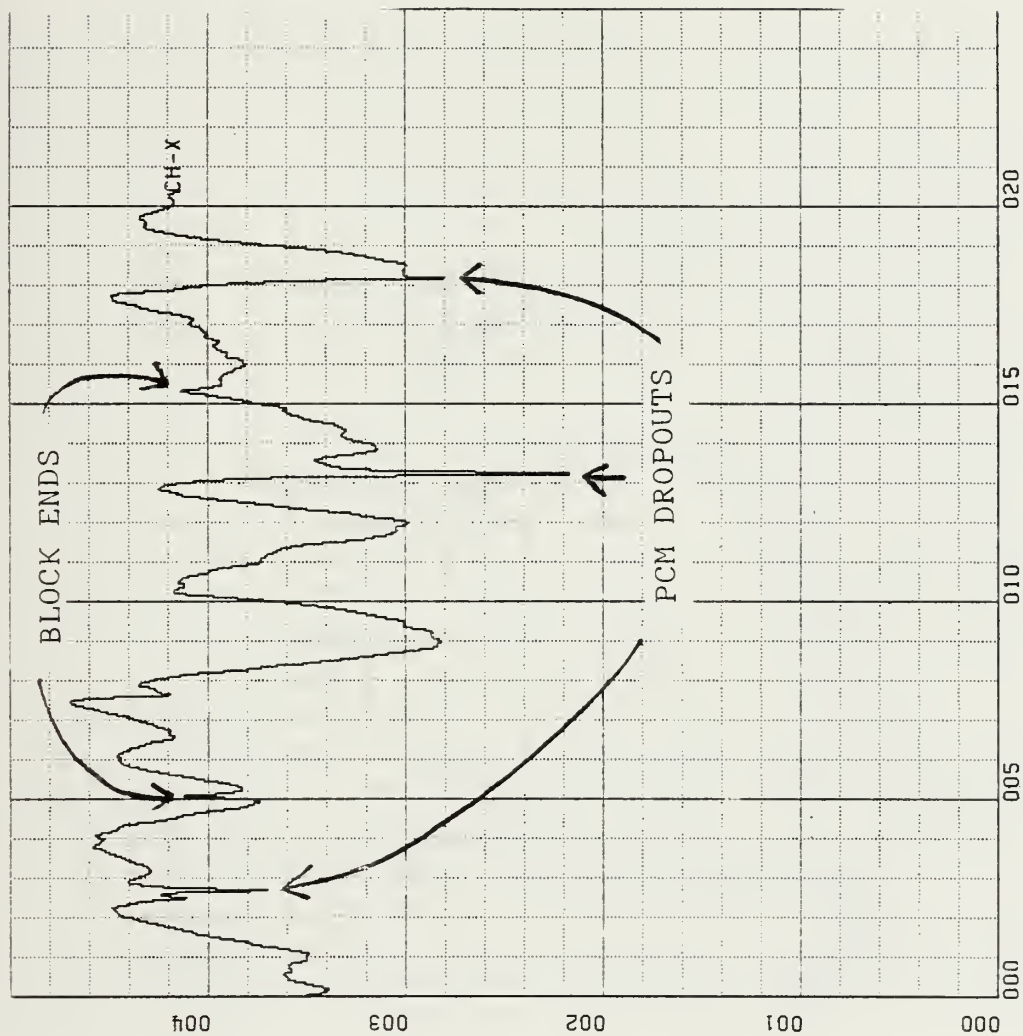


Figure 3.16. X Coil Magnetic Field, 17 August 82, 2241-2315, Local.  
Amplitude (nanoteslas : 1 unit/in) vs. Time (seconds : 500 units/in)



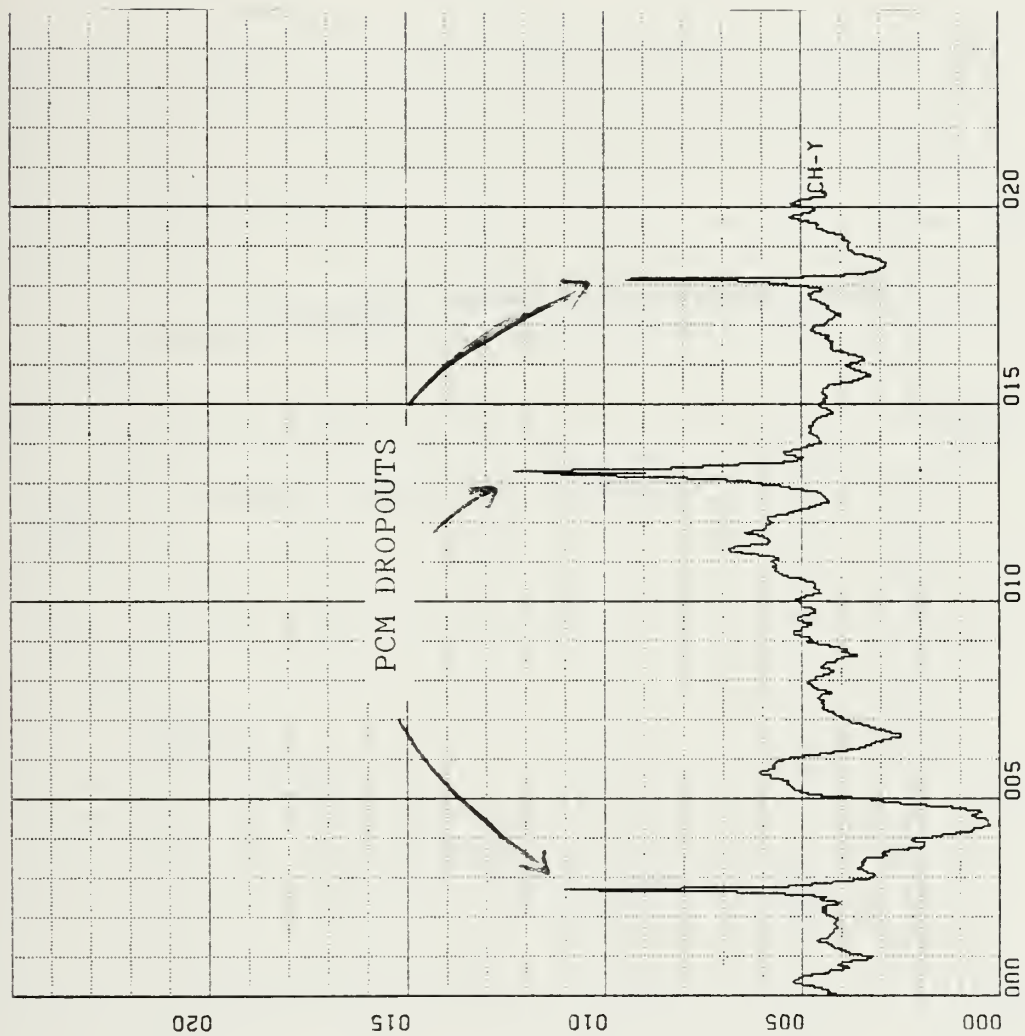


Figure 3.17. Y Coil Magnetic Field, 17 August 82, 2241-2315 Local.  
Amplitude (nanoteslas : 0.5 units/in) vs. Time (seconds : 500 units/in)



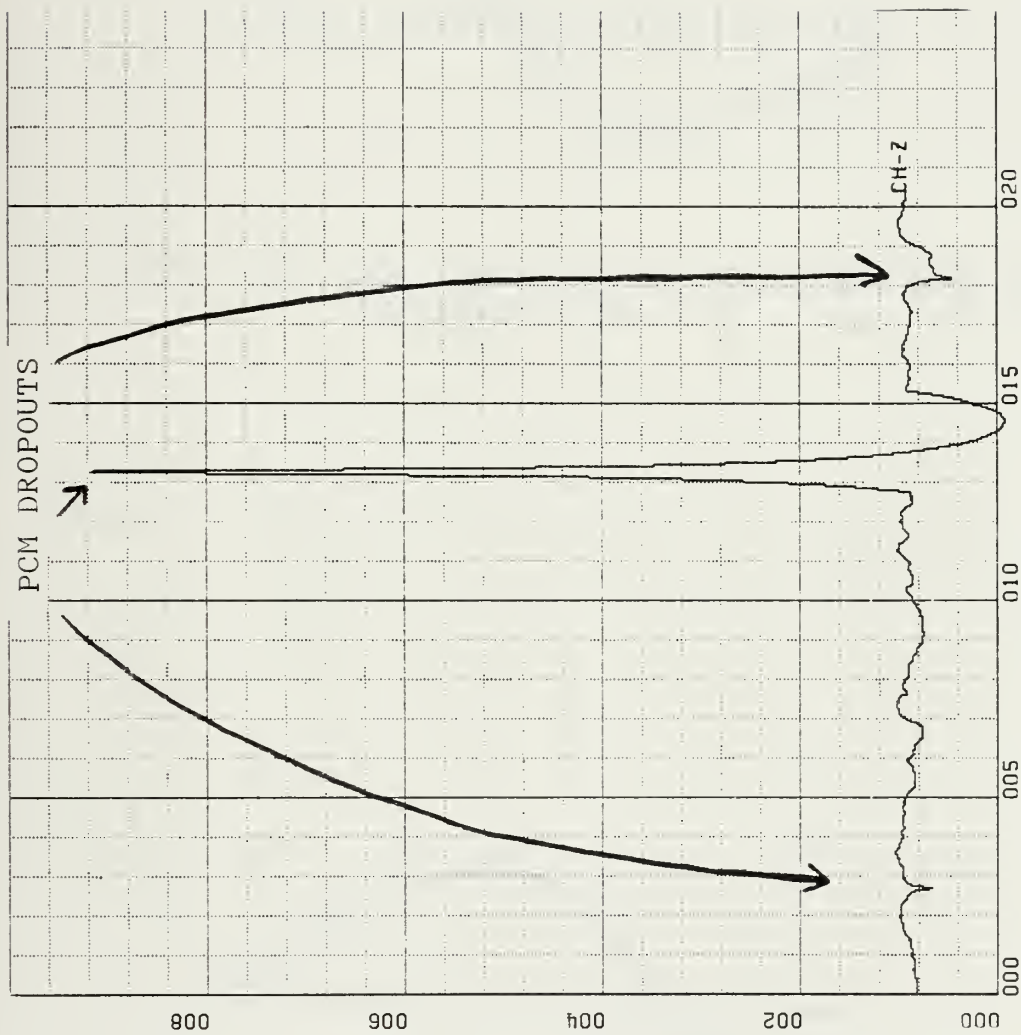


Figure 3.18. Z Coil Magnetic Field, 17 August 82, 2241-2315 Local.  
Amplitude (nanoteslas : 2 units/in) vs. Time (seconds : 500 units/in)







Figure 3.19. One Frame of Data with End Points Having the Same Value

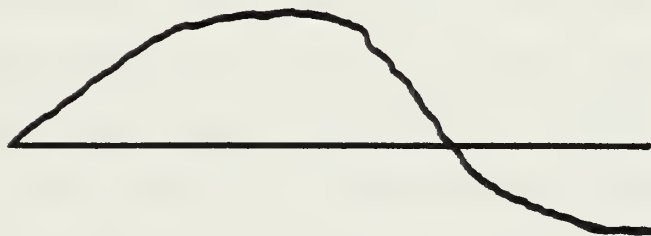


Figure 3.20. One Frame of Data with End Points Having Different Values



#### IV. SYSTEM AND SOFTWARE VALIDATION

##### A. EXPERIMENTAL APPARATUS

The inconsistencies in phase between the time series voltage and magnetic field plots prompted an experiment to validate the sensing system and software. The sensing apparatus consisted of the X-coil and a Schoenstadt fluxgate magnetometer. The sensing axis of both sensors were horizontal and oriented North-South. Figure 4.1 shows the test set-up. Instead of an on axis arrangement, the set-up shown was used because of limited resources. The fluxgate magnetometer is closer to the source since it has less sensitivity at the frequency of interest than the coils. Recorded on the usual X-channel was the output from the X-coil. The Y-channel contained data from the coil after passing through an additional Krohn-Hite model 3321 lowpass filter with a 10 hertz cutoff. On the Z-channel was the output from the fluxgate magnetometer. All three channels were recorded simultaneously and a 64 sample/second sample rate was used. An on-site chart recorder monitored the fluxgate and double filtered coil voltage output real time. The experiment produced two digital data tapes each approximately 46 minutes in length denoted GMTT1A and GMTT1B.

Artificial magnetic fields were introduced into the region by applying sinusoidal currents from a Wavetek signal generator to a cylinder (diameter = 0.13m) wrapped with 150 turns of wire. Location of the source is noted in Figure 4.1. The



Coil Sensing Axis

Fluxgate Sensing Axis

Source

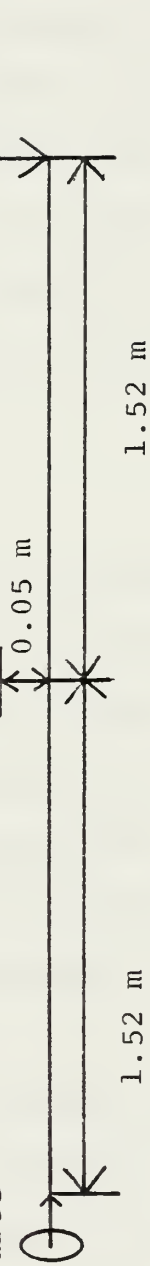


Figure 4.1. Test Arrangement



applied sinusoidal currents varied in frequency from 0.005 hertz to 10 hertz. For each frequency, two magnitude currents were applied to the source to demonstrate a linear response with amplitude.

The fluxgate magnetometer output is correct in phase and amplitude to at least 1 hertz. The transfer function between voltage and magnetic field for the fluxgate magnetometer is a constant of 10 nanoteslas/volt. Thus the fluxgate provides an excellent check for the coil transfer functions, the RD data stripping subroutine and the digital fourier transform.

## B. EXPERIMENT RESULTS

### 1. Voltage

From the real time chart record of voltage for the fluxgate and double filtered coil, we can check the computer generated voltages using VOLTR and VOLTS. Table 4.1 shows the chart record and computer generated voltages for the fluxgate and double filtered coil at various frequencies. Only the large amplitude oscillations are measured for the double filtered coil because of poor signal-to-noise, for the small amplitude oscillations.

Table 4.1 shows good agreement between the chart record and computer output for the double filtered coil. However, the fluxgate magnetometer voltages undergo a constant transformation of 0.831 from chart record to computer plot. This may be explained by a problem in the data stripping





Table 4.1. Coil and Fluxgate Voltage

FREQUENCY (HZ)	CHART RECORD VOLTAGE (V)			COMPUTER GENERATED VOLTAGE (V)		
	FLUXGATE		COIL	FLUXGATE		COIL
	<u>Large Amplitude Oscillation</u>	<u>Small Amplitude Oscillation</u>	<u>Large Amplitude Oscillation</u>	<u>Large Amplitude Oscillation</u>	<u>Small Amplitude Oscillation</u>	<u>Large Amplitude Oscillation</u>
0.1	2.45	0.78	0.90	2.00	0.60	0.90
0.09	2.45	0.80	0.76	1.98	0.60	0.83
0.08	2.45	0.78	0.69	2.00	0.60	0.70
0.07	2.44	0.70	0.66	2.00	0.60	0.68
0.06	2.46	0.77	0.50	1.97	0.60	0.50
0.05	2.45	0.79	0.40	2.20	0.75	0.40
0.04	2.41	0.78	0.40	2.15	0.70	0.37
0.03	2.50	0.82	0.30	2.02	0.65	0.33
0.02	2.50	0.76	0.20	2.03	0.60	0.31
0.01	2.50	0.78		1.96	0.57	

Double filtered coil and fluxgate magnetometer voltages,  
real time and computer generated.



algorithm. The present agreement between the chart record and computer generated voltages is shown in Table 4.2.

Another more serious problem became obvious during the examination of the computer generated voltage plots. For approximately the first 20 minutes of data recording the fluxgate magnetometer was not connected to the PCM board. Figures 4.2-4.4 show the two respective sensing devices. Figures 4.2 and 4.3 both contain "real" signal while Figure 4.4 does not contain "real" signal until the amplitude discontinuity indicating connection of the fluxgate magnetometer to the PCM board. Figures 4.2-4.4 indicate that "pick-up" is occurring probably between the channels at the PCM board. The amplitude of the cross-talk voltage is about 0.15 volts peak-to-peak at the frequency of 0.1 hertz. The amplitude of the "real" signal on the double filtered coil is 0.29 volts at 0.1 hertz. Thus 51 percent of the "real" signal is coupled to the disconnected channel. Coupling between channels of this magnitude raises serious questions about the computer generated data, especially for coherence. Discovering the amount of the channel pick-up if the channel is loaded requires further experimentation.

Figures 4.5-4.7 show an interesting feature of the coil data versus fluxgate magnetometer data. On the channels containing the coil output we see noise on top of the signal. This noise is not present on the channel containing the fluxgate magnetometer data. Since all three channels passed



Table 4.2. Percent Agreement Between the Chart Record  
and Computer Generated Voltages

<u>FREQUENCY (HZ)</u>	<u>FLUXGATE FIELD (%)</u>		<u>COIL FIELD (%)</u>	
	<u>Large Amplitude Oscillation</u>	<u>Small Amplitude Oscillation</u>	<u>Large Amplitude Oscillation</u>	
0.1	87	74	100	
0.09	87	72	94	
0.08	87	76	99	
0.07	87	84	98	
0.06	87	84	100	
0.05	87	97	100	
0.04	87	93	92	
0.03	87	84	94	
0.02	87	80	69	
0.01	86	80		



# 0.1 Hz with 60 Hz Aliasing

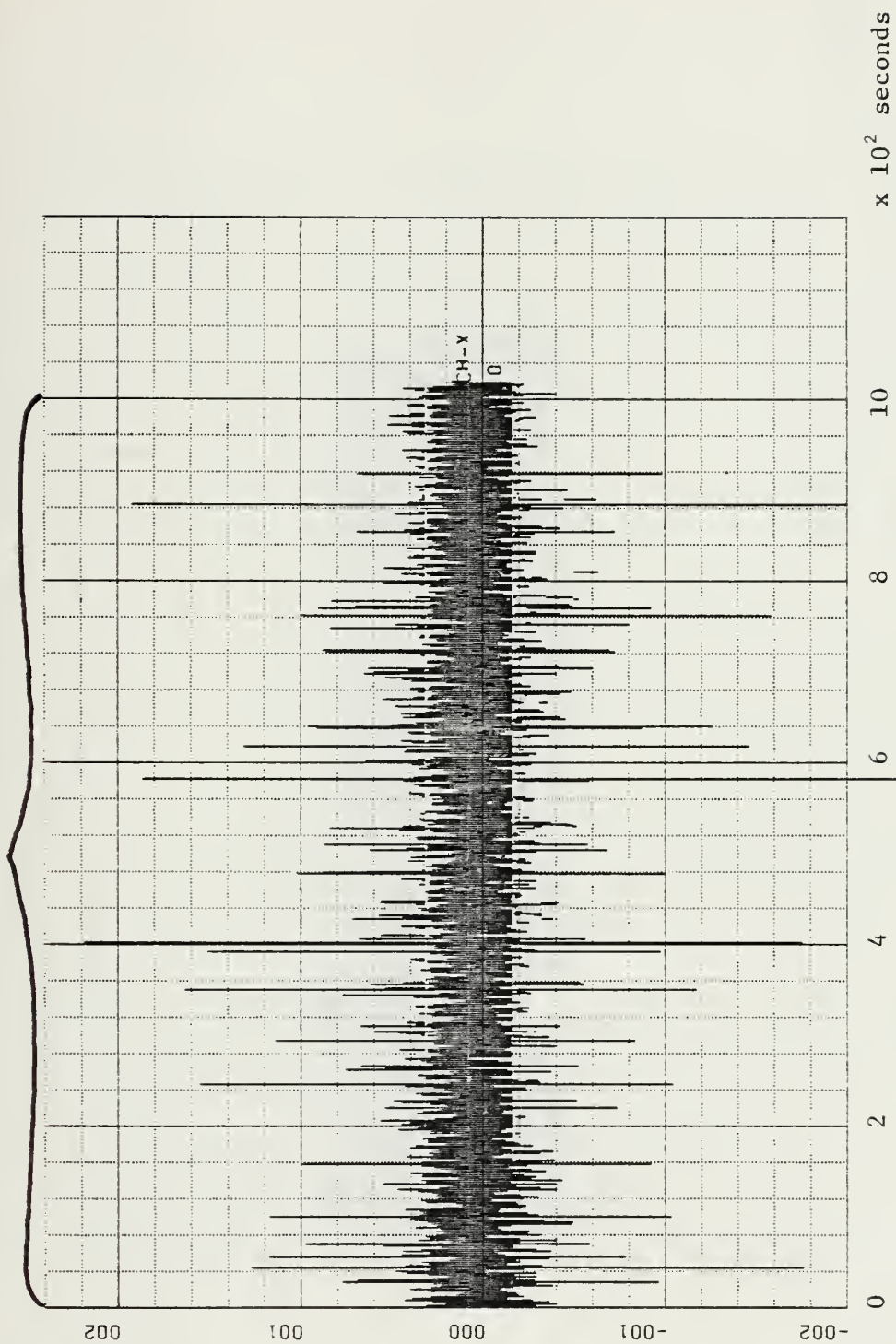


Figure 4.2. X-Coil Voltage, 26 April 83, 0931-0948 Local.  
Amplitude (volts : 1 unit/in) vs. Time (seconds : 200 units/in)





0.1 Hz

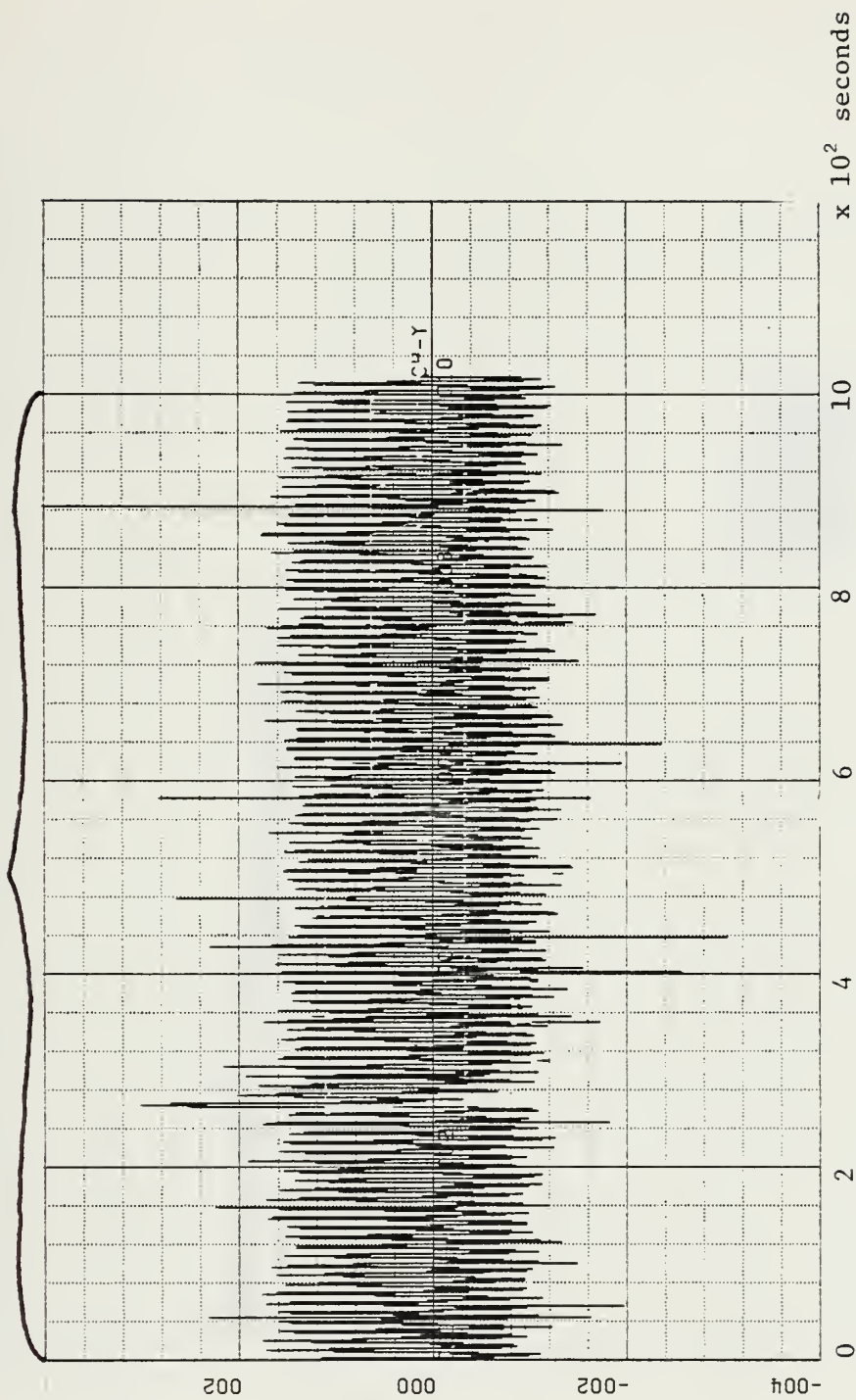


Figure 4.3. Filtered X-Coil Voltage, 26 April 83, 0931-0948 Local.  
Amplitude (volts : 0.2 units/in) vs. Time (seconds : 200 units/in)



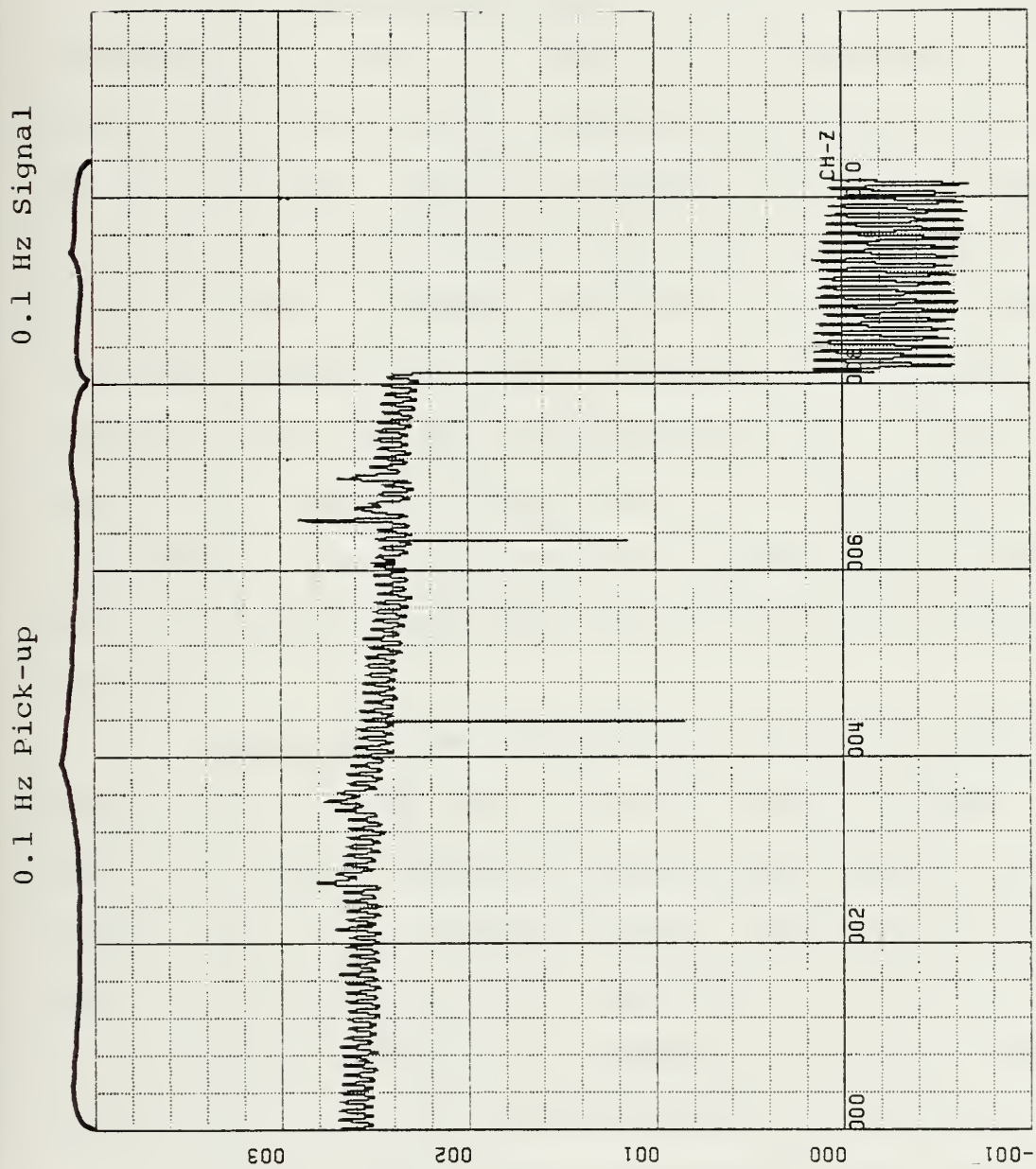


Figure 4.4. Fluxgate Voltage, 26 April 83, 0931-0948 Local.  
Amplitude (volts : 1 unit/in) vs. Time (seconds : 200 units/in)



through the PCM encoder and decoder, the noise is probably in the coil amplifiers or the coils themselves. An experiment to investigate the true origin of the noise should be done.

## 2. Magnetic Field

Given the dipole equation [Ref. 6] and the experimental arrangement in Figure 4.1, the ratio of magnitude of the magnetic field seen by the fluxgate to that seen by the coil can be calculated. From the geometry in Figure 4.1 the field at the coil would be a factor of 8 less than that seen by the fluxgate. This is because the source is a dipole and the field of a dipole falls off as  $1/R$ . Detailed consideration of the geometry gives a ratio of approximately 8.09. Table 4.3 contains the magnetic field measured at the fluxgate magnetometer. Using the ratio calculated from the geometry, the expected magnetic field amplitude at the coil is listed in Table 4.3.

A modified form of computer code LFVTC1 generated the magnetic field versus time plots for the test tapes. Table 4.3 shows the computer generated peak-to-peak magnetic field values read from the computer plots. From Table 4.3 it appears that the coil magnetic field amplitude is in error by a factor of approximately three (with exception to the low frequencies). One can conclude that a problem exists in the software.

Figures 4.8-4.9 show the magnetic field data for the second seventeen minutes of digital data tape GMTT1A. Figure 4.9 is the magnetic field measured by the fluxgate magnetometer



Table 4.3. Measured and Computer Generated Magnetic Field Magnitudes

FREQUENCY (Hz)	KNOWN FLUXGATE FIELD (nT)			EXPECTED COIL FIELD (nT)			EXPECTED RATIO FLUXGATE/COIL			COMPUTER COIL FIELD (nT)			ACTUAL RATIO FLUXGATE/COIL		
	LARGE AMPLITUDE OSCILLATION	SMALL AMPLITUDE OSCILLATION		LARGE AMPLITUDE OSCILLATION	SMALL AMPLITUDE OSCILLATION		LARGE AMPLITUDE OSCILLATION	SMALL AMPLITUDE OSCILLATION		LARGE AMPLITUDE OSCILLATION	SMALL AMPLITUDE OSCILLATION		LARGE AMPLITUDE OSCILLATION	SMALL AMPLITUDE OSCILLATION	
0.1	24.50	7.80		3.04	0.96		8.06	8.12		1.08	0.30		22.69	26.00	
0.09	24.50	8.00		3.03	0.99		8.09	8.08		1.00	0.35		24.50	22.86	
0.08	24.50	7.80		3.04	0.96		8.06	8.12		0.98	0.30		25.00	26.00	
0.07	24.40	7.00		3.02	0.87		8.08	8.05		0.98	0.32		24.89	21.88	
0.06	24.60	7.70		3.05	0.94		8.07	8.19		0.90	0.30		27.33	25.67	
0.05	24.50	7.90		3.03	0.98		8.09	8.06		0.76	0.35		32.23	22.57	
0.04	24.10	7.80		3.01	0.96		8.01	8.12		0.28	0.24		86.07	32.5	
0.03	25.00	8.20		3.09	1.01		8.09	8.12		0.32	0.14		78.13	58.57	
0.02	25.00	7.60		3.09	0.92		8.09	8.26		0.64	0.24		39.06	31.67	
0.01	25.00	7.80		3.09	0.96		8.09	8.12		0.40	0.14		62.50	55.71	





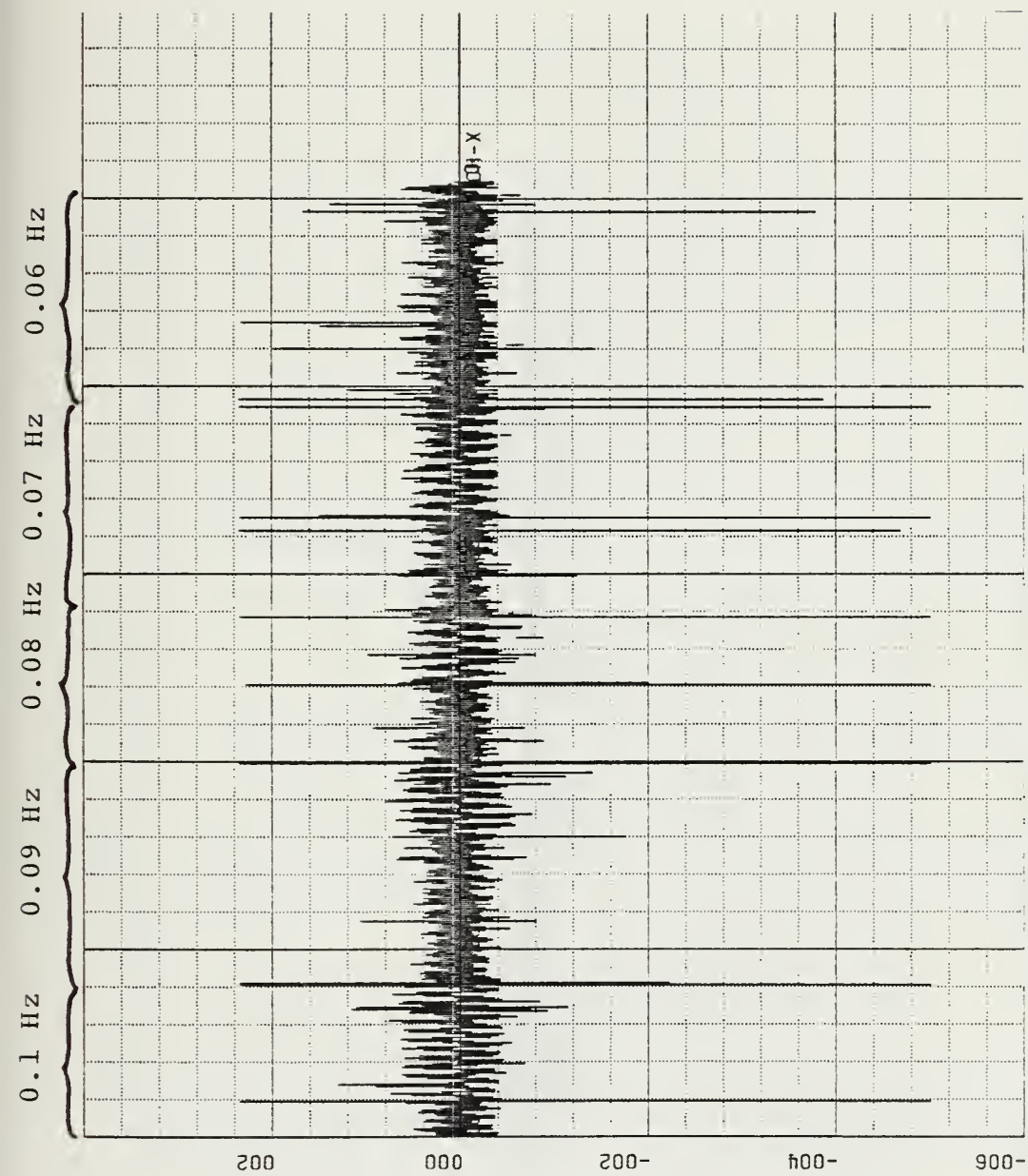


Figure 4.5. X-Coil Voltage, 26 April 83, 0948-1005 Local.  
Amplitude (volts : 2 units/in) vs. Time (seconds : 200 units/in)



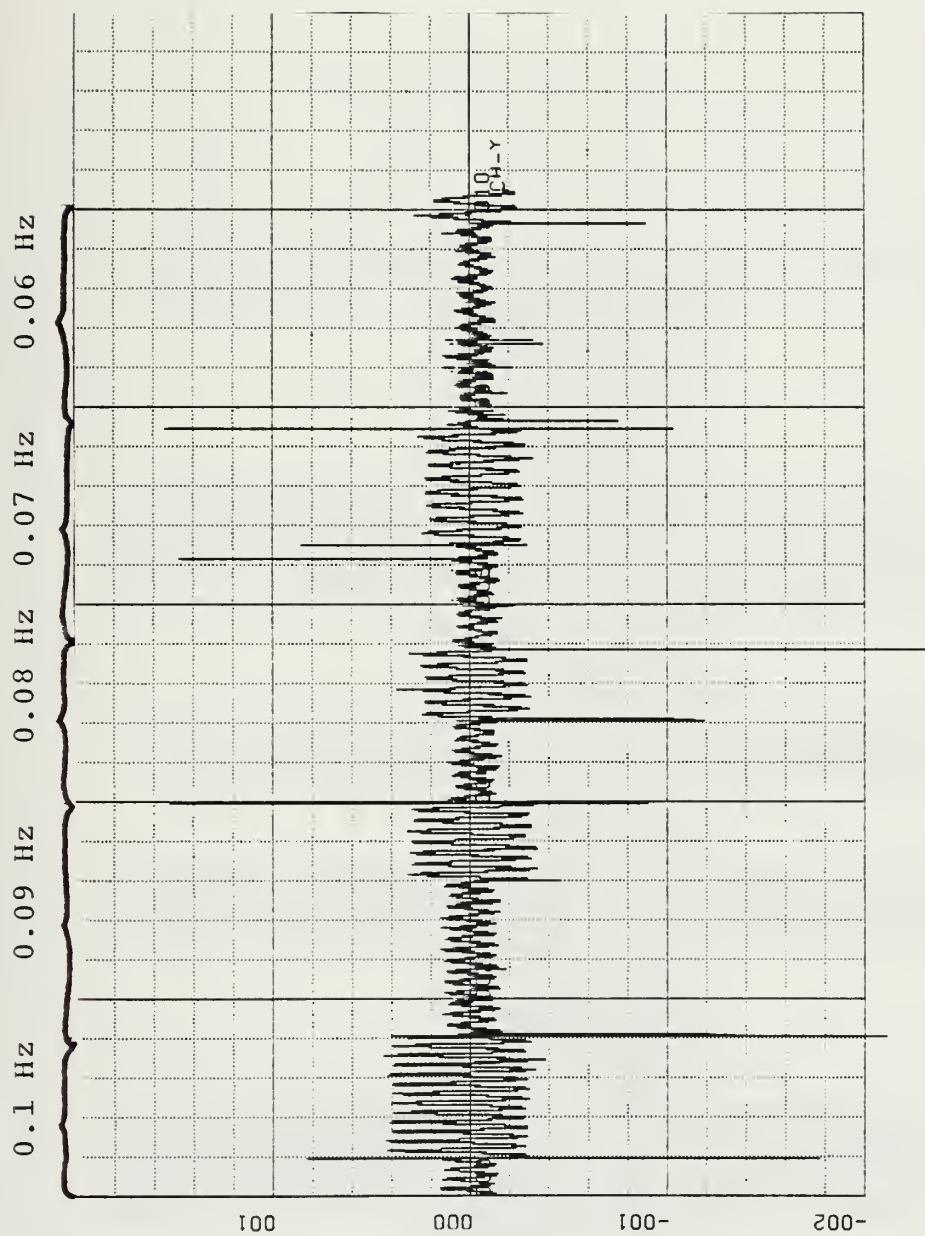


Figure 4.6. Filtered X-Coil Voltage, 26 April 83, 0948-1005 Local.  
Amplitude (volts : 1 unit/in) vs. Time (seconds : 200 units/in)



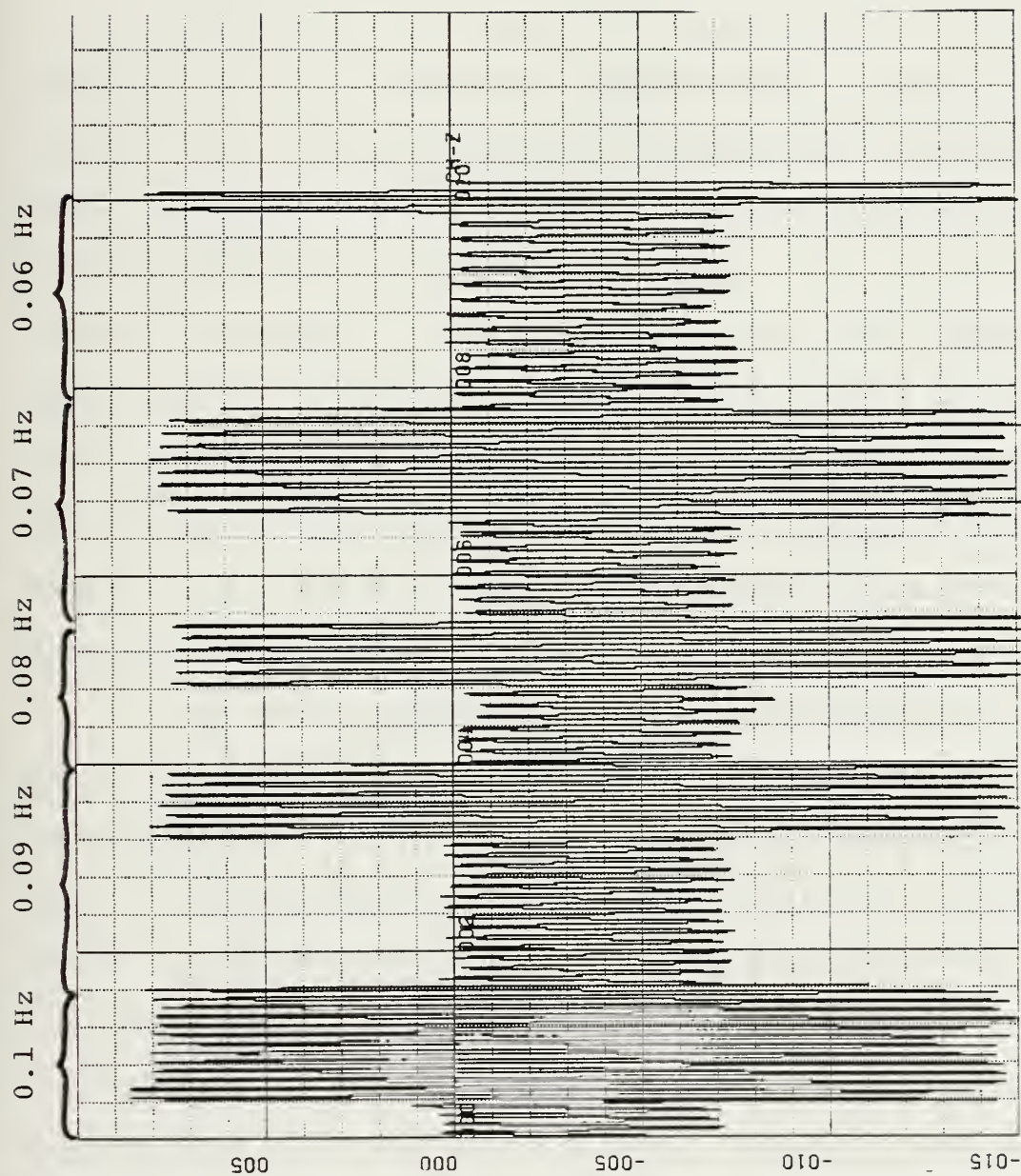


Figure 4.7. Fluxgate Voltage, 26 April 83, 0948-1005 Local.  
Amplitude (volts : 0.5 units/in) vs. Time (seconds : 200 units/in)





and Figure 4.8 is the magnetic field seen by the coil. For the coil we see discontinuities every 256 seconds corresponding to the block size of data. This indicates that the problems in the data block end points, as mentioned in Section III, do exist. It is not clear how to deal with this.

The first 300 seconds of Figures 4.8-4.9 is expanded in Figures 4.11-4.12. With the expanded data a phase difference between coil and fluxgate can be determined. By checking the phase difference, we can determine whether the phase independent transfer function is introducing error. For the 0.1 hertz field plotted in Figures 4.10-4.11 the coil lags the fluxgate by approximately 72 degrees. In Figures 4.12-4.13 we see that at 0.01 hertz the coil sensitivity has fallen and a reliable phase difference between the fluxgate and coil cannot be made. Figure 4.14 shows the relationship between phase angle and frequency.

The above experiment shows the advantages of having a real time "ground truth" record. With this, one can avoid "working in the blind". Computer products will have a check. Thus, a multi-channel chart recorder should be purchased to graph in real time the x, y, and z inputs to the PCM board. In addition, electronic circuitry should be developed and incorporated so that the chart records represent at least a low pass filtering of the coil voltages. Ideally, conversion of voltage to magnetic field could occur in real time at this point given the appropriate electronics.





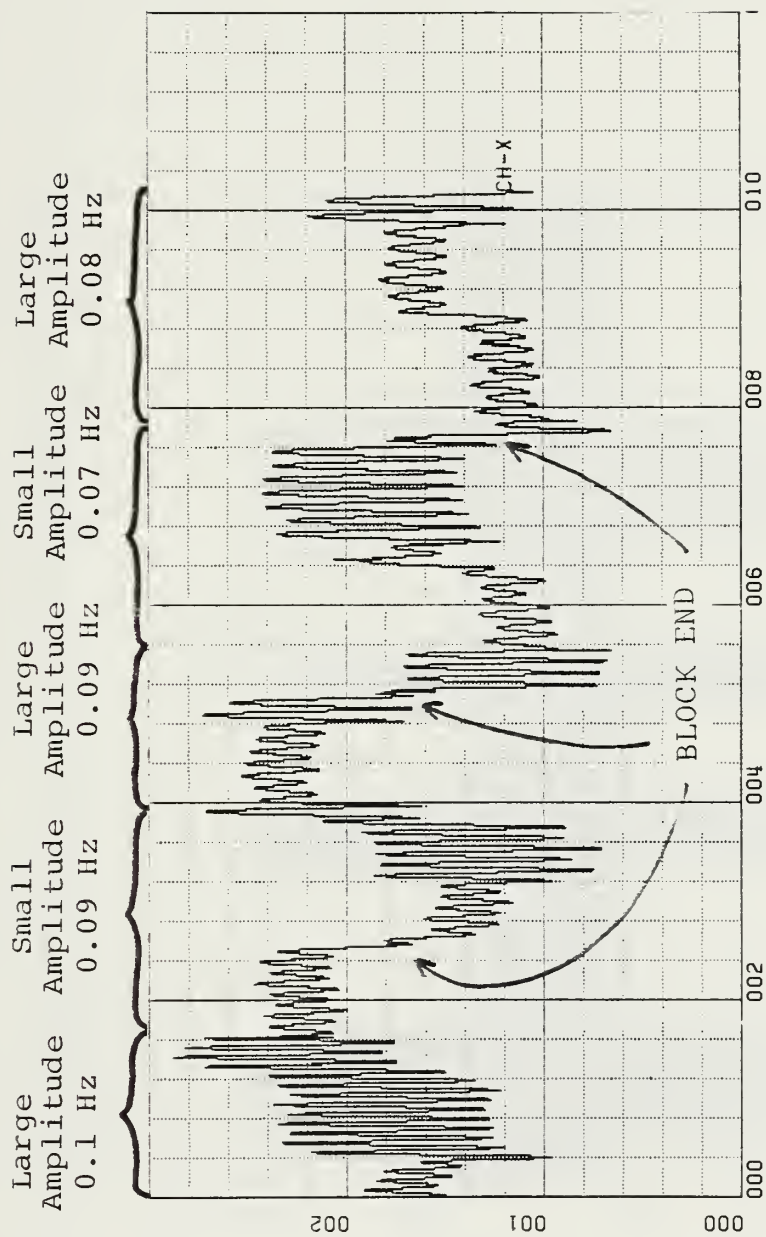


Figure 4.8. X-Coil Magnetic Field, 26 April 83, 0948-1005 Local.  
Amplitude (nanoteslas : 1 unit/in) vs. Time  
(seconds : 200 units/in)



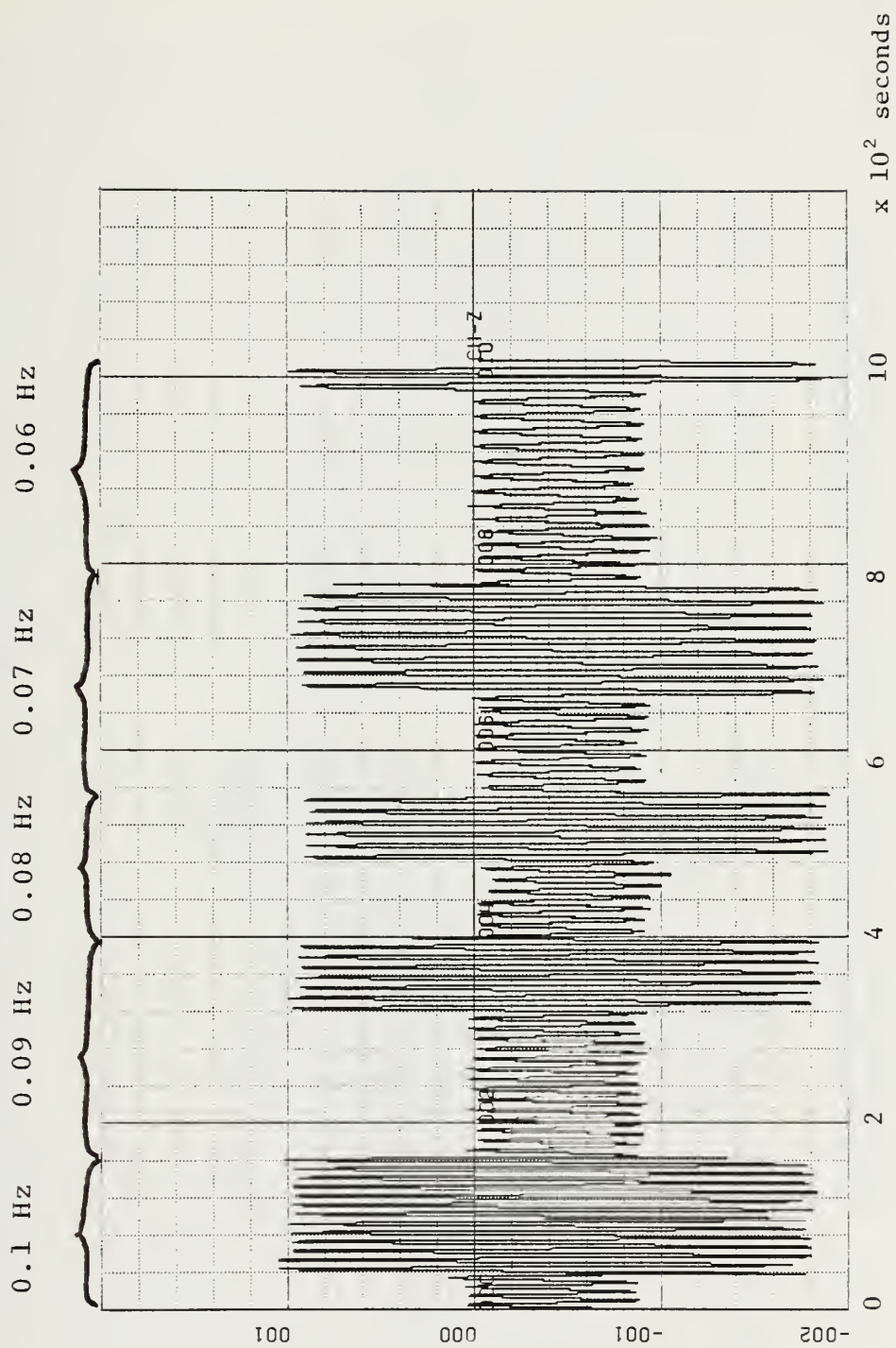


Figure 4.9. Fluxgate Magnetic Field, 26 April 83, 0948-1005 Local.  
 Amplitude (nanoteslas : 10 units/in) vs. Time  
 (seconds : 200 units/in)



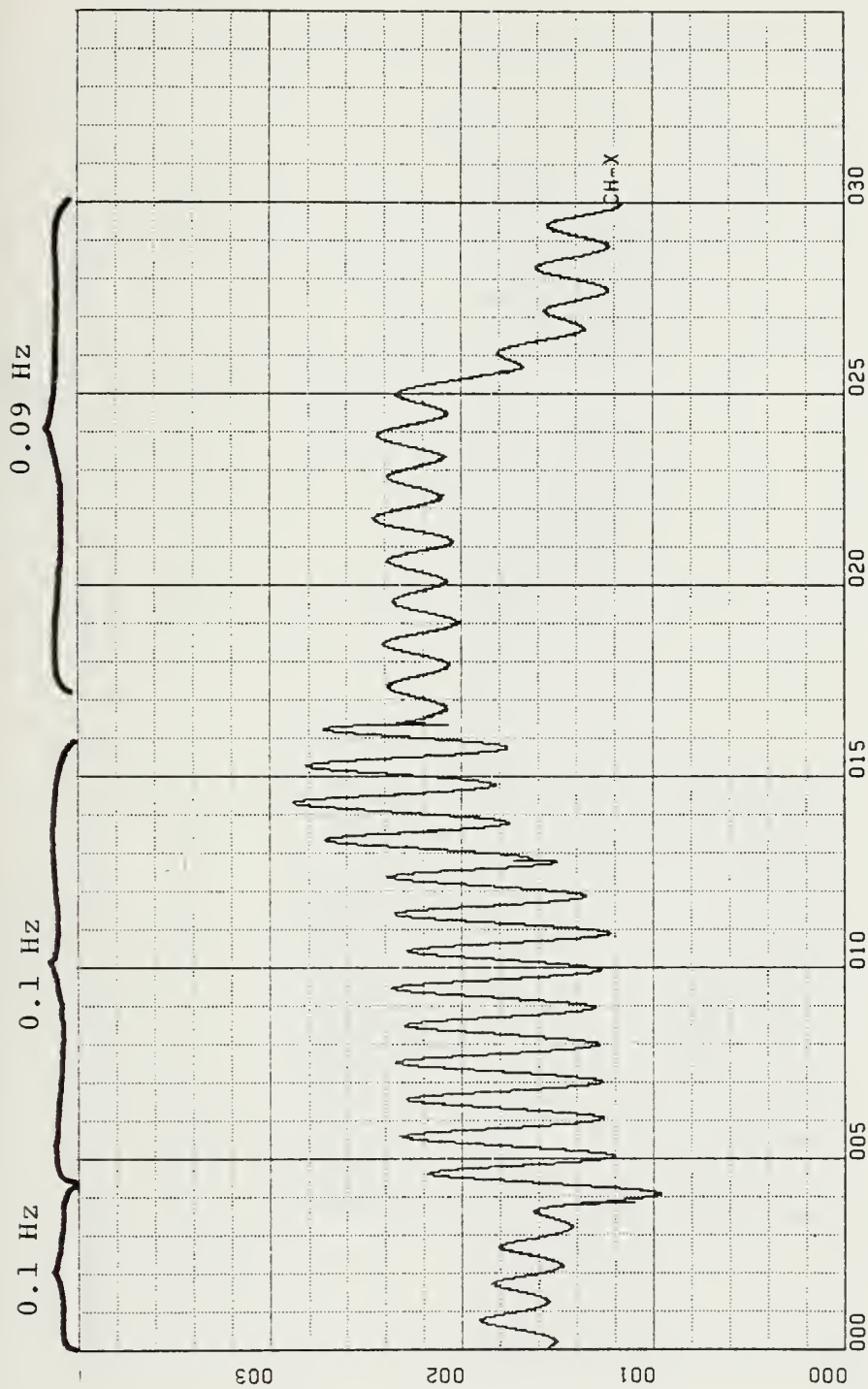


Figure 4.10. X-Coil Magnetic Field, 26 April 83, 0948-0953 Local.  
Amplitude (nanoteslas : 1 units/in) vs. Time (seconds : 50 units/in)



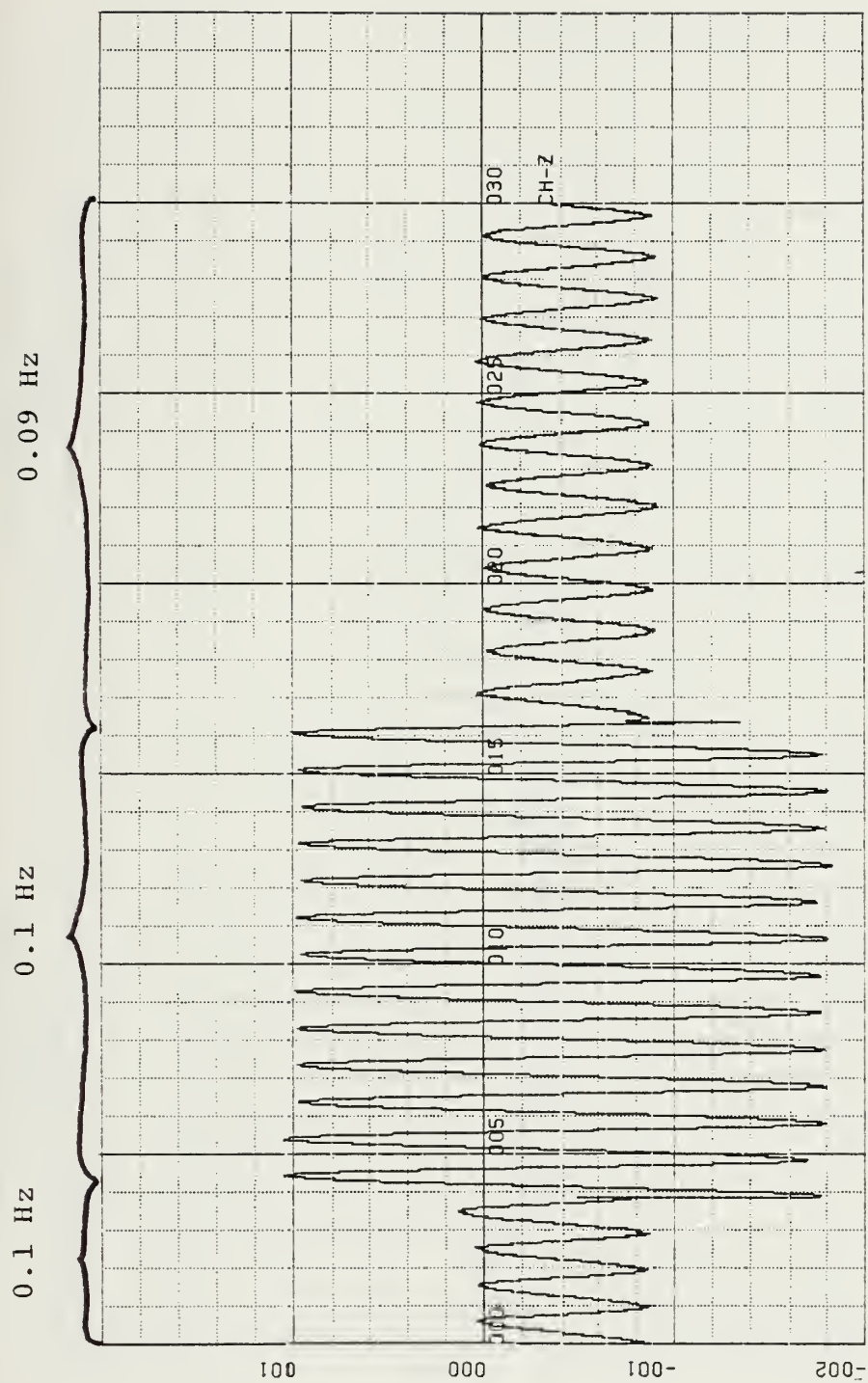


Figure 4.11. Fluxgate Magnetic Field, 26 April 83, 0948-0953 Local.  
Amplitude (nanoteslas : 10 units/in) vs. Time (seconds : 50 units/in)





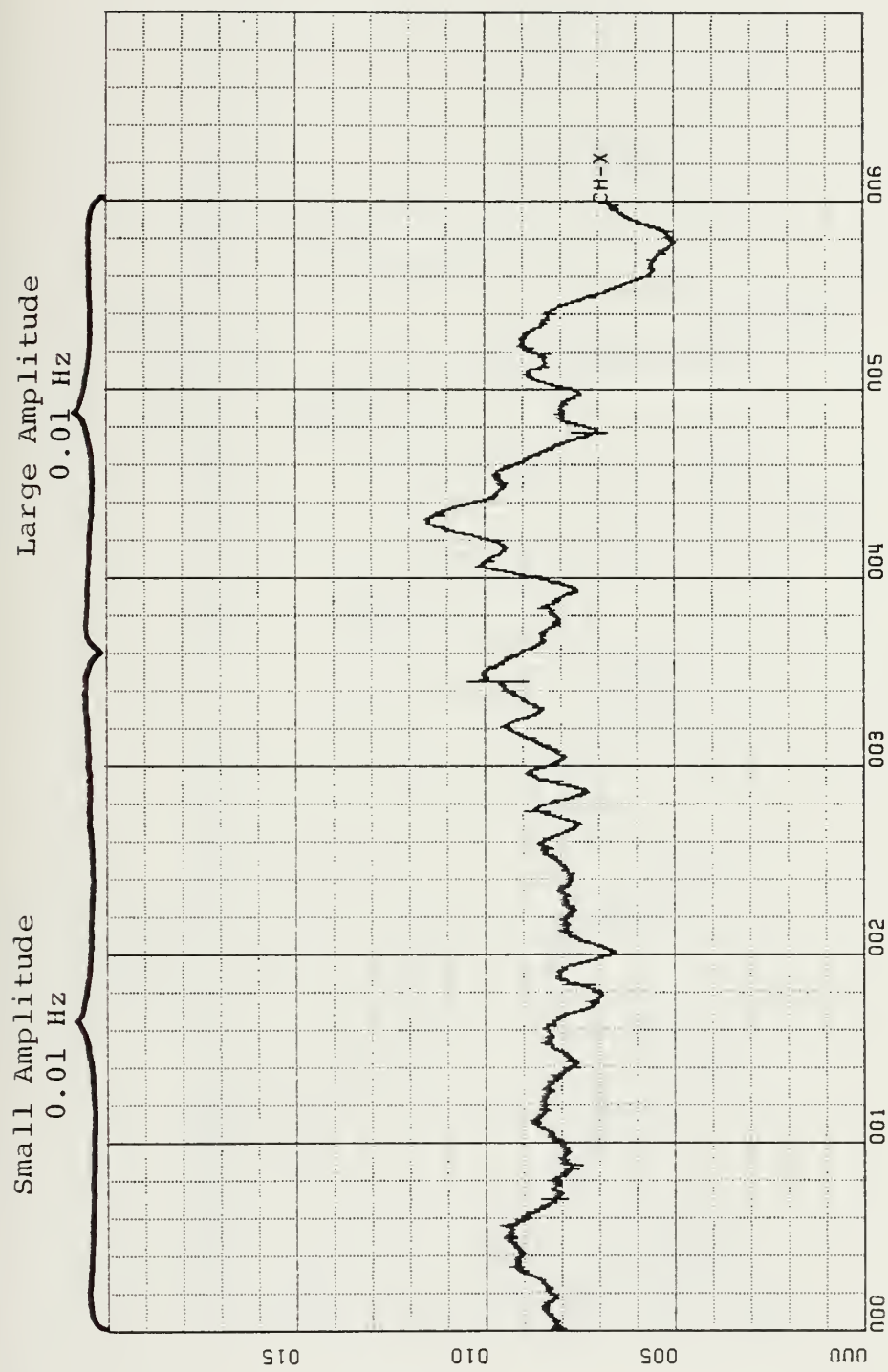


Figure 4.12. X-Coil Magnetic Field, 26 April 83, 1023-1033 Local.  
Amplitude (nanoteslas : 0.5 units/in) vs. Time (seconds : 100 units/in)



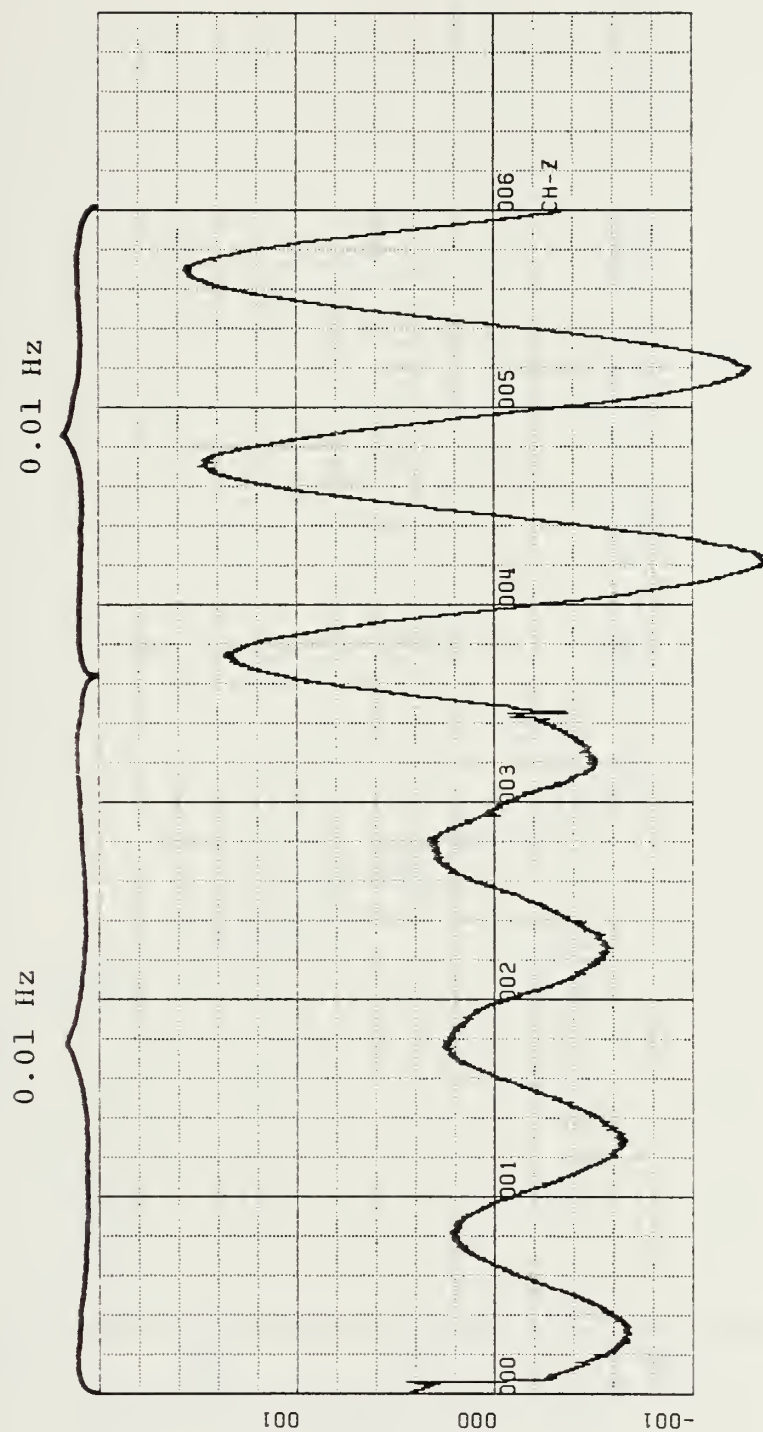


Figure 4.13. Fluxgate Magnetic Field, 26 April 83, 1023-1033 Local.  
Amplitude (nanoteslas : 10 units/in) vs. Time (seconds : 100 units/in)



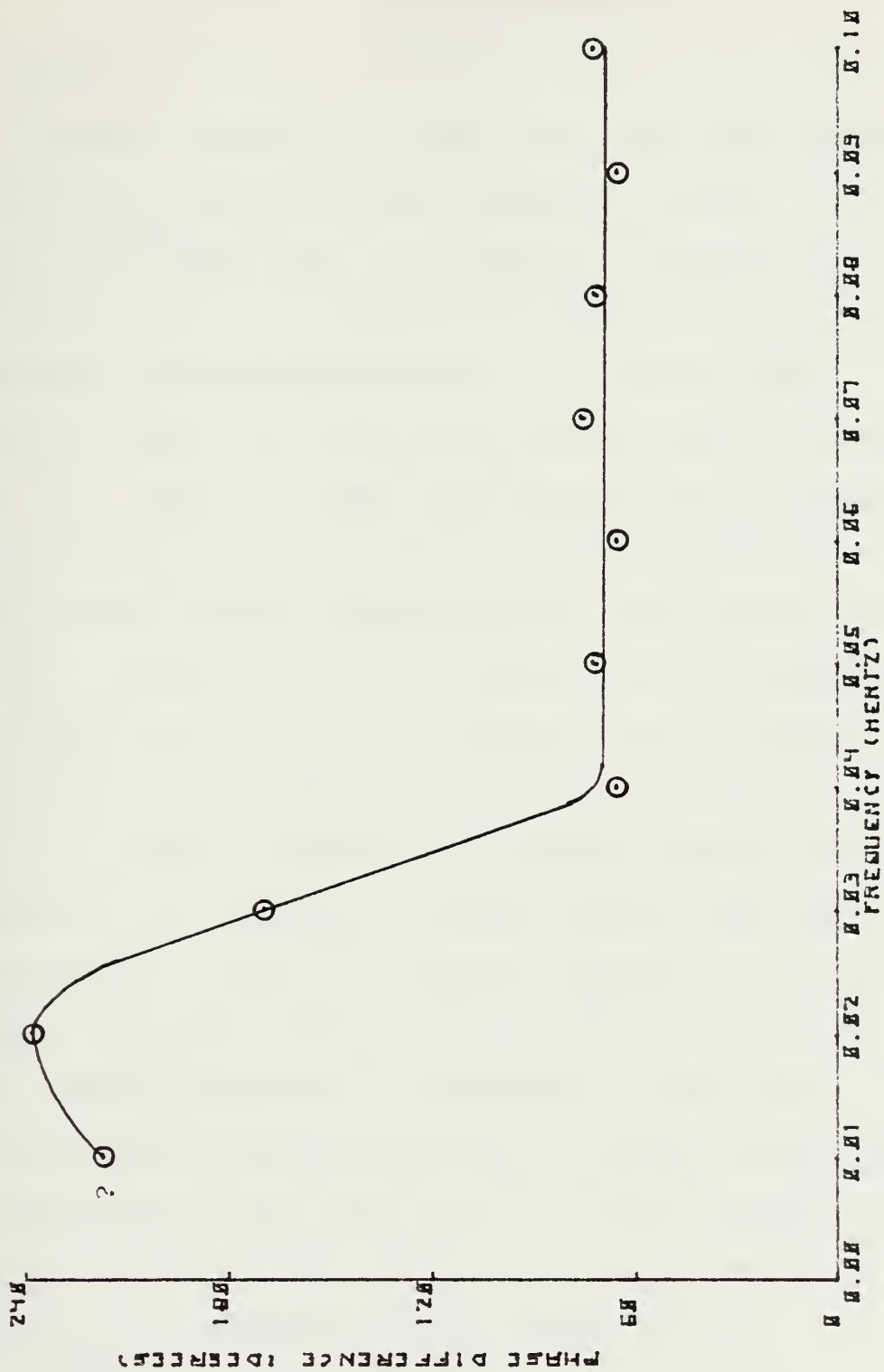


Figure 4.14. Phase Lag of Coil with Respect to Fluxgate



## V. MICROPULSATIONS

### A. THEORY

Currently there is no theory that completely models the observed micropulsations and geomagnetic noise. It is generally accepted that the generating mechanism for micropulsations is an interaction between the solar wind and the earth's magnetosphere [Ref. 5]. The observed micropulsations are classified by their period and regularity [Ref. 5]. Table 5.1 shows the micropulsation classification. The smoothing algorithm applied to the magnetic field data is designed to highlight micropulsations with periods between 10-45 seconds. Specifically we are interested in micropulsations classified as Pc 3. Pc 3 micropulsations are generally regular and have a more or less distinct period. Thus in the PSD plots we will be able to identify the micropulsation by an apparent anomaly at its frequency. Micropulsations have amplitudes of approximately 0.5 nT. This small amplitude is very small compared to a main magnetic field value of 50,000 nT, hence the term "micro" pulsations. Geomagnetic fluctuations are a combination of micropulsations and a general background noise. Micropulsation events grow out of the ever present background. The time series magnetic field plots will provide a means of obtaining the frequency of the micropulsation.





Table 5.1. Micropulsation Classification

<u>Notation</u>	<u>Period (seconds)</u>
Pc1	0.2-5
Pc2	5-10
Pc3	10-45
Pc4	45-150
Pc5	150-600



## B. MICROPULSATION DATA ANALYSIS

The first 1200 seconds of data after a 60 second tape advance on digital data tape GMDT 11, 17 August 82, 1301-1408 Local, may contain a micropulsation event. Figures 3.10-3.12 show the first 34 minutes of GMDT 11 after a 60 second advance. To determine whether the regular pulsations we see in the first third of Figures 3.10-3.12 (disregarding the suspicious "cusps") is a micropulsation, the scale must be expanded. Figures 5.1-5.3 show the regular pulsations on an expanded scale. From Figures 5.1-5.3 the period of the oscillation is calculated to be 17.2 seconds. Thus this section of data contains a type Pc 3 micropulsation.

Executing the computer code LANDXYZ [Ref. 1] on this section of data, we generate the PSD, coherence, degree of polarization, and ellipticity. Table 5.2 contains the amplitude, frequency, coherence, etc. for the micropulsation.

At the frequency of the micropulsation one would expect a good coherence, degree of polarization and ellipticity since the coil system is oriented arbitrarily with each coil sensing the micropulsation. The observed micropulsation exhibits a high coherence as shown in Table 5.2. The observed micropulsation has a high degree of polarization. Micropulsations are generally considered to be left-hand elliptically polarized [Ref. 5]. The observed micropulsation is elliptically polarized.

If the errors in phase and amplitude that were shown to exist in Section IV are constant, then that should not be a



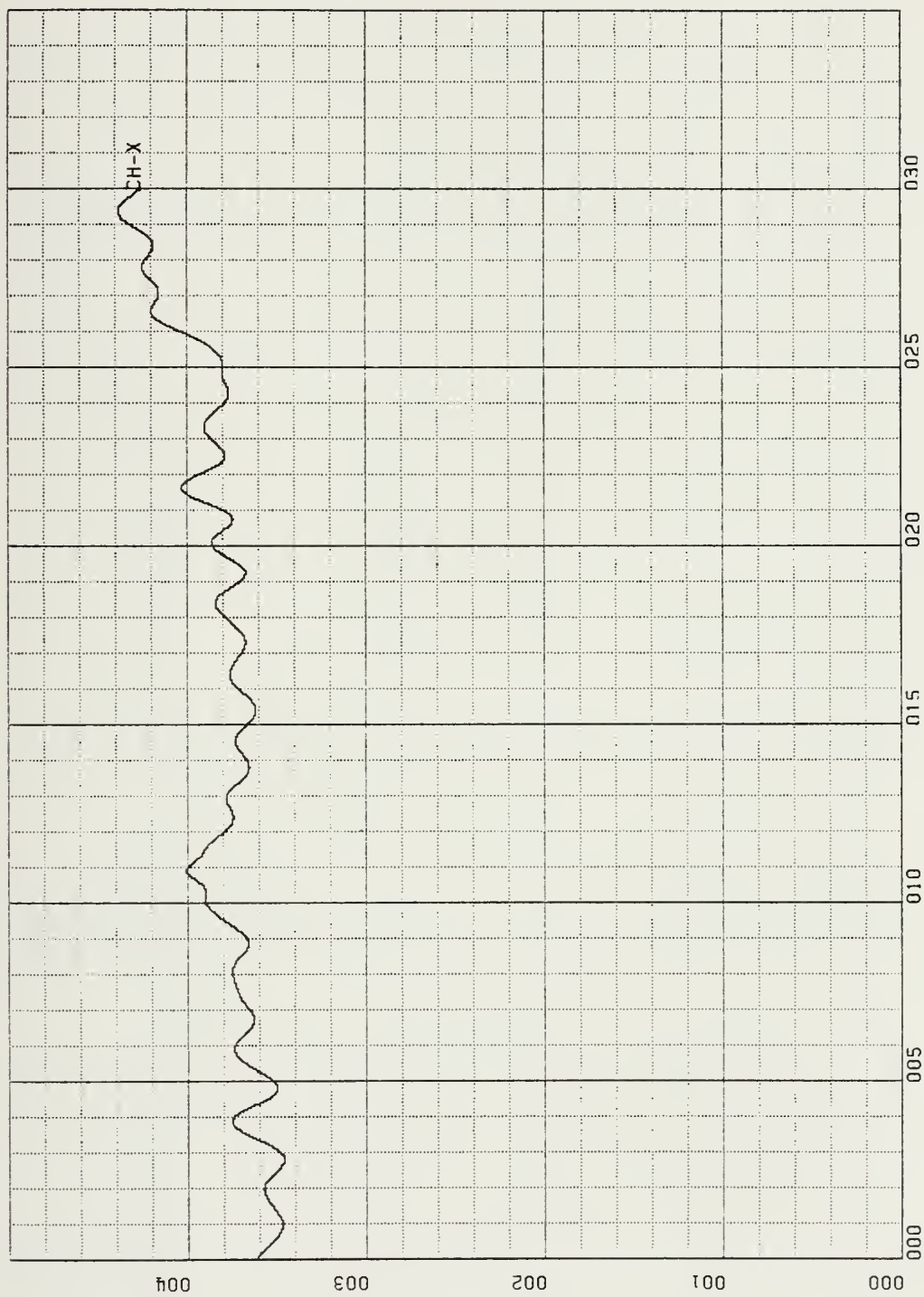


Figure 5.1. X-Coil Magnetic Field, 17 August 82, 1305-1310 Local.  
Amplitude (nanoteslas : 1 unit/in) vs. Time (seconds : 50 units/in)



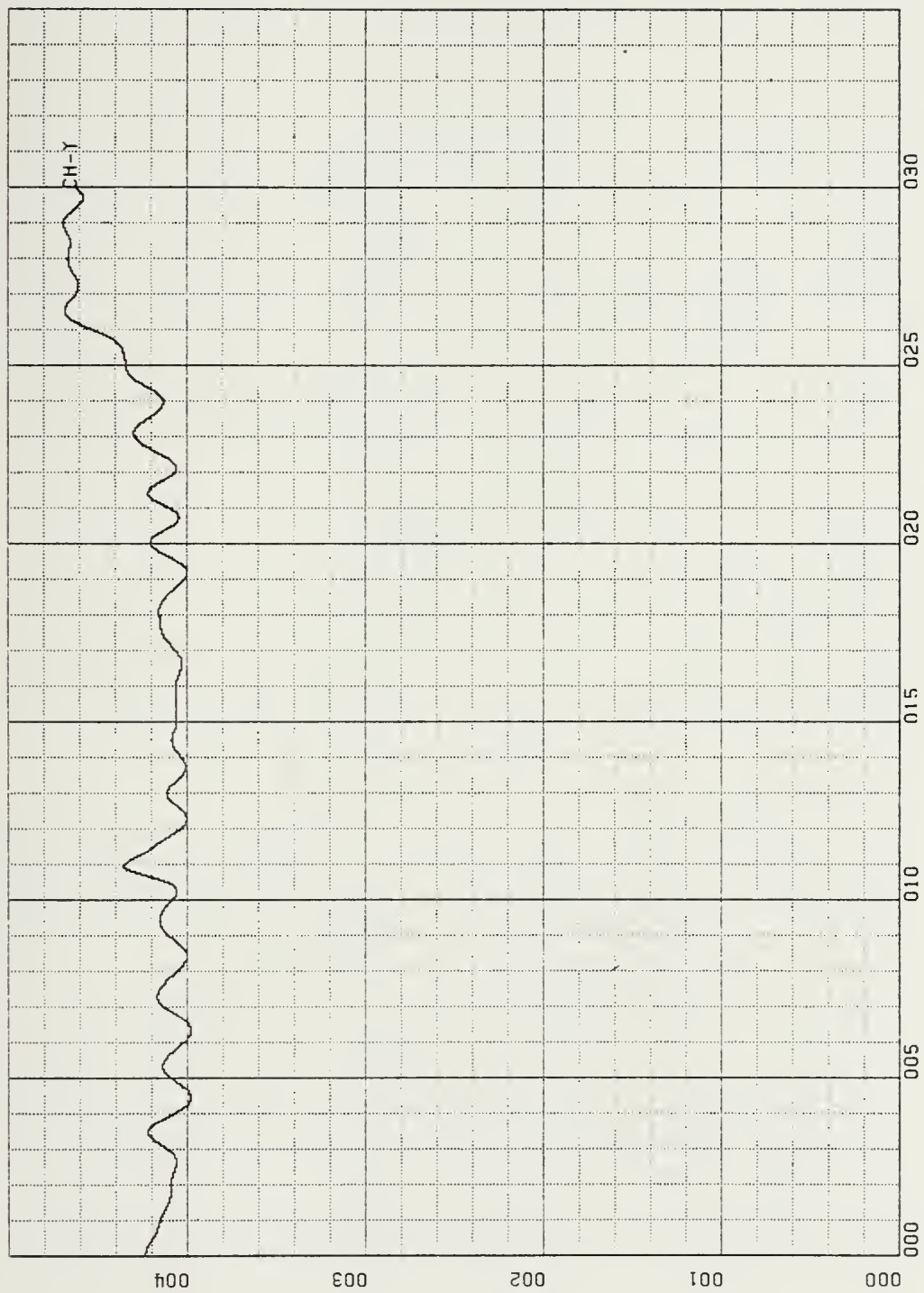


Figure 5.2. Y Coil Magnetic Field, 17 August 82, 1305-1310 Local.  
Amplitude (nanoteslas : 1 unit/in) vs. Time (seconds : 50 units/in)





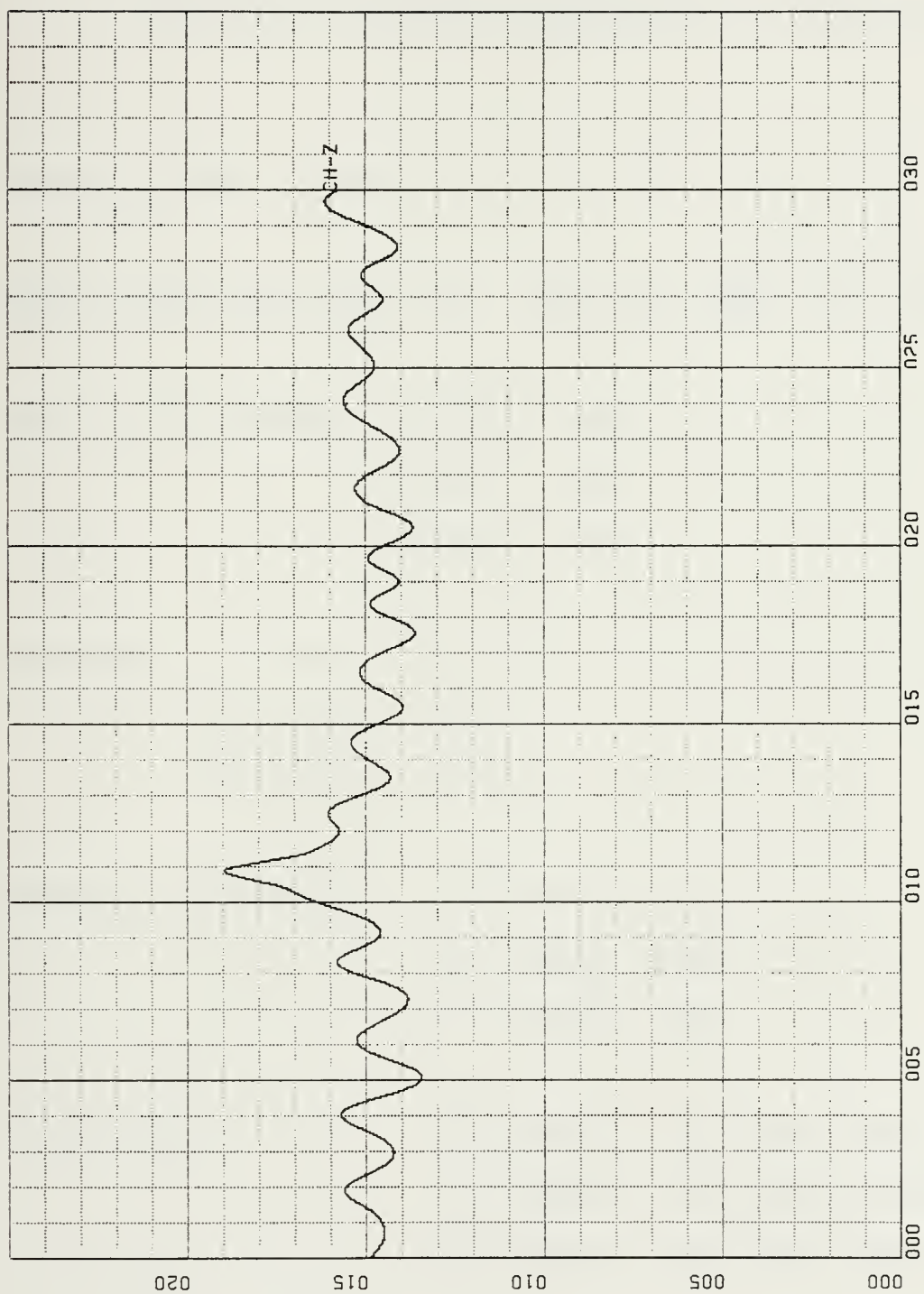


Figure 5.3. Z Coil Magnetic Field, 17 August 82, 1305-1310 Local.  
Amplitude (nanoteslas : 0.5 units/in) vs. Time (seconds : 50 units/in)



Table 5.2. Observed Micropulsation Properties

Frequency (Hz): 0.058

Peak-to-Peak Amplitude (nT): Amplitude  $= \sqrt{X^2 + Y^2 + Z^2} = 0.37$

PSD (dB) (Ref 1nT<sup>2</sup>/Hz): X-Coil: -3dB

Y-Coil: -4dB

Z-Coil: 1.5dB

Coherence: X-Y Coils: 0.99

Y-Z Coils: 0.99

Z-X Coils: 0.99

Degree of Polarization: X-Y Plane: 0.99

Y-Z Plane: 0.99

Z-X Plane: 0.99

Ellipticity: X-Y Plane: 0.45 (left hand)

Y-Z Plane: 0.10 (right hand)

Z-X Plane: 0.30 (left hand)



serious problem since we are dealing with a single frequency. Thus, the observed micropulsation exhibited definite structure decidedly different than the background.



## VI. CONCLUSIONS

A type PC-3 micropulsation event of peak-to-peak amplitude (0.37 nT) and period (17.2 seconds) was identified in a section of data. At the frequency of the micropulsation, the coherence between the three orthogonal coil sensors was about 0.99 for the xy-pair, 0.99 for the xz-pair, and 0.99 for the yz-pair. The degree of polarization was 0.99. The ellipticity was about 0.30.

The origin of the regular "hump"-like structure in the PSD's of previous coil data was found to be artificial and not representative in any way of natural phenomena in the geomagnetic field. Previous conclusions based on a frequency domain analysis of coil data characterized by a regular "hump" structure (strong or weak) in the PSD plots are known to be unsubstantiated.

Compared to a PSD frequency domain analysis of the data set, an analysis of geomagnetic field fluctuations in the time domain easily identifies data sets containing a micropulsation event. A double running average routine developed and applied to the time series data sets was found to be helpful in highlighting the micropulsation.

Detailed conclusions about the geomagnetic field from the coil measurements require a balance of analysis in the frequency and time domain.





An accurate reproduction of a time series plot for the geomagnetic field oscillations will require modification to the existing software.

Comparisons in the time or frequency domain between any pair of coils in the orthogonal system might be misleading as a result of cross talk between electrical inputs. The suspicion of cross talk is based on the observed pick-up on an unloaded input of the contents of an adjacent loaded and active input.

Further micropulsation studies should continue. This initial investigation of the coherence, polarization, and ellipticity features of micropulsation events shows promise that with more data, one might suggest novel physical mechanisms and models for the origin of micropulsations.



## APPENDIX A

### VOLTR COMPUTER PROGRAM

Appendix A contains the VOLTR computer program that provides unsmoothed time series voltage plots. VOLTR uses the subroutine RD to strip voltage data off digital tapes. The integer voltage data is normalized to  $\pm 5V$  and plotted using the DRAWP subroutine.



```

//VGLT$1L JOB (1029,0129),'STEVENS, SMC 2670',CLASS=G
//*MAIN ORG=NP GVM1.1029P,LINES=(65)
//*FCRMAT PR,DDNAME=PLOT,SYSVECTR,DEST=LOCAL
// EXEC FRITXCLGP,PARM.LKED='LIST,MAP,XREF',REGION.GO=2048K
//FORT.SYSIN DD *
  INTEGER*2 IN(16)
  ARRAY 'IN' IS USED IN READING DATA FROM TAPE
  REAL*4 XX(8192),YY(8192),ZZ(8192)
  THE ABOVE REAL*4 ARRAYS ARE USED TO ORDER INPUT DATA AND
  INITIALLY REPRESENT VOLTAGE - TIME SERIES INFORMATION.
  DIMENSION ZZ(1(65536)),ZZY1(65536),ZZV1(65536)
  DIMENSION TIME2(65536)
  INTEGER K,15
  INTEGER*4 ITB(12)/12*0/
  REAL*4 RTB(28)/28*0.0/
  REAL ALAB(3)/'CH-X','CH-Y','CH-Z'//
  REAL*8 TITLE(12)
  EQUIVALENCE(TITLE(1),RTB(5))
  ARRAYS 'ITB','RTB','ALAB',AND 'TITLE' ARE USED IN GENERATING
  THE VERTSATEC PLCTIER OUTPUT.
  DATA XX,YY/16384*0./
  DATA ZZ/8192*0./
  K=0
  I5=1
  DC 31 IN1=1,65536
  ZZX1(IN1)=0.0
  ZZY1(IN1)=0.0
  ZZV1(IN1)=0.0
  TIME2(IN1)=0.0
  CCNT INUE
31 THE NEXT FIVE LINES SERVE AS A TIME DELAY IN STARTING THE
   DATA ANALYSIS. ISEC IS THE NUMBER OF SECCNDS DELAYED.
   ISEC=2048
   ITL=ISEC*32
  DC 55 JJ=1,ITL
  CALL KD(20,IN,200,IKEC,IRR)
55 CCNT INUE
   IFRAME=8192
   NR=8
   FNR=FLOAT(NR)
  DC 70 LI=1,NR
  THE DO LOOP ENDING WITH STATEMENT 70 ENABLES THE PROGRAM TO
  PROCESS A LARGE AMOUNT OF DATA BY REPEATING THE PROCESS IN
  BLOCKS.
  NR REPRESENTS THE NUMBER OF DATA SEQUENCES. ONE
  SEQUENCE CURRENTLY EQUALS 8192 DATA POINTS FOR EACH CHANNEL
  OR 256 SECCNDS OF DATA.

```

```

VTH000010
VTH000020
VTH000030
VTH000040
VTH000050
VTH000060
VTH000070
VTH000080
VTH000090
VTH000100
VTH000110
VTH000120
VTH000130
VTH000140
VTH000150
VTH000160
VTH000170
VTH000180
VTH000190
VTH000200
VTH000210
VTH000220
VTH000230
VTH000240
VTH000250
VTH000260
VTH000270
VTH000280
VTH000290
VTH000300
VTH000310
VTH000320
VTH000330
VTH000340
VTH000350
VTH000360
VTH000370
VTH000380
VTH000390
VTH000400
VTH000410
VTH000420
VTH000430
VTH000440
VTH000450
VTH000460
VTH000470
VTH000480

```



```

C      THE DO LCCP ENDING WITH 60 READS THE DATA FROM THE PCM FRAME
C      STRIPS OUT THE SYNC CODE, AND SORTS OUT THE DATA BY COIL
C      CHANNEL.
      DO 60 JJ=1,IFRAME
      CALL RD(20,IN,1000,IREC,IRR)
      XX(JJ)=IN(2)
      YY(JJ)=IN(3)
      ZZ(JJ)=IN(4)
      CCNT INUE
60      N=8192
      FN=FLOAT(N)
      DELTAT=1./32.
      DO 20 J=1,N
      THE FOLLOWING CALCULATIONS NORMALIZE THE DATA TO +5V AND -5V.
      XX(J)=(XX(J)-1966.)*5./1966.
      YY(J)=(YY(J)-2085.)*5./2085.
      ZZ(J)=(ZZ(J)-2539.)*5./2539.
      *XX* IS THE X-COIL DATA, *YY* IS THE Y-COIL DATA,
      *ZZ* IS THE Z-COIL DATA
      NORTH-SOUTH COMPONENT (XX) AND THE VERTICAL COMPONENT (ZZ)
20      CCNT INUE
      DC 91 I3=1,8192
      ZZX1(I5)=XX(I3)
      ZZY1(I5)=YY(I3)
      ZZV1(I5)=ZZ(I3)
      TIME2(I5)=(DELTAT*FLOAT(I3))+(256.0*FLOAT(K))
      I5=I5+1
91      CCNT INUE
      K=K+1
70      CCNT INUE

C      VERSATEC PLOT OF V - TIME SERIES VOLTAGE
C      NPTS=2048./DELTAT +1.
C      *NPTS* DETERMINES NUMBER OF POINTS NECESSARY IN ORDER FOR
C      THE 0 TO 2047 SECS RANGE TO BE PLOTTED.
C      FOR THE FOLLOWING *ITB* AND *RTB* VALUES REVIEW THE WRITE-UP
C      FOR THE SUBROUTINE PROCEDURE 'DRAWP'.
      ITB(3)=20
      ITB(4)=8
      ITB(7)=1
      ITB(12)=0.0
      RTB(1)=0.0
      RTB(2)=0.0
      RTB(3)=ALAB(1)
      READ(5,3000)TITLE
      CALL DRAWP(NPTS,TIME2,ZZX1,ITB,RTB)
      RTB(3)=ALAB(2)
      VTH00490
      VTH00500
      VTH00510
      VTH00520
      VTH00530
      VTH00540
      VTH00550
      VTH00560
      VTH00570
      VTH00580
      VTH00590
      VTH00600
      VTH00610
      VTH00620
      VTH00630
      VTH00640
      VTH00650
      VTH00660
      VTH00670
      VTH00680
      VTH00690
      VTH00700
      VTH00710
      VTH00720
      VTH00730
      VTH00740
      VTH00750
      VTH00760
      VTH00770
      VTH00780
      VTH00790
      VTH00800
      VTH00810
      VTH00820
      VTH00830
      VTH00840
      VTH00850
      VTH00860
      VTH00870
      VTH00880
      VTH00890
      VTH00900
      VTH00910
      VTH00920
      VTH00930
      VTH00940
      VTH00950
      VTH00960

```





```

      READ(5,3000)TITLE
      CALL DRAWP(NPTS,TIME2,ZZX1,ITB,RTB)
      RTB(3)=ALAB(3)
      READ(5,3000)TITLE
      CALL DRAWP(NPTS,TIME2,ZZV1,ITB,RTB)
      ITB(3)=7
      ITB(4)=5
      ITB(12)=0
      RTB(3)=ALAB(1)
      READ(5,3000)TITLE
      CALL DRAWP(NPTS,TIME2,ZZX1,ITB,RTB)
      RTB(3)=ALAB(2)
      READ(5,3000)TITLE
      CALL DRAWP(NPTS,TIME2,ZZX1,ITB,RTB)
      RTB(3)=ALAB(3)
      READ(5,3000)TITLE
      CALL DRAWP(NPTS,TIME2,ZZV1,ITB,RTB)
      FORMAT(6A8)
3000 STOP
      END
      SUBROUTINE RD(IUN,IO,IRS,IREC,IRQ)
      THIS PROCEDURE FURNISHED BY DR. TIM STANTON,
      DEPARTMENT OF OCEANOGRAPHY.
      READ DATA FROM IUN, ALIGN, CHECK & RETURN
      IUN=TAPE NUMBER, EG 20
      IO=INTEGER*2 ARRAY, 16 LONG, (VALUES 0-4095, SUBTRACT 2048)*5
      /2028. GIVES VOLTAGE
      IRS= NUMBER OF RESINCS ALLOWED (ERRORS)
      IREC= COUNTER OF RECORDS (FRAMES OF DATA)
      BLOCK 512 BITS, 32 BITS = RECORD
      800 BPI TAPE UNLABLED
      IRQ= NUMBER OF ACTUAL RESINCS (ERRORS)
      INTEGER * 2 IO(16),IP(16)
      DATA IRK /C/
      IF (IREC.EQ.0) IS=0
      IER=0
      FORMAT(16A2)
      IF (IS.NE.0) GO TO 50
      READ (IUN,20,END=900) IP
      IREC=IREC+1
      IS=IS+1
      IF (IS.LT.17) GO TO 50
      READ (IUN,20,END=900) IP

```

```

VTH00970
VTH00980
VTH00990
VTH01000
VTH01010
VTH01020
VTH01030
VTH01040
VTH01050
VTH01060
VTH01070
VTH01080
VTH01090
VTH01100
VTH01110
VTH01120
VTH01130
VTH01140
VTH01150
VTH01160
VTH01170
VTH01180
VTH01190
VTH01200
VTH01210
VTH01220
VTH01230
VTH01240
VTH01250
VTH01260
VTH01270
VTH01280
VTH01290
VTH01300
VTH01310
VTH01320
VTH01330
VTH01340
VTH01350
VTH01360
VTH01370
VTH01380
VTH01390
VTH01400
VTH01410
VTH01420
VTH01430
VTH01440

```



50	IS=I	VTH01450
C	I	VTH01460
55	ICH=IMASK(IP(IS),3,0)+1	VTH01470
C	WRITE(6,55) ICH,IS,IUN,IREC	VTH01480
	FORMAT(' RE SYNCING ICH,IS,IUN,IREC ',418)	VTH01490
		VTH01500
	IF (ICH.NE.1) GO TO 40	VTH01510
	DO 100 I=1,16	VTH01520
	IO(I)=ISHIFT(IP(IS),4)	VTH01530
	ICH=IMASK(IP(IS),3,0)+1	VTH01540
	IF (ICH.EQ.1) GO TO 80	VTH01550
	IER=IER+1	VTH01560
	WRITE(6,70) IUN,IREC,I,ICH,IER	VTH01570
70	FORMAT(' UNIT ',13,' RECORD ',16,'CHAN & DATA CH ',214,	VTH01580
	' ERRORS ',17)	VTH01590
80	IS=IS+1	VTH01600
	IF (IS.LT.17) GO TO 100	VTH01610
	READ (IUN,20,END=900) IP	VTH01620
	IS=1	VTH01630
	IREC=IREC+1	VTH01640
100	CONTINUE	VTH01650
C		VTH01660
	IF (IER.EC.0) GO TO 150	VTH01670
	IRR=IRR+1	VTH01680
	IF (IRR.LT.IRS) GO TO 120	VTH01690
110	WRITE(6,110)	VTH01700
	FORMAT(' I STOPPED IN SUB RD BECAUSE GF IRR.GT.',I6,' AT 1110')	VTH01710
	IRR=IRR	VTH01720
	STOP	VTH01730
	CONTINUE	VTH01740
120	WRITE(6,130) IREC,IRR	VTH01750
130	FORMAT(' RESYNC AT FRAME ',I6,' WITH TOTAL ERRORS ',I7)	VTH01760
	IER=0	VTH01770
	IRQ=IRR	VTH01780
	GO TO 50	VTH01790
150	CONTINUE	VTH01800
	RETURN	VTH01810
900	WRITE(6,510) IUN,IREC	VTH01820
910	FORMAT(' I END OF UNIT ',I3,' AT REC ',I7)	VTH01830
	STOP	VTH01840
	END	VTH01850
		VTH01860
	FUNCTION ISHIFT(IN,NPLC)	VTH01870
C	RETURNS SHIFTED VALUE OF I*2 WORD IN	VTH01880
C	-VE LEFT,+VE RIGHT SHIFT	VTH01890
C		VTH01900
	INTEGER * 2 IN	VTH01910
	IP=IN	VTH01920



VTH01930  
 VTH01940  
 VTH01950  
 VTH01960  
 VTH01970  
 VTH01980  
 VTH01990  
 VTH02000  
 VTH02010  
 VTH02020  
 VTH02030  
 VTH02040  
 VTH02050  
 VTH02060  
 VTH02070  
 VTH02080  
 VTH02090  
 VTH02100  
 VTH02110  
 VTH02120  
 VTH02130  
 VTH02140  
 VTH02150  
 VTH02160  
 VTH02170  
 VTH02180  
 VTH02190  
 VTH02200  
 VTH02210  
 VTH02220  
 VTH02230  
 VTH02240  
 VTH02250  
 VTH02260  
 VTH02270  
 VTH02280  
 VTH02290  
 VTH02300  
 VTH02310  
 VTH02320  
 VTH02330  
 VTH02340

```

IF (IP.LT.0) IP=IP+65536
IF (NPLC.LT.0) GO TO 30
IShift=IP/(2**IABS(NPLC))
RETURN
IShift=IP*(2**IABS(NPLC))
IF (IShift.GT.65535) IShift=MOD(IShift,65536)
RETURN
END
FUNCTION IMASK (IN,IBL,IBR)
  MASK 1#2 WORD IN OUTSIDE BITS IBL & IBR
  INTEGER * 2 IN,IO
  IO=IN
  IF (IBR.EQ.0) GO TO 50
  IT=IShift(IN,IBR)
  IO=IT
  IP=IShift(IO,IBL-15-IBR)
  IO=IP
  IMASK=IShift(IO,15-IBL)
  RETURN
END

/*GO.SYSIN DD *
LA MESA VILLAGE, 17 AUG 82, 1324-1358 LOCAL
X COIL AMP IN VOLTS
LA MESA VILLAGE, 17 AUG 82, 2240-2314 LOCAL
Y COIL AMP IN VOLTS
LA MESA VILLAGE, 17 AUG 82, 1324-1358 LOCAL
Z COIL AMP IN VOLTS
LA MESA VILLAGE, 17 AUG 82, 1324-1358 LOCAL
X COIL AMP IN VOLTS
LA MESA VILLAGE, 17 AUG 82, 1324-1358 LOCAL
Y COIL AMP IN VOLTS
LA MESA VILLAGE, 17 AUG 82, 1324-1358 LOCAL
Z COIL AMP IN VOLTS
/*
//GO.FT20F001 DD UNIT=3400-4,VOL=SER=GMDT11,DISP=(OLD,KEEP),
// LABEL=(1,NL,IN),
// DCB=(RECFM=FB,LRECL=32,BLKSIZE=512,DEN=2)
//GO.SYSDUMP DD SYSOUT=A
//
//

```



APPENDIX B  
VOLTS COMPUTER PROGRAM

Appendix B contains the VOLTS computer program that provides smoothed time series voltage plots. VOLTS uses the subroutine RD to strip voltage data off digital tapes. The integer voltage data is normalized to  $\pm 5V$ . A double 144 point running average is applied to the data. The DRAWP subroutine plots the data.





```

//VLTS$ILL JOB (1029,0129),'STEVENS SMC 2670',CLASS=G
//*MAIN ORG=MPGVML1029P,LINES=(65)
//**FORMAT PR,DDNAME=PLOT.SYSVECTOR,DEST=LUCAL
// EXEC FR TXCLGP,PARM.LKED='LIST,MAP,XREF',REGION.GC=2048K
//FORT. SYSIN DD *
  INTEGER*2 IN(16)
  C ARRAY IN IS USED IN READING DATA FROM TAPE
  REAL*4 XX(8192),YY(8192),ZZ(8192)
  C THE ABOVE REAL*4 ARRAYS ARE USED TO ORDER INPUT DATA AND
  C INITIALLY REPRESENT VOLTAGE - TIME SERIES INFORMATION.
  DIMENSION ZZ1(65536),ZZY1(65536),ZZV1(65536)
  DIMENSION TIME2(65536)
  INTEGER K,G,I5
  REAL SUMX,SUMY,SUMZ,SUMT,AVE1,AVE2,AVE3,AVE4
  INTEGER*4 ITB(12)/12*0/
  REAL*4 RIB(28)/28*0.0/
  REAL ALAB(4)/'CH-X','CH-Y','CH-Z','TOT'/
  REAL*8 TITLE(12)
  EQUIVALENCE(TITLE(1),RIB(5))
  C ARRAYS ITB,'RIB',ALAB,AND 'TITLE' ARE USED IN GENERATING
  C THE VERTSATEC PLOTTER OUTPUT.
  DATA XX,YY/16384*0.0/
  DATA ZZ/8192*0.0/
  K=0
  I5=1
  SUMX=0.0
  SUMY=0.0
  SUMZ=0.0
  DO 31 IN1=1,65536
    ZZX1(IN1)=0.0
    ZZY1(IN1)=0.0
    ZZV1(IN1)=0.0
    TIME2(IN1)=0.0
  31 CONTINUE
  C THE NEXT FIVE LINES SERVE AS A TIME DELAY IN STARTING THE
  C DATA ANALYSIS
  ISEC=60
  ITL=ISEC*32
  DO 55 JJ=1,ITL
    CALL RD(20,IN,200,IREC,IRR)
    CCNT INUE
    IFRAME=8192
    NR=8
    FNR=FLCAT(NR)
    DO 70 LI=1,NR
      THE DO LOOP ENDING WITH STATEMENT 70 ENABLES THE PROGRAM TO
      C PROCESS A LARGE AMOUNT OF DATA BY REPEATING THE PROCESS IN
      C BLOCKS.

```



```

C      •NR• REPRESENTS THE NUMBER OF DATA SEQUENCES.
C      I SEQUENCE CURRENTLY EQUALS 8192 DATA POINTS FOR EACH CHANNEL
C      OR 256 SECONDS OF DATA.
C
C      THE DA LOOP ENDING WITH 60 READS THE DATA FROM THE PCM FRAME
C      STRIPS OUT THE SYNC CODE, AND SORTS OUT THE DATA BY COIL
C      CHANNEL
C      DO 60 JJ=1,IFRAME
C      CALL RD(20,IN,IOUO,IREC,IRR)
C      XX(JJ)=IN(2)
C      YY(JJ)=IN(3)
C      ZZ(JJ)=IN(4)
C      60 CONTINUE
C      N=8192
C      FN=FLOAT(N)
C      DELTAT=1./32.
C      DO 20 J=1,N
C      XX(J)=(XX(J)-1966.)*5./1966.
C      YY(J)=(YY(J)-2085.)*5./2085.
C      ZZ(J)=(ZZ(J)-2539.)*5./2539.
C      •XX• IS THE X-COIL DATA, •YY• IS THE Y-COIL DATA,
C      •ZZ• IS THE Z-COIL DATA
C      NORTH-SOUTH COMPONENT (XX) AND THE VERTICAL COMPONENT (ZZ)
C      20 CONTINUE
C      DO 91 I3=1,8192
C      ZZX1(I3)=XX(I3)
C      ZZY1(I3)=YY(I3)
C      ZZV1(I3)=ZZ(I3)
C      TIME2(I3)=(DELTAT*FLCAT(I3))+(256.0*FLOAT(K))
C      I5=I3+1
C      91 CONTINUE
C      K=K+1
C      70 CONTINUE
C      DOUBLE RUNNING POINT AVERAGE
C      DO 73 L2=1,2
C      Q=0
C      DO 74 IS=1,65318
C      SUMX=0.0
C      SUMY=0.0
C      SUMZ=0.0
C      DO 75 J=1,144
C      SUMX=ZZX1(Q+J)+SUMX
C      SUMY=ZZY1(Q+J)+SUMY
C      SUMZ=ZZV1(Q+J)+SUMZ
C      75 CONTINUE
C      ZZX1(IS)=SUMX/144.
C      ZZY1(IS)=SUMY/144.
C      ZZV1(IS)=SUMZ/144.
VTH00490
VTH00500
VTH00510
VTH00520
VTH00530
VTH00540
VTH00550
VTH00560
VTH00570
VTH00580
VTH00590
VTH00600
VTH00610
VTH00620
VTH00630
VTH00640
VTH00650
VTH00660
VTH00670
VTH00680
VTH00690
VTH00700
VTH00710
VTH00720
VTH00730
VTH00740
VTH00750
VTH00760
VTH00770
VTH00780
VTH00790
VTH00800
VTH00810
VTH00820
VTH00830
VTH00840
VTH00850
VTH00860
VTH00870
VTH00880
VTH00890
VTH00900
VTH00910
VTH00920
VTH00930
VTH00940
VTH00950
VTH00960

```



```

C
C
C
74 CONTINUE
73 CONTINUE
Q=Q+1
VERSATEC PLOT OF V - TIME SERIES VOLTAGE SMOOTHED
NPTS=2041./DELTA+1.
  NPTS* DETERMINES NUMBER OF POINTS NECESSARY IN ORDER FOR
  THE 0 TO 2041 SECS RANGE TO BE PLOTTED.
  FOR THE FOLLOWING ITB, AND RTB VALUES REVIEW THE WRITE-UP
  FOR THE SUBROUTINE PROCEDURE 'DRAWP'.
  ITB(3)=20
  ITB(4)=8
  ITB(7)=1
  ITB(12)=0
  RTB(1)=0.0
  RTB(2)=0.0
  RTB(3)=ALAB(1)
  READ(5,3000)ITL
  CALL DRAWP(NPTS,TIME2,ZZX1,ITB,RTB)
  RTB(3)=ALAB(2)
  READ(5,3000)ITL
  CALL DRAWP(NPTS,TIME2,ZZY1,ITB,RTB)
  RTB(3)=ALAB(3)
  READ(5,3000)ITL
  CALL DRAWP(NPTS,TIME2,ZZV1,ITB,RTB)
  ITB(3)=7
  ITB(4)=5
  ITB(12)=0
  RTB(3)=ALAB(1)
  READ(5,3000)ITL
  CALL DRAWP(NPTS,TIME2,ZZX1,ITB,RTB)
  RTB(3)=ALAB(2)
  READ(5,3000)ITL
  CALL DRAWP(NPTS,TIME2,ZZY1,ITB,RTB)
  RTB(3)=ALAB(3)
  READ(5,3000)ITL
  CALL DRAWP(NPTS,TIME2,ZZV1,ITB,RTB)
  3000 FORMAT(6A8)
      STOP
      END
/*GG.SYSIN DD *
LA MESA VILLAGE, 17 AUG 82, 1302-1336 LOCAL
XCUIL AMP IN VOLTS
LA MESA VILLAGE, 17 AUG 82, 1302-1336 LOCAL
YCUIL AMP IN VOLTS
LA MESA VILLAGE, 17 AUG 82, 1302-1336 LOCAL
VTH00970
VTH00980
VTH00990
VTH01000
VTH01010
VTH01020
VTH01030
VTH01040
VTH01050
VTH01060
VTH01070
VTH01080
VTH01090
VTH01100
VTH01110
VTH01120
VTH01130
VTH01140
VTH01150
VTH01160
VTH01170
VTH01180
VTH01190
VTH01200
VTH01210
VTH01220
VTH01230
VTH01240
VTH01250
VTH01260
VTH01270
VTH01280
VTH01290
VTH01300
VTH01310
VTH01320
VTH01330
VTH01340
VTH01350
VTH01360
VTH01370
VTH01380
VTH01390
VTH01400
VTH01410
VTH01420
VTH01430
VTH01440

```



```

Z COIL AMP IN VOLTS
LA MESA VILLAGE, 17 AUG 82, 1302-1330 LOCAL
X COIL AMP IN VOLTS
LA MESA VILLAGE, 17 AUG 82, 1302-1330 LOCAL
Y COIL AMP IN VOLTS
LA MESA VILLAGE, 17 AUG 82, 1302-1336 LOCAL
Z COIL AMP IN VOLTS
/*
//GO.FT20F001 DD UNIT=3400-4, VOL=SER=GMDT3A, DISP=(OLD,KEEP),
// LABEL=(1,NL,IN),
// DCB=(RECFM=FB, LRECL=32, BLKSIZE=512, DEN=2)
//GO.SYSDUMP DD SYSOUT=A
/*
//

```

```

VTH01450
VTH01460
VTH01470
VTH01480
VTH01490
VTH01500
VTH01510
VTH01520
VTH01530
VTH01540
VTH01550
VTH01560
VTH01570
VTH01580

```





APPENDIX C  
LFVTC1 COMPUTER PROGRAM

Appendix C contains the LFVTC1 computer program that provides smoothed time series magnetic field plots. LFVTC1 uses the subroutine RD to strip voltage data off digital tapes. The voltage data is normalized to  $\pm 5V$ . The voltage data is fast fourier transformed using the FOURT subroutine. The transfer function is applied and forward transform taken. The resulting magnetic field data undergoes a double 144 point running average and is plotted using the DRAWP subroutine.



```

//LFVIT$IL JOB (1029,0129), 'STEVENS SMC 2670', CLASS=G
//*MAIN ORG=NPGVML,1029P,LINES=(65)
//*FORMAT PR,DDNAME=PLOT,SYSVECTR,DEST=LOCAL
// EXEC FR TXCLGP,PARM.LKED='LIST,MAP,XREF',REGION.GD=2048K
//FCRT,SYNIN DD *
INTEG R#2 IN(16)
C ARRAY IN IS USED IN READING DATA FROM TAPE
C COMPLEX*8 XX(8192),YY(8192),ZZ(8192),IF(8192)
C THE ABOVE COMPLEX*8 ARRAYS ARE USED TO ORDER INPUT DATA AND
C INITIALLY REPRESENT VOLTAGE - TIME SERIES INFORMATION.
DIMENSION ZT1(8192),FREQ(8192),WORK(16384),FRQ2(8192)
DIMENSION ZY1(8192),ZY1(65536),ZZY1(65536)
DIMENSION ZT1(65536),TIME2(65536)
C THE Z ARRAYS REPRESENT FREQUENCY DOMAIN (FF TRANSFORMED)
C MAGNITUDE DATA AND ARE EVENTUALLY CONVERTED TO POWER SPECTRAL
C DENSITY INFORMATION. ZY1,ZY1,ZY1,AND ZT1 REPRESENT MAGNITUDE
C VALUES.
INTEG K,14,15,Q
REAL SUMX,SUMY,SUMZ,SUMT,AVE1,AVE2,AVE3,AVE4
REAL CONSTX,CONSTY,CONSTZ,CONSTT
INTEG R#4 ITB(12)/12*0/
REAL*4 RTB(28)/28*0.0/
REAL ALAB(4)/CH-X',CH-Y',CH-Z',TGT'/
REAL*8 TITLE(12)
EQUIVALENCE(TITLE(1),RTB(5))
C ARRAYS ITB,RTB,ALAB,AND TITLE ARE USED IN GENERATING
C THE VERTSATEC PLOTTER OUTPUT.
DATA XX,YY/16384*(0.,0.)//
DATA ZZ,IF/16384*(0.,0.)//
DATA ZY1,ZY1/16384*0.//
DATA ZT1,ZT1/16384*0.//
DATA TIME,FREQ/16384*0.//
K=0
I4=1
I5=1
C CONS IX=0.0
C CONS IY=0.0
C CONS IZ=0.0
C CONS IT=0.0
C SUMX=0.0
C SUMY=0.0
C SUMZ=0.0
C SUMT=0.0
C AVE1=0.0
C AVE2=0.0
C AVE3=0.0
C AVE4=0.0
MAG000010
MAG000020
MAG000030
MAG000040
MAG000050
MAG000060
MAG000070
MAG000080
MAG000090
MAG000100
MAG000110
MAG000120
MAG000130
MAG000140
MAG000150
MAG000160
MAG000170
MAG000180
MAG000190
MAG000200
MAG000210
MAG000220
MAG000230
MAG000240
MAG000250
MAG000260
MAG000270
MAG000280
MAG000290
MAG000300
MAG000310
MAG000320
MAG000330
MAG000340
MAG000350
MAG000360
MAG000370
MAG000380
MAG000390
MAG000400
MAG000410
MAG000420
MAG000430
MAG000440
MAG000450
MAG000460
MAG000470
MAG000480

```



```

TWOPI=6.2831853
COS60=COS(TWOPI/6.)
COS30=COS(TWOPI/12.)
D=16.75*TWOPI/360.
CCSD=COS(D)
CCSD1=COS((90.-D)*TWOPI/360.)
C      D IS THE DECLINATION OR MAGNETIC VARIATION AT THE MAGNETOMETER
C      SITE.
DO 31 IN1=1,65536
ZZX1(IN1)=0.0
ZZY1(IN1)=0.0
ZZV1(IN1)=0.0
ZZT1(IN1)=0.0
TIME2(IN1)=0.0
31 CONTINUE
C      THE NEXT FIVE LINES SERVE AS A TIME DELAY IN STARTING THE
C      DATA ANALYSIS
ISEC=60
ITL=ISEC*32
DO 55 JJ=1,ITL
CALL RD(20,IN,200,IREC,IRR)
55 CONTINUE
IFRAME=8192
NR=8
FNR=FLOAT(NR)
DO 70 LI=1,NR
C      THE DO LOOP ENDING WITH STATEMENT 70 ENABLES THE PROGRAM TO
C      PROCESS A LARGE AMOUNT OF DATA BY REPEATING THE PROCESS IN
C      BLOCKS.
;NR; REPRESENTS THE NUMBER OF DATA SEQUENCES TO BE AVERAGED.
1 SEQUENCE CURRENTLY EQUALS 8192 DATA POINTS FOR EACH CHANNEL
OR 256 SECONDS OF DATA.
C      THE DO LOOP ENDING WITH 60 READS THE DATA FROM THE PCM FRAME
C      STRIPS OUT THE SYNC CODE, AND SORTS OUT THE DATA BY COIL
C      CHANNEL
DO 60 JJ=1,IFRAME
CALL RD(20,IN,1000,IREC,IRR)
XX(JJ)=IN(2)
YY(JJ)=IN(3)
ZZ(JJ)=IN(4)
60 CONTINUE
C      THE FOLLOWING SECTION GENERATES THE TIME AND FREQUENCY
C      ARRAYS AND NORMALIZES THE INPUT PCM DATA TO VOLTAGE FORM
C      IN PREPARATION FOR FAST FOURIER TRANSFORM TO THE FREQUENCY
C      DOMAIN.
N=8192
FN=FLOAT(N)

```

MAG00490  
MAG00500  
MAG00510  
MAG00520  
MAG00530  
MAG00540  
MAG00550  
MAG00560  
MAG00570  
MAG00580  
MAG00590  
MAG00600  
MAG00610  
MAG00620  
MAG00630  
MAG00640  
MAG00650  
MAG00660  
MAG00670  
MAG00680  
MAG00690  
MAG00700  
MAG00710  
MAG00720  
MAG00730  
MAG00740  
MAG00750  
MAG00760  
MAG00770  
MAG00780  
MAG00790  
MAG00800  
MAG00810  
MAG00820  
MAG00830  
MAG00840  
MAG00850  
MAG00860  
MAG00870  
MAG00880  
MAG00890  
MAG00900  
MAG00910  
MAG00920  
MAG00930  
MAG00940  
MAG00950  
MAG00960



```

DELTAT=1./32.
DELTAF=1./ (FN*DELTAT)
DC 20 J=1,N
TIME(J)=DELTAT*FLOAT(J)
FREQ(J)=DELTAF*FLOAT(J)
XX(J)=(XX(J)-1966.)*5./1966.
XX(J)=REAL(XX(J))
YY(J)=(YY(J)-2085.)*5./2085.
YY(J)=REAL(YY(J))
ZZ(J)=(ZZ(J)-2539.)*5./2539.
ZZ(J)=REAL(ZZ(J))
*XX* IS THE X-COIL DATA, 'YY' IS THE Y-COIL DATA,
*ZZ* IS THE Z-COIL DATA, AND 'TF' IS THE PROJECTION OF THE
NORTH-SOUTH COMPONENT (XX) AND THE VERTICAL COMPONENT (ZZ)
ON THE TOTAL GEOMAGNETIC FIELD VECTOR.
20 CONTINUE
DC 21 J=1,N
FREQ2(J)=ALOG10(FREQ(J))
21 CONTINUE
THE NEXT FOUR STATEMENTS PERFORM AN FFT ON THE INPUT
TIME SERIES DATA. SEE THE WRITEUP ON 'FOURT' FOR
FURTHER INFORMATION.
CALL FOURT(XX,N,1,-1,0,WORK)
CALL FOURT(YY,N,1,-1,0,WORK)
CALL FOURT(ZZ,N,1,-1,0,WORK)
B-FIELD) TRANSFER FUNCTION TO THE SYSTEM (VOLTAGE TO
DOMAIN DATA. THIS BLOCK ENDS AT STATEMENT 9.
THE TRANSFER FUNCTION CONVERTS VOLTS TO NANOTESLAS (GAMMAS).
***WARNING*** THIS TRANSFER FUNCTIONS YIELDS AN INACCURATE
PHASE. USE A DIFFERENT TRANSFER FUNCTION IF PHASE INFORMATION
NEEDED.
DC 9 L=1,N
FREQ=FRQ(L)
IF (FRQ.LE.25.) GO TO 1
XX(L)=XX(L)/28.
GO TO 8
1 IF (FRQ.LE.15.) GO TO 2
XX(L)=XX(L)/(105.5-3.14*FRQ)
YY(L)=YY(L)/(181.32-7.588*FRQ)
ZZ(L)=ZZ(L)/(177.26-7.484*FRQ)
GO TO 8
2 IF (FRQ.LE.10.) GO TO 3
XX(L)=XX(L)/(5.958*FRQ-30.97)
YY(L)=YY(L)/(7.166*FRQ-39.99)
ZZ(L)=ZZ(L)/(6.49*FRQ-32.35)
GO TO 8
3 IF (FRQ.LE.7.5) GO TO 4

```

MAG00970  
MAG00980  
MAG00990  
MAG01000  
MAG01010  
MAG01020  
MAG01030  
MAG01040  
MAG01050  
MAG01060  
MAG01070  
MAG01080  
MAG01090  
MAG01100  
MAG01110  
MAG01120  
MAG01130  
MAG01140  
MAG01150  
MAG01160  
MAG01170  
MAG01180  
MAG01190  
MAG01200  
MAG01210  
MAG01220  
MAG01230  
MAG01240  
MAG01250  
MAG01260  
MAG01270  
MAG01280  
MAG01290  
MAG01300  
MAG01310  
MAG01320  
MAG01330  
MAG01340  
MAG01350  
MAG01360  
MAG01370  
MAG01380  
MAG01390  
MAG01400  
MAG01410  
MAG01420  
MAG01430  
MAG01440





MAG01450  
MAG01460  
MAG01470  
MAG01480  
MAG01490  
MAG01500  
MAG01510  
MAG01520  
MAG01530  
MAG01540  
MAG01550  
MAG01560  
MAG01570  
MAG01580  
MAG01590  
MAG01600  
MAG01610  
MAG01620  
MAG01630  
MAG01640  
MAG01650  
MAG01660  
MAG01670  
MAG01680  
MAG01690  
MAG01700  
MAG01710  
MAG01720  
MAG01730  
MAG01740  
MAG01750  
MAG01760  
MAG01770  
MAG01780  
MAG01790  
MAG01800  
MAG01810  
MAG01820  
MAG01830  
MAG01840  
MAG01850  
MAG01860  
MAG01870  
MAG01880  
MAG01890  
MAG01900  
MAG01910  
MAG01920

```

XX(L)=XX(L)/(3.492*FRQ-6.31)
YY(L)=YY(L)/(4.252*FRQ-10.85)
ZZ(L)=ZZ(L)/(4.044*FRQ-7.89)
GO TO 8
4 IF(FRQ.LE.5.)GO TO 5
  XX(L)=XX(L)/(2.6311*FRQ+0.14667)
  YY(L)=YY(L)/(3.012*FRQ-1.55)
  ZZ(L)=ZZ(L)/(3.184*FRQ-1.44)
GO TO 8
5 IF(FRQ.LE.3.)GO TO 6
  XX(L)=XX(L)/(2.6311*FRQ+0.14667)
  YY(L)=YY(L)/(2.702*FRQ)
  ZZ(L)=ZZ(L)/(2.92*FRQ)
GO TO 8
6 XX(L)=XX(L)/(2.72*FRQ)
GO TO 7
8 CCNTINUE
  TF(L)=(XX(L)*COSD + YY(L)*CUSD1)*COS60 + ZZ(L)*COS30
9 CCNTINUE
  CALL FCURT(XX,N,1,1,1,1,WORK)
  CALL FCURT(YY,N,1,1,1,1,WORK)
  CALL FCURT(ZZ,N,1,1,1,1,WORK)
  CALL FCURT(TF,N,1,1,1,1,WORK)
DO 57 J=1,N
  XX(J)=XX(J)/FN
  YY(J)=YY(J)/FN
  ZZ(J)=ZZ(J)/FN
  TF(J)=TF(J)/FN
57 CCNTINUE
  DC 56 I3=1,N
  ZX(I3)=CABS(XX(I3))
  ZY(I3)=CABS(YY(I3))
  ZV(I3)=CABS(ZZ(I3))
  ZT(I3)=CABS(TF(I3))
66 CCNTINUE
  THE NEXT 44 LINES OF CODE CORRECT DATA BLOCK END JUMPS.
  IF(K.NE.0) GO TO 36
DO 66 IS=8048,8192
  SUMX=ZX(I3)+SUMX
  SUMY=ZY(I3)+SUMY
  SUMZ=ZV(I3)+SUMZ
  SUMT=ZT(I3)+SUMT
66 CCNTINUE
  CCNSTX=SUMX/144.
  CCNSTY=SUMY/144.
  CCNSTZ=SUMZ/144.
  CCNSTT=SUMT/144.
DO 67 IS=1,8192

```



MAG01930  
MAG01940  
MAG01950  
MAG01960  
MAG01970  
MAG01980  
MAG01990  
MAG02000  
MAG02010  
MAG02020  
MAG02030  
MAG02040  
MAG02050  
MAG02060  
MAG02070  
MAG02080  
MAG02090  
MAG02100  
MAG02110  
MAG02120  
MAG02130  
MAG02140  
MAG02150  
MAG02160  
MAG02170  
MAG02180  
MAG02190  
MAG02200  
MAG02210  
MAG02220  
MAG02230  
MAG02240  
MAG02250  
MAG02260  
MAG02270  
MAG02280  
MAG02290  
MAG02300  
MAG02310  
MAG02320  
MAG02330  
MAG02340  
MAG02350  
MAG02360  
MAG02370  
MAG02380  
MAG02390  
MAG02400

```

ZZX1(I4)=ZX1(IS)
ZZY1(I4)=ZY1(IS)
ZZV1(I4)=ZV1(IS)
ZZT1(I4)=ZT1(IS)
I4=I4+1
67 CONTINUE
GO TO 37
36 CONTINUE
SUMX=0.0
SUMY=0.0
SUMZ=0.0
SUMT=0.0
DO 68 IS=1,144
SUMX=ZX1(IS)+SUMX
SUMY=ZY1(IS)+SUMY
SUMZ=ZV1(IS)+SUMZ
SUMT=ZT1(IS)+SUMT
68 CONTINUE
AVE1=SUMX/144.
AVE2=SUMY/144.
AVE3=SUMZ/144.
AVE4=SUMT/144.
DO 69 IS=1,8192
ZZX1(I4)=ZX1(IS)+(CONSTX-AVE1)
ZZY1(I4)=ZY1(IS)+(CONSTY-AVE2)
ZZV1(I4)=ZV1(IS)+(CONSTZ-AVE3)
ZZT1(I4)=ZT1(IS)+(CONSTT-AVE4)
I4=I4+1
69 CONTINUE
37 CONTINUE
DC 91 I3=1,8192
TIME2(I5)=(DELTA*FLOAT(I3))+(256.0*FLOAT(K))
I5=I5+1
91 CONTINUE
K=K+1
70 CONTINUE
THE FOLLOWING LINES OF CODE PERFORMS A DOUBLE RUNNING POINT
AVERAGE ON THE DATA.
DC 73 L2=1,2
Q=0
DO 74 IS=1,65318
SUMX=0.0
SUMY=0.0
SUMZ=0.0
SUMT=0.0
DO 75 J=1,144
SUMX=ZZX1(Q+J)+SUMX
SUMY=ZZY1(Q+J)+SUMY

```



MAG02410  
MAG02420  
MAG02430  
MAG02440  
MAG02450  
MAG02460  
MAG02470  
MAG02480  
MAG02490  
MAG02500  
MAG02510  
MAG02520  
MAG02530  
MAG02540  
MAG02550  
MAG02560  
MAG02570  
MAG02580  
MAG02590  
MAG02600  
MAG02610  
MAG02620  
MAG02630  
MAG02640  
MAG02650  
MAG02660  
MAG02670  
MAG02680  
MAG02690  
MAG02700  
MAG02710  
MAG02720  
MAG02730  
MAG02740  
MAG02750  
MAG02760  
MAG02770  
MAG02780  
MAG02790  
MAG02800  
MAG02810  
MAG02820  
MAG02830  
MAG02840  
MAG02850  
MAG02860  
MAG02870  
MAG02880

```

SUMZ=ZZV1(Q+J)+SUMZ
SUMT=ZZT1(Q+J)+SUMT
75 CCNT INUE
  ZZX1(I)=SUMX/144.
  ZZY1(I)=SUMY/144.
  ZZV1(I)=SUMZ/144.
  ZZT1(I)=SUMT/144.
  Q=Q+1
74 CCNT INUE
73 CCNT INUE

  VERSATEC PLOT OF B - MAGNETIC FIELD (SMOOTHED)

  NPTS=2041./DELTA T +1.
  NPTS DETERMINES NUMBER OF POINTS NECESSARY IN ORDER FOR
  THE 0 TO 2041 SECS RANGE TO BE PLOTTED.
  FOR THE FOLLOWING 'ITB' AND 'RTB' VALUES REVIEW THE WRITE-UP
  FOR THE SUBROUTINE PROCEDURE 'DRAWP'.
  ITB(3)=20
  ITB(4)=8
  ITB(7)=1
  ITB(12)=0
  RTB(1)=0.0
  RTB(2)=0.0
  RTB(3)=ALAE(1)
  READ(5,3000)ITILE
  CALL DRAWP(NPTS,TIME2,ZZX1,ITB,RTB)
  RTB(3)=ALAB(2)
  READ(5,3000)ITILE
  CALL DRAWP(NPTS,TIME2,ZZY1,ITB,RTB)
  RTB(3)=ALAE(3)
  READ(5,3000)ITILE
  CALL DRAWP(NPTS,TIME2,ZZV1,ITB,RTB)
  ITB(12)=1
  RTB(3)=ALAB(4)
  READ(5,3000)ITILE
  CALL DRAWP(NPTS,TIME2,ZZT1,ITB,RTB)
  ITB(3)=7
  ITB(4)=5
  ITB(12)=0
  RTB(3)=ALAB(1)
  READ(5,3000)ITILE
  CALL DRAWP(NPTS,TIME2,ZZX1,ITB,RTB)
  RTB(3)=ALAB(2)
  READ(5,3000)ITILE
  CALL DRAWP(NPTS,TIME2,ZZY1,ITB,RTB)
  RTB(3)=ALAE(3)
  READ(5,3000)ITILE

```



```

CALL DRAWP(NPTS,TIME2,ZZV1,ITB,RTB)
ITB(12)=1
RTB(3)=ALAB(4)
READ(5,3000)TITLE
CALL DRAWP(NPTS,TIME2,ZZT1,ITB,RTB)
3000 STOP
END

```

```

/*
//GO.SYSIN DC *
LA MESA VILLAGE, 18 AUG 82, 1825-1859 LOCAL
X COIL AMP IN NT
LA MESA VILLAGE, 18 AUG 82, 1825-1859 LOCAL
Y COIL AMP IN NT
LA MESA VILLAGE, 18 AUG 82, 1825-1859 LOCAL
Z COIL AMP IN NT
LA MESA VILLAGE, 18 AUG 82, 1825-1859 LOCAL
TCTAL FIELD AMP IN NT
LA MESA VILLAGE, 18 AUG 82, 1825-1859 LOCAL
X COIL AMP IN NT
LA MESA VILLAGE, 18 AUG 82, 1825-1859 LOCAL
Y COIL AMP IN NT
LA MESA VILLAGE, 18 AUG 82, 1825-1859 LOCAL
Z COIL AMP IN NT
LA MESA VILLAGE, 17 AUG 82, 1825-1859 LOCAL
TCTAL FIELD AMP IN NT
//GO.FT20F001 DD UNIT=3400-4,VUL=SER=GMDT21,DISP=(OLD,KEEP),
// LABEL=(1,NL,IN),
// DCB=(RECFM=FB,LRECL=32,BLKSIZE=512,DEN=2)
//GO.SYSDUMP DD SYSOUT=A
/*
//

```

```

MAG02890
MAG02900
MAG02910
MAG02920
MAG02930
MAG02940
MAG02950
MAG02960
MAG02970
MAG02980
MAG02990
MAG03000
MAG03010
MAG03020
MAG03030
MAG03040
MAG03050
MAG03060
MAG03070
MAG03080
MAG03090
MAG03100
MAG03110
MAG03120
MAG03130
MAG03140
MAG03150
MAG03160
MAG03170
MAG03180
MAG03190
MAG03200
MAG03210

```





## LIST OF REFERENCES

1. Pogue, E. W., "Experimental Observations of Geomagnetic Micropulsations: Land and Sea", Master's Thesis, Naval Postgraduate School, Monterey, September 1982.
2. Gritzke, A. R. and Johnson, R. H., "Ocean Floor Geomagnetic Data Collection System", Master's Thesis, Naval Postgraduate School, Monterey, December 1982.
3. Fisher, J. T., "Coherence in the Horizontal Plane of the Geomagnetic Field in the Frequency Range of 0-10 Hz", Master's Thesis, Naval Postgraduate School, Monterey, December 1982.
4. Schweiger, J. M., "Evaluation of Geomagnetic Activity in the MAD Frequency Band (.04 to .06 Hz)", Master's Thesis, Naval Postgraduate School, Monterey, September 1982.
5. Jacobs, J. A., "Geomagnetic Micropulsations", p. 35-39, Springer-Verlag, 1970.
6. Jackson, J. D., "Classical Electrodynamics", p. 145-148, John Wiley and Sons, Inc., 1962.
7. Moose, P. A. and Thomas M. E., "Polarization Characteristics of Geomagnetic Fluctuations", Transactions American Geophysical Union, vol. 64, no. 18, p. 212, May 1983.



INITIAL DISTRIBUTION LIST

	<u>No. Copies</u>
1. Defense Technical Information Center Cameron Station Alexandria, Virginia 22314	2
2. Library, Code 0142 Naval Postgraduate School Monterey, California 93940	2
3. Dr. Otto Heinz, Code 61Hz Department of Physics Naval Postgraduate School Monterey, California 93940	2
4. Dr. Andrew R. Ochadlick Jr., Code 610C Department of Physics Naval Postgraduate School Monterey, California 93940	2
5. Dr. Paul Moose, Code 62Me Department of Electrical Engineering Naval Postgraduate School Monterey, California 93940	1
6. Dr. Michael Thomas Applied Physics Lab, JHU Submarine Technology Division Johns Hopkins Road Laurel, MD 20707	1
7. CPT Kurt B. Stevens 45 Tuscarora Street Addison, New York 14801	2
8. Office of Naval Research Attn: Mr. John G. Heacock Code 425 GG 800 N. Quincy Street Arlington, VA 22217	1
9. Naval Air Development Center Attn: Mr. Edward Yannuzzi Code 30 Warminster, PA 18974	1



10. Naval Air Systems Command  
Attn: Mr. Barry Dillon  
Code AIR-340J  
Washington, DC 20361

1









Thesis  
S7129  
c.1

Stevens

202325

An analysis of a PC-3  
micropulsation in the  
geomagnetic field.

Thesis  
S7129  
c.1

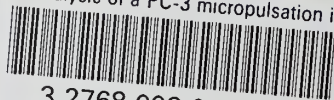
Stevens

202325

An analysis of a PC-3  
micropulsation in the  
geomagnetic field.

thesS7129

An analysis of a PC-3 micropulsation in



3 2768 002 02282 4

DUDLEY KNOX LIBRARY